UNITED NATIONS EDUCATIONAL, SCIENTIFIC AND CULTURAL ORGANIZATION
INTERNATIONAL ATOMIC ENERGY AGENCY
INTERNATIONAL CENTRE FOR THEORETICAL PHYSICS
I.C.T.P., P.O. BOX 586, 34100 TRIESTE, ITALY, CABLE: CENTRATOM TRIESTE

H4.SMR/1011 - 8

Fourth Workshop on Non-Linear Dynamics and Earthquake Prediction

6 - 24 October 1997

Application of Earthquake Prediction Algorithms to Italy and Microzoning

G.F. PANZA

Universita' degli Studi di Trieste
Dept. of Earth Sciences
/ ICTP - SAND Group, Trieste
ITALY

MONITORING OF SEISMICITY WITH ALGORITHM CN IN ITALY

Antonella Peresan[1] Giovanni Costa[1,2] and Giuliano Francesco Panza[1,2]

1) Dipartimento di Scienze della Terra, Università degli Studi di Trieste, via E. Weiss 1, 34127 Trieste, Italy

2) International Center for Theoretical Physics - SAND Group - ICTP, 34100 Trieste Miramar, Italy

ABSTRACT

The choice of the regions is essential in the application of the algorithm CN, therefore a seismotectonic criterion for their definition is tested.

In the previous analysis (Keilis-Borok et al., 1990; Costa et al., 1995; Costa et al., 1996), made using CN and taking into account both the distribution of the epicentres and the seismotectonic model, three main areas are defined, where to look for the premonitory instability patterns associated to an impending earthquake. The separation among these areas is not marked by sharp boundaries, and it is possible to identify intersection areas, which could be assigned to either bordering main area; in each main area the TIPs duration decreases when the intersection areas are included.

In a further step, to take into account the geodinamic complexity characterizing the Italian peninsula, we established to follow strictly the seismotectonic model, including in each region only zones with similar seismogenic behaviour and the transitional zones connected to them. Three regions have been succesfully defined in this way, corresponding approximatively to the North, Centre and South of Italy. The reduction of the space-time uncertainty and the increase of the stability of prediction results obtained with this regionalization, with respect to the previous investigations, can be interpreted as a validation of the seismotectonic model of the Italian territory.

1. INTRODUCTION

Algorithm CN has been originally designed by retrospective analysis of seismicity in the California-Nevada region to diagnose the Time of Increased Probability (TIPs) for events with magnitude above a fixed threshold M_0. Thanks to the normalisation of the functions used by the algorithm, CN can be applied without any adjustment of parameters to areas with different dimensions and seismicity.

A first application of CN in Italy was performed by Keilis-Borok et al. (1990), over an area chosen considering simply the completeness of the used catalogue. Subsequently Costa et al. (1995) showed that seismological and tectonic arguments permit to narrow the region, leading at the same time to a reduction of failures to predict and of TIPs, while increasing the stability of the algorithm. In a further step the analysis was extended to the whole Italian territory by Costa et al. (1996), selecting three main areas, Northern, Central and Southern Italy, accordingly both to the seismotectonic model (Scandone et al., 1990) and to the spatial distribution of epicentres. These experiments evidenced that the CN algorithm permits to deal with the development of regional geodynamic models, involving relationships between the structural features that control the seismicity and the selection of the optimal causative fault system for prediction purposes (Rundkvist et al., 1994).

In this work we want to test the possibility to trace the boundary of regions following closely the seismogenic zones, independently defined by GNDT (Scandone et al., 1990), to check if it's possible to reduce the time-space uncertainty and the number of false alarms.

A new catalogue, the CCI1996 (Costa et al. 1997; Peresan et al., 1997) has been compiled revising and updating the PFGING catalogue (Postpischl, 1985; Costa et al., 1995) to take into account recent informations, mainly concerning historical seismicity, supplied by Boschi et al. (1995).

2. REGIONALIZATION

The choice of the area where a strong earthquake has to be predicted, is a relevant factor to obtain reliable results and to minimise the time-space uncertainty. Regions defined for prediction purposes have to be as small as possible and must include the zones with higher seismicity level, where stronger earthquakes are likely to occurr. This choice affects clearly the frequency-magnitude distribution for events occurred within each region, because the log-linearity of the Gutemberg-Richter relation is preserved only on a global scale or, according to a multiscale

approach (Molchan et al., 1996 and 1997), within a zone of the appropriate hierarchical scale, depending on the maximum magnitude considered. To reduce the spatial uncertainty of prediction, the area has to be relatively small, therefore the frequency-magnitude distribution exhibits a good linearity only for lower magnitudes, with increasing fluctuations due to the small number of events for larger magnitudes. According to the standard procedure, the magnitude threshold M_0, for the selection of the events to be predicted, is chosen close to a minimum in the frequency-magnitude distribution, and this guarantees the stability of results (e.g. Costa et al., 1995). In other words, CN makes use of the informations given by small and moderate earthquakes, having a quite good statistic, to predict the stronger earthquakes, that are rare events.

The area selected for predictions, using the algorithm CN, must satisfy three general rules: 1) its linear dimensions must be greater or equal to 5L-10L, where L is the length of the expected source; 2) on average, at least 3 events with magnitude over the completeness threshold should occur inside the region each year; 3) the border of the region must correspond, as much as possible, to minima in the seismicity (Keilis-Borok et al., 1996). This indicates that the detection level controls, to some extent, the time space uncertainty of prediction (Keilis-Borok, 1996) and then the possibility to reduce the spatial uncertainty is limited by the difficulty to keep an high level of detection, due to unavoidable logistic problems.

The Italian peninsula and the whole Mediterranean area are characterised by a very complex geodinamic behaviour (fig. 1), as revealed by the coexistence of fragmented seismogenic structures of greatly different kind. Even if the normalization of it's functions guarantees the applicability of the algorithm CN to regions with a different level of seismic activity, it was designed by retrospective analysis of seismicity in a region quite homogeneous, from the seismogenic point of view. Compared to the California-Nevada region, that is characterized by strike-slip source mechanisms, Italy exhibits a considerable heterogeneity in the focal mechanisms and this aspect should not be neglected. As an example, the number of aftershocks generated by an earthquake is not independent from the fault mechanism, therefore mixing sources of different kind may alter the time clustering of events (bursts of aftershocks).

In the regionalization proposed by Costa et al. (1996), the borders between the three main areas, Northern, Central and Southern Italy, are not sharply defined. In each main region, in order to analyze the effect on the prediction of the transition domains seismicity, two different regions were tested, following blandly the border

of the seismotectonic zones. In all the cases considered, the best results were obtained for the regions which include the transition areas.

Here, wishing to take into account the seismotectonic complexity of the Italian peninsula, we propose to define the regions following strictly the seismotectonic zones. Considering the general rules and the sizes of the seismotectonic zones, a preliminary grouping appears necessary, so we established to include in each region only adjacent zones with the same seismotectonic characteristics or with transitional properties. A transitional zone is included in a region if it is between zones of the same kind or if it is located at the edges of the region. In the latter case we have taken into account the space distribution of the aftershocks to reveal if they may be connected or not. For this purpose the selection of aftershocks is performed (Molchan et al., 1995) using the "minimax" method proposed by Molchan and Dmitrieva (1992).

3. CN ANALYSIS IN NORTHERN ITALY

Northern Italy is characterized by the presence of a main structure, the Alpine arc, which is generally uplifting (Mueller, 1982) with some westerly strike-slip motion (Pavoni et al., 1992) and therefore the majority of focal mechanisms are compressive or transpressive.

The presence of many different political borders, across the Alpine arc, introduces two problems. First of all the catalogue CCI1996 covers an area that, toward to the North, follows the Italian border and consequently it's fairly incomplete for our purposes; this problem has been solved (Costa et al., 1996) filling the gap with data contained in two other catalogues, ALPOR (Catalogo delle Alpi Orientali, 1987) and NEIC (1992).The catalogue obtained for Northern Italy can be considered complete for $M \geq 3.0$ starting from 1960. The operating magnitude is selected as follows:

$$M = MAX \begin{vmatrix} M_{ALPOR}(M_L, M_I) \\ M_{PFGING}(M_L, M_d, M_I) \\ M_{NEIC}(M_L, M_S, m_b) \end{vmatrix} \qquad (1)$$

This means that the operating magnitude is the maximum of the three magnitudes selected for each catalogue according to the priority order given in brackets. Magnitudes are indicated as follow: M_L is the local magnitude, M_d the duration magnitude, M_I is the magnitude from intensities, while M_S and m_b are the magnitudes from surface and body waves. Aftershocks are removed following the

criteria proposed by Keilis-Borok et al. (1980) and, according to the standard rules of the algorithm CN, the magnitude for the selection of the events to be predicted is chosen to be $M_0 = 5.4$. The period 1960-1992 is analyzed, because of the significant incompleteness of the catalogue before 1960 (Costa et al., 1996).

The second problem, due to the presence of political borders, arises from the necessity to use an adequate seismotectonic zoning for the neighbouring countries. Till recently the available zones for the Slovenian-Croatian region were designed with different purposes and criteria (Lapajne et al., 1995), consequently the easternmost border of the region could only be defined on the base of seismicity. Recently, following criteria quite similar to those used for Italy by Scandone et al. (1990), a seismotectonic zoning has been proposed by Zivcic et al. (1997) and consequently it is possible to redraw the boundaries of the north-eastern part of the region closely following the seismogenic zones (fig. 2c and fig. 3).

Our final choice of the region to be used with CN algorithm is based on the prediction experiments described below. When performing prediction experiments, with the aim to optimise the regionalization, we must preserve the predictive power reached with the previous regionalizations. Therefore, since the old regionalizations allow us to predict the strong earthquakes, in the following we consider satisfactory only the experiments with no failures to predict.

Experiment 1. We consider the region defined by the compressional band and the adjacent transpressive zones that cover the whole Alpine arc, from the Istrian peninsula to Liguria (fig.2a-1 and tab. 1). This experiment is unsuccessful, probably due to the different completeness of the catalogue (Molchan et al., 1995) and to the different level of seismic activity in different parts of the Alpine arc.

Experiment 2. Within the smaller region defined by Costa et al. (1996) for Northern Italy (fig. 2a-2) we keep only the compressional and transpressive adjacent zones in Italy, while in Austria, Slovenia and Croatia we keep the boundaries proposed by Costa et al. (1996), except towards the North, where we follow the minimum of seismicity located in correspondence of the 47°N parallel. The seismogenic properties of the zone at the west side of Garda's lake (central part of Southern Alps) have been subject of debate, as can be seen by recent revisions of the seismotectonic model (Scandone et al., 1990 and 1994). Therefore we define two regions, one including and the other excluding the zone west of Garda (GZ), as shown respectively in fig. 2a-3 and fig. 2a-4. The results obtained for these two regions are given in table 1 and can be considered satisfactory only for the region shown in fig. 2a-4. Then we deduce that the seismicity contained in this small zone

plays a critical role, revealing a certain instability with respect to the choice of the areas represented in fig. 2a-2, 3 and 4 (see also fig. 4).

Experiment 3. For a deeper analysis of the instability detected with experiment 2, we remember the hypothesis that the seismicity at the Northern edge of the Apennines may be related to the seismicity of the Alpine Arc (Costa et al., 1996), that led to define the region in fig. 2b-5. Therefore we extend the region of fig. 2a-4 to the transition seismogenic zone at the northern edge of the Appennines, even if it's not directly connected to the others (fig. 2b-6). In such a way the percentage of total TIPs is reduced. Subsequently the area is further extended to the whole compressional band along the Adriatic coast (fig. 2b-7). With this extension the destabilizing effect of the zone at the west side of Garda's lake zone is removed (fig. 2a-3, 4 and tab. 1).

Experiment 4. The north-eastern border of the region shown in fig. 2b-8 is modified considering the seismotectonic zoning for the Slovenian-Croatian territory (Zivcic, 1997) and including only compressional and transpressive zones. Where there is an overlapping of the two zonings the priority is given to the model proposed by Scandone et al. in 1994 (fig. 2c and fig. 3).

The results obtained for the area finally selected (fig. 2c) can be summarised as follows: both events with $M \geq M_0$, occurred in the period under analysis (M=6.5, May 6, 1976 and M=5.4, February 1, 1988), are predicted with 20% of the total time considered occupied by TIPs and 2 false alarms. The M=6.0 September 15, 1976 event is a strong aftershock, identified as Related Strong Earthquake by Vorobieva and Panza (1993), and therefore it is not a target of the CN algorithm. The improvement with respect to the results obtained by Costa et al. (1996) is a reduction in the percentage of TIPs (from 27% to 20%) and in the spatial uncertainty (around 38%). The diagram of the time distribution of TIPs, obtained in the monitoring with the catalogue updated to July 1997, is shown in figure 10-a. These results are stable with respect to changes in the learning period and to the exclusion of the transition zone containing the Ortona-Roccamonfina line (fig. 4).

The new regionalization is compatible with the cinematic model of rotation and subduction of the Adriatic microplate and supports the hypothesis of a possible connection between the earthquakes that occur within the compressional band, marking the zone of subduction along the Southern Alps and Northern Apennines (Ward, 1994; Anderson and Jackson, 1987).

A common feature to the different successful regionalization experiments performed is the persistence of a TIP in the time interval from 1972 to 1976.

Starting in January 1973, remarkable tilt perturbations have been recorded by the horizontal pendulums of Grotta Gigante, near Trieste (Zadro, 1978). These anomalies have been interpreted as a "slow earthquake" (Dragoni, 1985) and therefore it seems reasonable to formulate the hypothesis that the persisting TIP, from September 1972 to January 1976, is related to these creeping phenomena. In this case, the symptoms of instability detected by the algorithm CN could reveal a stress accumulation, partially released through events of small and moderate size ($M \leq 4.5$) and not ended with a strong earthquake, because of creep. This interpretation is an alternative to the explanation given in the framework of the dilatancy model, where a volume increase is expected under the effect of tectonic stresses, due to fluid migration in a volume of cracked rocks; accordingly the anomalies are viewed as precursors, indicating accumulation rather than relaxation of stress.

4. CN ANALYSIS IN CENTRAL ITALY

The central part of the Italian peninsula along the Appennines, is characterised by a band with tensional seismotectonic behaviour, with prevailing dip-slip focal mechanism. Two belts run parallel to it: the western one is composed by the tensive zones near to the Tyrrhenian coast and the eastern one by the compressional zones along the Adriatic sea, from the Ortona-Roccamonfina line (fig. 1) to the Po plain. Costa et al. (1996) evidenced that the central band may be considered individually and this fact seems to be supported by the model proposed by Meletti at al. (1995) for the deep structure of the Northern Appenines. The model indicates a connection at depth between the Adriatic compressional front and the uplifting astenosphere along the Tyrrhenian sea, in agreement with the geometries of the litosphere-astenosphere system outlined by Calcagnile and Panza (1981), Della Vedova et al. (1991) and Marson et al. (1995) on the base of the available relevant geophysical data (surface waves, body waves tomography, heat flow, gravity). According to the seismogenic zoning, the foreland Gargano region must be excluded from the region of Central Italy.

The CN algorithm has been initially applied to Central Italy (Keilis-Borok et al., 1990), because the catalogue PFGING is rather complete there; subsequently a regionalization based on seismotectonic consideration has been proposed by Costa et al.(1995).

The new region defined for Central Italy is presented in fig. 5-3. In this region the catalogue CCI1966, starting from 1950, can be considered complete for $M \geq 3.0$

(Molchan et al., 1995). The operating magnitude is chosen following the priority: M_L, M_d, M_I. Aftershocks are removed as in Northern Italy and, according to the general rules of the algorithm CN, only crustal earthquakes are considered, and the threshold for the selection of strong events is $M_0 = 5.6$. In any case, the inclusion, according to the model proposed in Marson et al. (1995), of the few deep and intermediate earthquakes occurred in Central Italy, does not affect the results, since their number and size is small. The events to be predicted inside this region (fig. 5-3) are three: M=5.8 and M=6.0, both on August 21, 1962 and the Irpinia's earthquake, with M=6.5, on November 23, 1980. All of them are predicted with TIPs covering 19% of the total time and with two false alarms (tab. 2). The distribution of TIPs is shown in fig. 10-b. The exclusion of the transition zones at both edges of the extensional band doesn't affect significantly the results, that are very stable over this area (Costa et al., 1995).

The whole extensional band, running along the peninsula, from the Po plain to the Messina strait, can be considered to form a single region (fig. 5-2), but this leads only to an increase of the spatial uncertainty (tab.2 and fig. 6). On the contrary, the attempt to divide this tensional band along the Ortona-Roccamonfina discontinuity shows that, in this case, a proper retrospective description of seismicity is impossible, because the strong Irpinia's earthquake and its precursors seem to affect significantly the activation in the whole peninsula. Comparing the region defined in fig. 5-3 to that defined for Central Italy by Costa et al. (1996), we observe that even if the same seismogenic structures are considered, the new criteria allows us a reduction of the spatial uncertainty by about 30%.

The results obtained using different regionalizations for Central Italy (Keilis-Borok et al, 1990; Costa et al., 1996), all show the persistence of a false alarm within a period that goes from July 1984 to March 1988. Similarly to the case observed in Northern Italy, anomalous deformations, modelled as aseismic dislocations processes (Dragoni, 1988), have been recorded in this region during 1985 (Bella et al., 1987).

5. CN ANALYSIS IN SOUTHERN ITALY

The extremity of the Italian peninsula, together with Sicily, is characterised by a seismotectonic profile connected with the sinking of the Adriatic-Ionic plate under the Southern Appennines and the Calabrian arc. The cinematic model proposed by Scandone et al. (1990) for Southern Italy seems to indicate a possible relation among the events occurring along the arc that goes from Ortona-Roccamonfina

discontinuity to the western edge of Sicily. This hypothesis is supported by the unsuccessful experiment reported by Costa et al. (1996) for the region that excludes the Irpinia's area (fig. 7-2 and tab. 3).

The role played by foreland zones is particularly critical in the south of Italy, because their inclusion in the analysis leads to unsuccessful or very unstable experiments. When they are excluded, both in the Gargano region and in Sicily, the algorithm gives satisfactory results (fig. 7-3,4 and tab. 3).

The transition zone corresponding to the Ortona-Roccamonfina line is not included in the South Italy region, thought it is adjacent to the region, since the distribution of the aftershocks for strong events occurred over this area (Molchan et al., 1995) indicates a strong connection between the transition zone and the northward part of the tensional band, but not with its southward extension (fig. 9).

Following the standard priority (M_L, M_d, M_I) for the operating magnitude, in the region shown in figure 7-4 we can fix the completeness threshold for the catalogue CCI1996, starting from 1950, at M=3.0 and choose $M_0 = 5.6$. All the four events (M=5.8, May 20, 1957; M=5.8 and M=6.0 on August, 1962; M=6.5 on November 23, 1980) with $M \geq M_0$ are predicted with TIPs occupying 33% of the total time interval and 3 false alarms. With respect to the region defined by Costa et al. (1996) and shown in fig. 7-1, the reduction of the spatial uncertainty can be estimated around 72%.

4. CONCLUSIONS

The new regionalization defined for the Italian territory and based on the seismotectonic zoning allows us both to improve the predictions and to validate the seismotectonic model.

Three regions have been selected, for Northern, Central and Southern Italy respectively, following strictly the boundaries of the seismogenic zones; each region contains only adjacent zones with the same characteristics or with transitional properties.

The Northern Italy region appears compatible with the cinematic model of rotation and subduction of the Adriatic microplate, and the results of the analysis with the CN algorithm support the hypothesis of the connection between earthquakes that occur within the compressional band along the subduction zone in the Southern Alps and Northern Apennines. Similarly, the Southern Italy region is defined by the seismotectonic structures associated with the sinking of the Adriatic-Ionian plate under the Southern Appennines and the Calabrian Arc. The choice of

the Central region, instead, is related to the deep structure of the Northern Appenines, characterised by the subduction of the Adria microplate and by the uplifting of the astenosphere along the Thyrrenian rim.

Since earthquake catalogues, as complete and homogeneous as possible, are essential for intermediate-term prediction based on the representation of the lithosphere as a non-linear system, we have used a revised version of the PFGING catalogue, named CCI1996 (Peresan et al., 1997), obtained considering the most recent available revisions of source parameters of individual events (Boschi et al, 1995; ISC, 1976-1990). Particularly relevant it appears the problem of completeness and homogeneity of catalogues when the studied area is crossed by political boundaries and this calls for the strengthening of data collection at European level.

The results obtained for the three regions show a general reduction of time and space uncertainty of the predictions of strong events, with respect to the regionalizations not following the seismotectonic zones (Costa et al., 1996). In addition, the new regionalization, based on the seismotectonic model, makes it possible to apply the algorithm with standard and homogeneous criteria over the whole area considered and it appears adequate for the forward monitoring since the results of the retrospective analysis reach a score very close to the one obtained globally.

Costa et al. (1996), on the basis of the results obtained, concluded that the separation among the three regions proposed is not sharp, and that it is possible to identify intersection areas, which can be assigned to either bordering main areas. When these intersection areas are included in the CN analysis, an improvement of the results is obtained. This improvement has been confirmed, for Southern and Central Italy, by the results obtained using the new regionalization proposed here.

ACKNOWLEDGEMENTS

The authors are very grateful to Prof. I.M. Rotwain, to Prof. P. Scandone and to Prof. L. Pietronero for their precious suggestions and stimulating discussions. This research has been developed in the framework of the project 414 UNESCO-IGCP and has been supported by funds MURST (40% and 60%), funds CNR (contracts n° 95.00608.PF54 and n° 96.02968.PF54) and by INTAS funds (contract n° 95-856).

REFERENCES

ALPOR (1987) - *Catalogue of the Eastern Alps.* Osservatorio Geofisico Sperimentale, Trieste, Italy.

H. Anderson; J. Jackson (1987) - *Active tectonics in the Adriatic region.* Geophys. J. R. Astr. Soc., **91** , 937-983.

F. Bella; R.Bella; P.F.Biagi; G. Della Monica; A. Ermini; V. Sgrigna (1987)- *Tilt measurements and seismicity in Central Italy over a period of approximately three years.* Tectonophysics, **139**, 333-338.

E. Boschi; G. Ferrari; P. Gasperini; E. Guidoboni; G. Smriglio; G. Valensise (1995), *Catalogo dei forti terremoti in Italia dal 461 a.C. al 1980.* Istituto Nazionale di Geofisica e Storia Geofisica Ambiente.

G. Calcagnile; G.F. Panza (1981), *The main characteristics of the litosphere-astenosphere system in Italy and surrounding regions.* Pure and Appl. Geophys., **119,** 865-879.

G. Costa; G.F. Panza; I.M. Rotwain (1995), *Stability of premonitory seismicity pattern and intermediate-term earthquake prediction in central Italy.* Pageoph, **145,** 2, 259-275.

G. Costa; I.O. Stanishkova; G.F. Panza; I.M. Rotwain (1996), *Seismotectonic models and CN algorithm: the case of Italy.* Pageoph, **147**, 1, 1-12.

G. Costa; A. Peresan; I. Orozova; G.F. Panza; I.M. Rotwain (1996), *CN algorithm in Italy: intermediate-term earthquake prediction and seismotectonic model validation.* Proceedings of the 30th International Geological Congress, Vol. 5,1996. Beijing, China. In press.

B. Della Vedova; I. Marson; G.F. Panza; P. Suhadolc (1991), *Upper mantle properties of the Tuscan-Tyrrhenian Area: a key for understanding the recent tectonic evolution of the italian region.* Tectonophys, **195,** 311-318.

M. Dragoni; M. Bonafede; E. Boschi (1985), *On the interpretation of slow ground deformation precursory to the 1976 Friuli earthquake.* Pageoph., **122**, 784-792.

M. Dragoni (1988), *Aseismic propagation of dislocations:a model for tilt anomalies.* Proceedings National Meeting, National Research Council of Italy. ESA ed., Rome, 923-939.

A.M. Gabrielov; O.E. Dmitrieva; V.I. Keilis-Borok; V.G. Kossobokov; I.V. Kutznetsov; T.A. Levshina; K.M. Mirzoev; G.M. Molchan; S.Kh. Negmatullaev;

V.F. Pisarenko; A.G. Prozorov; W. Rinheart; I.M. Rotwain; P.N. Shelbalin; M.G. Shnirman; S.Yu Schreider (1986) - *Algorithms of long-term earthquakes' prediction.* International School for Research Oriented to Earthquake Prediction-algorithms, Software and Data Handling (Lima, Perù, 1986).

Y.Y. Kagan; L. Knopoff (1980) - *Spatial distribution of earthquakes: the two point correlation function.* Geophys. J. R. Astron. Soc., 62, 303-320.

V.I. Keilis-Borok (1996) - *Intermediate term earthquake prediction.* Proc. Natl. Acad Sci. USA, **93**, 3748-3755.

V.I. Keilis-Borok; L. Knopoff; I.M. Rotwain (1980) - *Bursts of aftershocks, long term precursors of strong earthquakes.* Nature, **283**, 259-263.

V.I. Keilis-Borok; I.V. Kutznetsov; G.F. Panza; I.M. Rotwain; G. Costa (1980) - *On intermediate-term earthquake prediction in Central Italy.* Pure and Appl. Geophys., **134**, 79-92.

V.I. Keilis-Borok; I.M. Rotwain (1990) - *Diagnosis of time of increased probability of strong earthquakes in different regions of the world: algorithm CN.* Phys. Earth Planet. Inter., **61**, 57-72.

ISC (1976-1990) - Bulletins of the International Seismological Centre, **13** (1)- **27** (3).

J. K. Lapajne; B. Sket Motnikar; P. Zupancic (1995) - *Delineation of seismic hazard areas in Slovenia. Seismic Zonation.* Proceeding of the 5th international conference on seismic zonation, 1995. Nice, France, **1**, 429-436.

I. Marson; G.F. Panza; P. Suhadolc (1995) - *Crust and upper mantle models along the active Tyrrhenian rim.* Terra Nova., **7**, 348-357.

C. Meletti; E. Patacca; P. Scandone (1995) - *Il sistema compressione-distensione in Appennino.* In G. Bonardi, B. De Vivo, P. Gasperini, A. Vallario (Eds.): "Cinquanta anni di attività didattica e scientifica del Prof. Felice Ippolito". Ed. Liguori - Napoli, 361-370.

G.M. Molchan (1990) - *Strategies in strong earthquake prediction.* Phys. of the Earth and Planet. Int., **61**, 84-98.

G.M. Molchan (1996) - *Earthquake prediction as a decision-making problem.* Pageoph., **147**, 1, 1-15.

G.M. Molchan; O.E. Dmitrieva (1992), *Aftershocks identification: methods and new approaches.* Geophys. J. Int., **190**, 501-516.

G.M. Molchan; T.L. Kronrod; O.E. Dmitrieva (1995) - *Statistical parameters of main shocks and aftershocks in the Italian region.* ICTP. Internal report.

G.M. Molchan; T.L. Kronrod; G.F. Panza (1996) - *Hazard oriented multiscale seismicity model: Italy.* International Centre for Theoretical Physics. Internal report IC/96/23. Trieste. Italy.

G.M. Molchan; T.L. Kronrod; G.F. Panza (1997) - *Multiscale seismicity model for seismic risk.* B.S.S.A.. In press.

S. Mueller (1982) - *Deep structure and recent dynamics in the Alps.* In *Mountain Building Process* (ed. K.J. Hsu). Academic Press, 181-199.

NEIC , *National Earthquake Information Center: Italy.* U.S.G.S. Denver, USA.

G.F. Panza; G. Calcagnile; P. Scandone; S. Mueller (1980) - *Struttura profonda dell'area mediterranea.* Le Scienze, **24**, 60-69.

G.F. Panza; A. Peresan; G.Costa (1997) - *Zone sismogenetiche e previsione a medio termine dei terremoti in Italia.* Il Quaternario. In press.

N. Pavoni; T. Ahjos; R. Freeman; S. Gregersen; H. Langer; G. Leydecker; Ph. Roth; P. Suhadolc; M. Uski (1992) - *Seismicity and focal mechanism.* In *A continent revealed - The European Geotraverse: Atlas of compiled data* (eds. R. Freeman and S. Mueller). Cambridge University Press, 14-19.

A. Peresan; G. Costa; F. Vaccari (1997) - *CCI1996: the Current Catalogue of Italy.* International Centre for Theoretical Physics. Internal report IC/IR/97/9. Trieste. Italy.

D. Postpischl (1980) - *Catalogo dei terremoti italiani dall'anno 1000 al 1980.* C.N.R.-Progetto Finalizzato Geodinamica.

D.V. Rundkvist; I.M. Rotwain (1994) - *Present-day geodynamics and seismicity of Asia Minor.* Computation of Seismology, **27**, 201-245.

P. Scandone; E. Patacca; C. Meletti; M. Bellatalla; N. Perilli; U. Santini (1990) - *Struttura geologica, evoluzione cinematica e schema sismotettonico della penisola italiana.* Atti del Convegno GNDT 1990, **1**, 119-135.

P. Scandone; E. Patacca; C. Meletti; M. Bellatalla; N. Perilli; U. Santini (1994) - *Seismotectonic zoning of the italian peninsula: revised version.* Working file NOV94.

D. L. Turcotte (1992), *Fractals and chaos in geology and geophysics.* Cambridge University Press.

I.A. Vorobieva; G.F. Panza (1993) - *Prediction of Occurrence of Related Strong Earthquakes in Italy.* Pageoph, **141**, 25-41.

S.N. Ward (1994) - *Constraints on the seismotectonics of the Central Mediterranean from Very Long Baseline Interferometry.* Geophys. J. Int., **117**, 441-452.

M. Zadro (1978) - *Use of tiltmeters for the detection of forerunning in seismic areas.* Boll. Geod: Sci. Aff., **37**, 597-618.

M. Zivcic; M. Poljak (1997) - *Seismogenetic areas of Slovenia.* Quantitative Seismic Zoning of the Circum Pannonian Region. QSEZ-CIPAR. Project CIPA CT 94-0238. Second year report.

FIGURE CAPTIONS.

Fig. 1 - Seismotectonic model of Italy (Scandone et al., 1994), revised version of the preliminary zoning described in Scandone et al. (1990).

Fig. 2a - Regionalization for Northern Italy, considering simply connected seismogenic zones: 1) first variant based on the seismotectonic model, including the whole Alpine Arc; 2) small region defined by Costa et al. (1996); 3) second variant, including the zone at the West of Garda's Lake (GZ); 4) third variant, excluding the GZ zone.

Fig. 2b - Regionalization for Northern Italy, considering also disconnected zones: 1) extended region defined by Costa et al. (1996); 2) first variant based on the seismotectonic model, including the transitional zone at the northern edge of the Appennines; 3) second variant, including the whole compressional band, but without the GZ zone; 4) third variant, including the GZ zone.

Fig. 2c - Regionalization for Northern Italy that takes into account the seismogenic zoning of the slovenian-croatian territory (Zivcic et al., 1997); the transition zones are included at both edges.

Fig. 3 - Preliminary seismogenic zoning of Slovenia and adjacent regions proposed by Zivcic et al. (1997); the areas extend beyond the margins of the map.

Fig. 4 - Diagram of the percentage of total TIPs versus the percentage of failures to predict ($\eta - \tau$ diagram) for the results obtained in Northern Italy for the different regions shown in fig. 2a, 2b and 2c. Some other variants (not shown in pictures) including or not the GZ zone have been considered. All the regions with GZ (zone at the west side of Garda's Lake) give unsatisfactory results. The diagonal line indicates the results of a random guess (Molchan, 1990).

Fig. 5 - 1) Regionalization for Central Italy defined by Costa et al. (1996); 2) region including the whole extensional band; 3) new region defined for Central Italy, including the transition zones at the edges.

Fig. 6 - Errors diagram for the results obtained in Central Italy considering the different regions shown in fig. 5.

Fig. 7 - 1) Region defined for Southern Italy by Costa et al. (1996); 2) region tested by Costa et al. (1995); 3) region defined following the seismotectonic model and including the foreland zones of Sicily; 4) region defined for Southern Italy, excluding all the foreland zones.

Fig. 8 - Diagram η-τ of the results, obtained using algorithm CN, for the different regions tested for Southern Italy and shown in fig. 7.

Fig. 9 - a) Map of the mainshocks (dots) and corresponding aftershocks (triangles) selected with the "minimax" method proposed by Molchan et al. (1995). Only events with at least 10 aftershocks and occurred in the period of time 1900-1993 are considered. The small box indicates the area shown in detail in part b) centered around the transitional zone corresponding to the Ortona-Roccamonfina line. Aftershocks evidence a connection only with the northward part of the extensional band, but not with its southward extension.

Fig. 10 - Diagrams of the TIPs obtained with the updated catalogue (up to 31 March 1997), over the regions defined for: a) Northern (fig. 2c-9), b) Central (fig. 5-3) and c) Southern Italy (fig. 6-4). The learning period is indicated in brackets, while the times of occurrence of a strong earthquake is indicated by a triangle with a number above, giving its magnitude. These diagrams corresponds to the results indicated in tables 1, 2 and 3, respectively.

TABLE CAPTIONS

Tab. 1 - Table of results obtained with the algorithm CN in Northern Italy, using the different regions represented in figures 2a, 2b and 2c. For regions 2 and 5 the catalogue PFGING has been used by Costa et al. (1996). The last line indicates results updated at July 1, 1997, whose corresponding TIPs diagram is shown in fig. 10-a.

Tab. 2 - Results obtained over the regions defined for Central Italy and shown in fig. 5. The first line indicates results given by Costa et al. (1996), using the PFGING catalogue. The diagram of TIPs for the updated catalogue and with the new region is shown in fig. 10-b.

Tab. 3 - Table of results given by the algorithm CN with the four variants of the Southern Region shown in fig. 7. The results given by Costa et al. (1996) for the regions 1 and 2 were obtained using the PFGING catalogue, including deep events and considering their maximum magnitude. Updated predictions (July 1, 1997) for the new region are represented with a TIPs diagram in fig. 10-c.

Northern Italy							
Region	Time	Learning Period	Mo	Events predicted	Failure to predict	TIPS %	False alarms
1	1960-1995	1964-1995	5.4	0	2	32.5	6
2*	1960-1994	1964-1994	5.4	2	0	34	2
3	1960-1995	1964-1995	5.4	1	1	35.1	4
4	1960-1995	1964-1995	5.4	2	0	28.8	2
5*	1960-1994	1964-1994	5.4	2	0	27	1
6	1960-1995	1964-1995	5.4	2	0	24.7	2
7	1960-1995	1964-1995	5.4	2	0	24.7	3
8	1960-1995	1964-1995	5.4	2	0	20.5	2
9	1960-1995	1964-1995	5.4	2	0	19.9	2
9**	1960-1997	1964-1995	5.4	2	0	19.3	2
* Catalogue: PFGING ** Updated Catalogue							

tab. 1

Central Italy							
Region	Time	Learning Period	Mo	Events predicted	Failure to predict	TIPS %	False alarms
1*	1950-1994	1950-1986	5.6	3	0	23	2
2	1950-1995	1950-1986	5.6	3	0	22.3	3
3	1950-1995	1950-1986	5.6	3	0	18.7	2
3**	1950-1997	1950-1986	5.6	3	0	18.4	2
* Catalogue: PFGING ** Updated Catalogue							

tab. 2

Southern Italy							
Region	Time	Learning Period	Mo	Events predicted	Failure to predict	TIPS %	False alarms
1*	1950-1994	1954-1994	6.5	3	0	33	5
2*	1950-1994	1954-1994	6.5	1	1	25	2
3	1948-1995	1952-1995	6.5	0	1	42.6	7
4	1950-1995	1954-1995	5.6	4	0	32.8	3
4**	1950-1997	1954-1995	5.6	4	0	32.7	3
* Magnitude=MAX Catalogue: PFGING Also deep events are included ** Updated Catalogue							

tab. 3

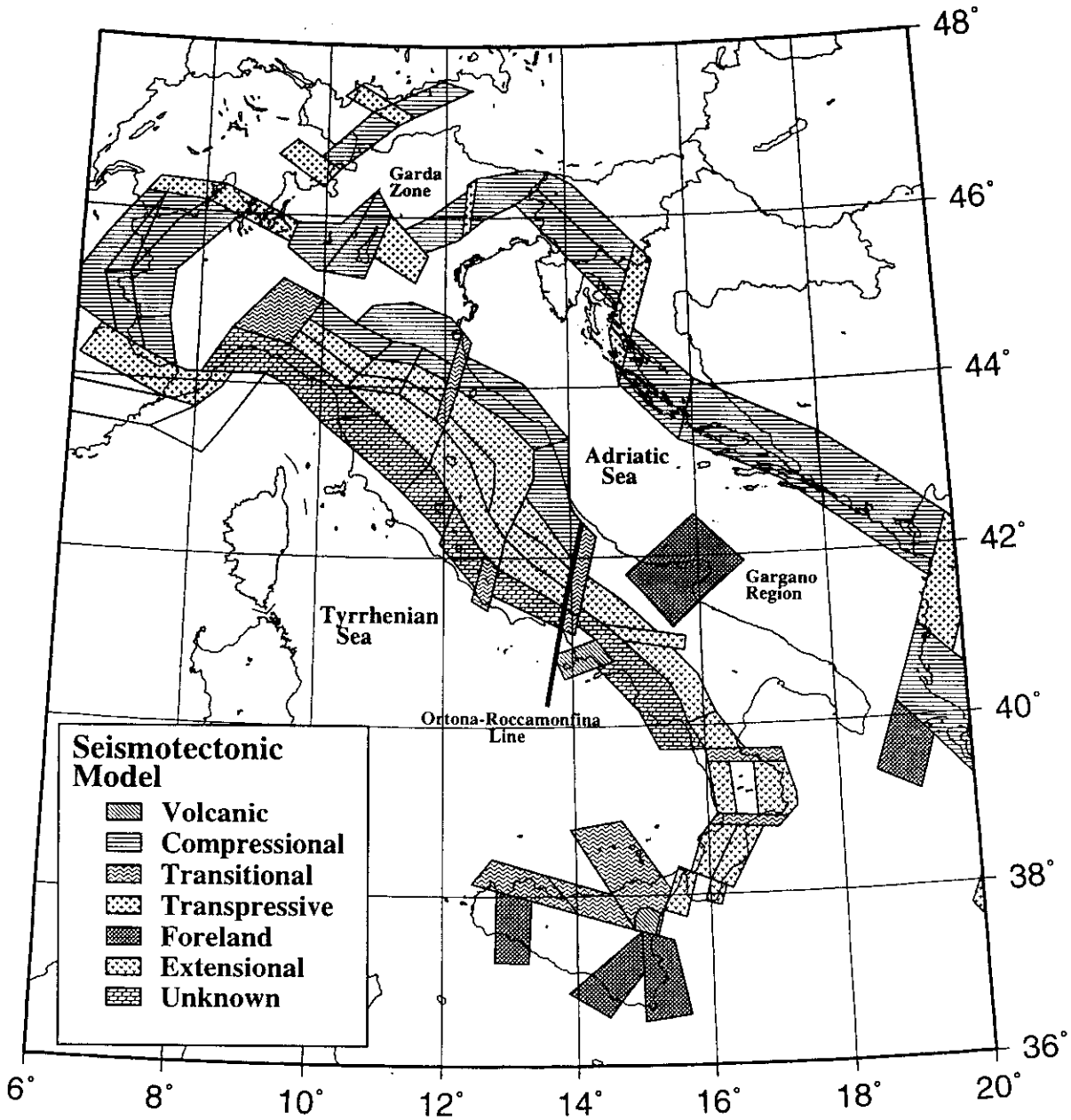
48°
46°
44°
42°
40°
38°
36°
6°
8°
10°
12°
14°
16°
18°
20°
Garda Zone
Adriatic Sea
Gargano Region
Tyrrhenian Sea
Ortona-Roccamonfina Line
Seismotectonic Model
Volcanic
Compressional
Transitional
Transpressive
Foreland
Extensional
Unknown

fig. 1

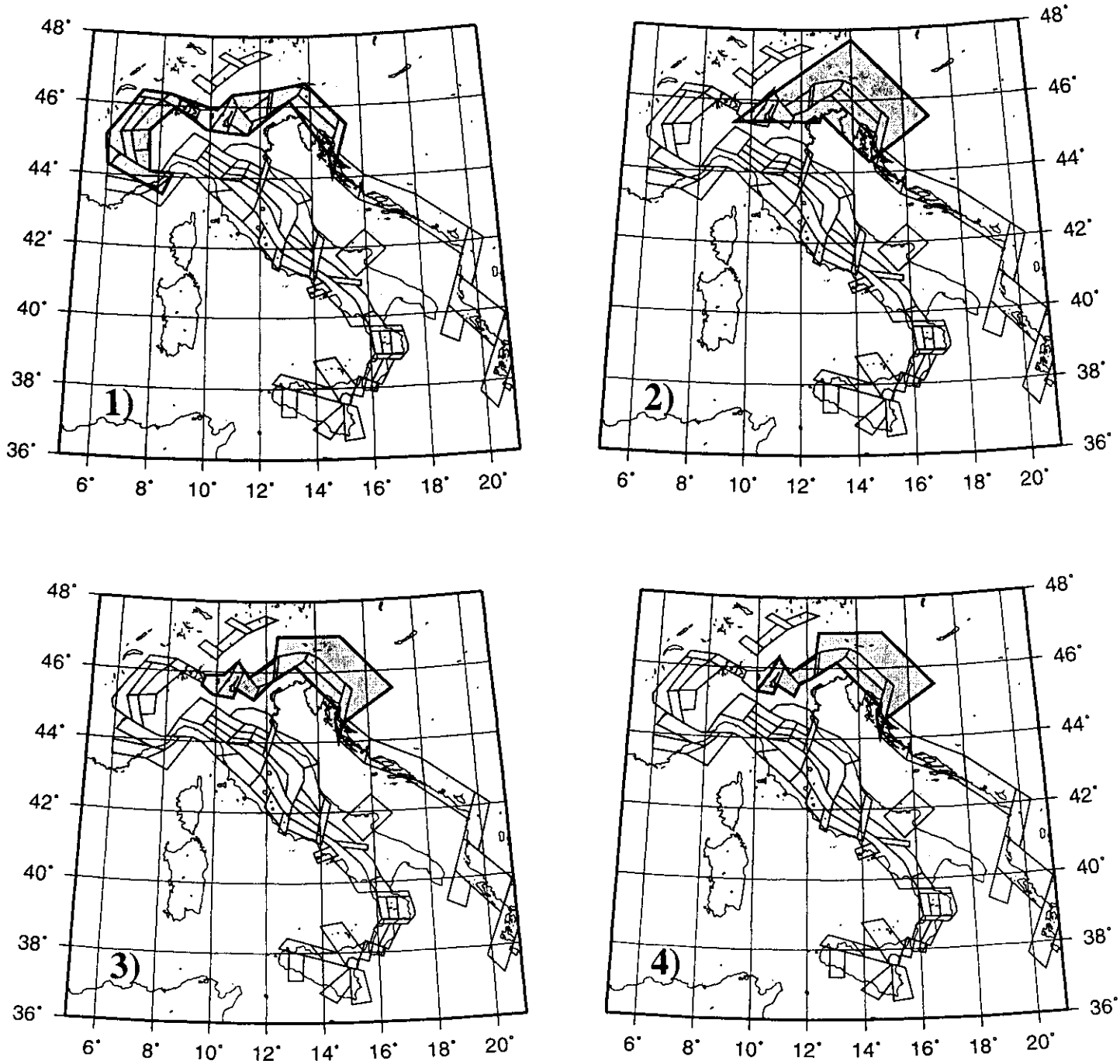

fig. 2a

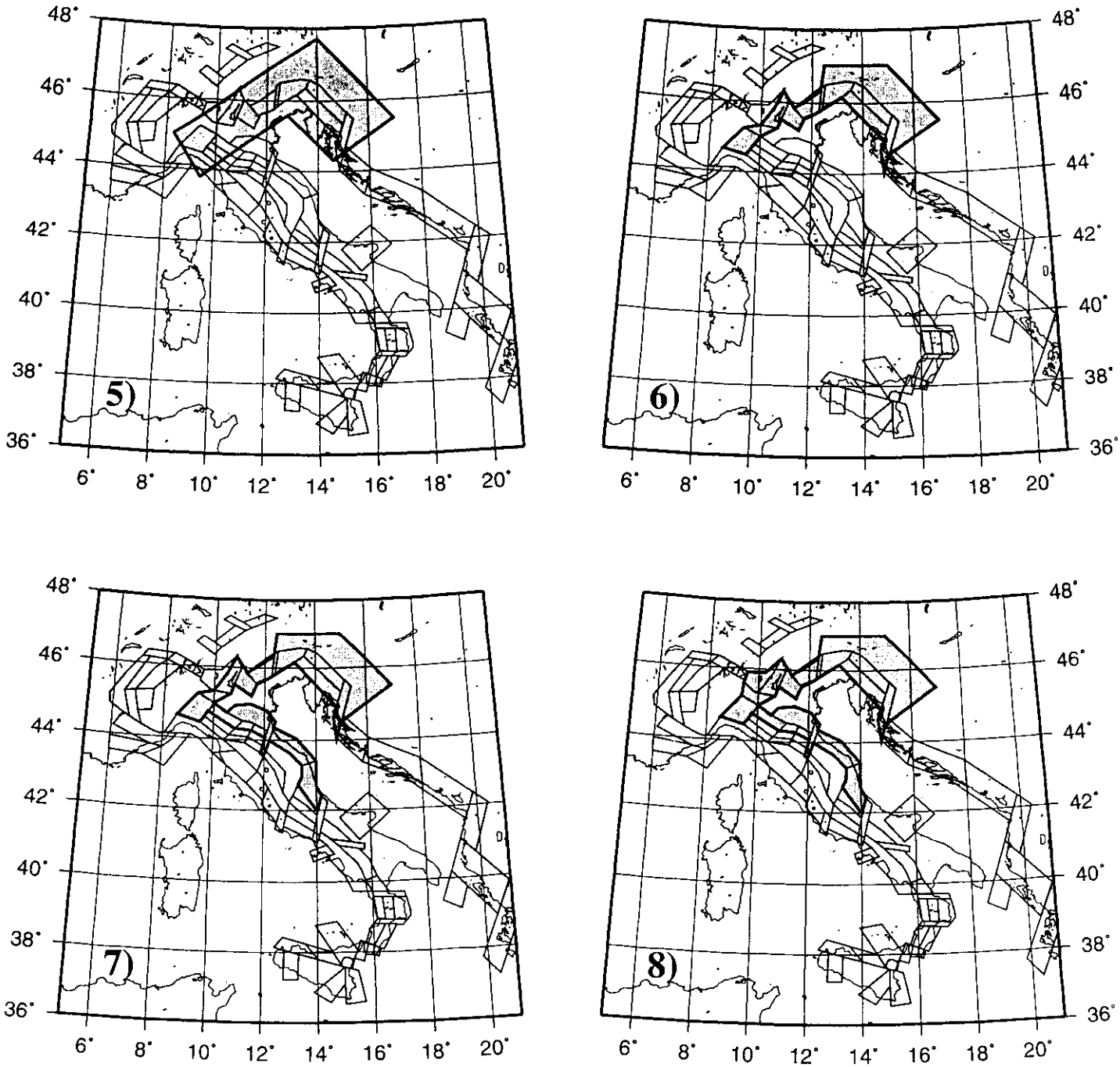

fig. 2b

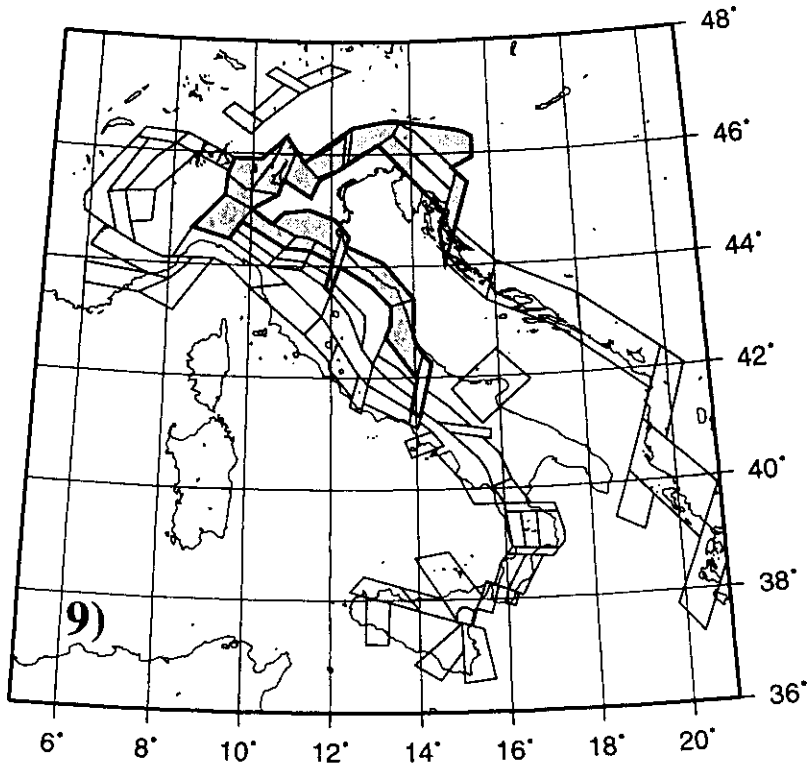
48°
46°
44°
42°
40°
38°
36°
6°
8°
10°
12°
14°
16°
18°
20°
9)

fig. 2c

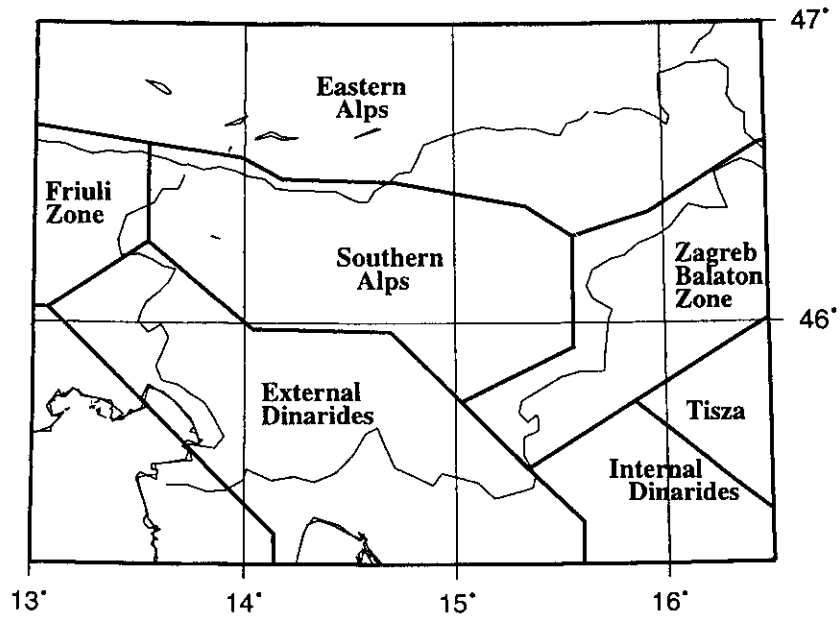
47°
46°
Eastern Alps
Friuli Zone
Southern Alps
Zagreb Balaton Zone
External Dinarides
Tisza
Internal Dinarides
13°
14°
15°
16°

fig. 3

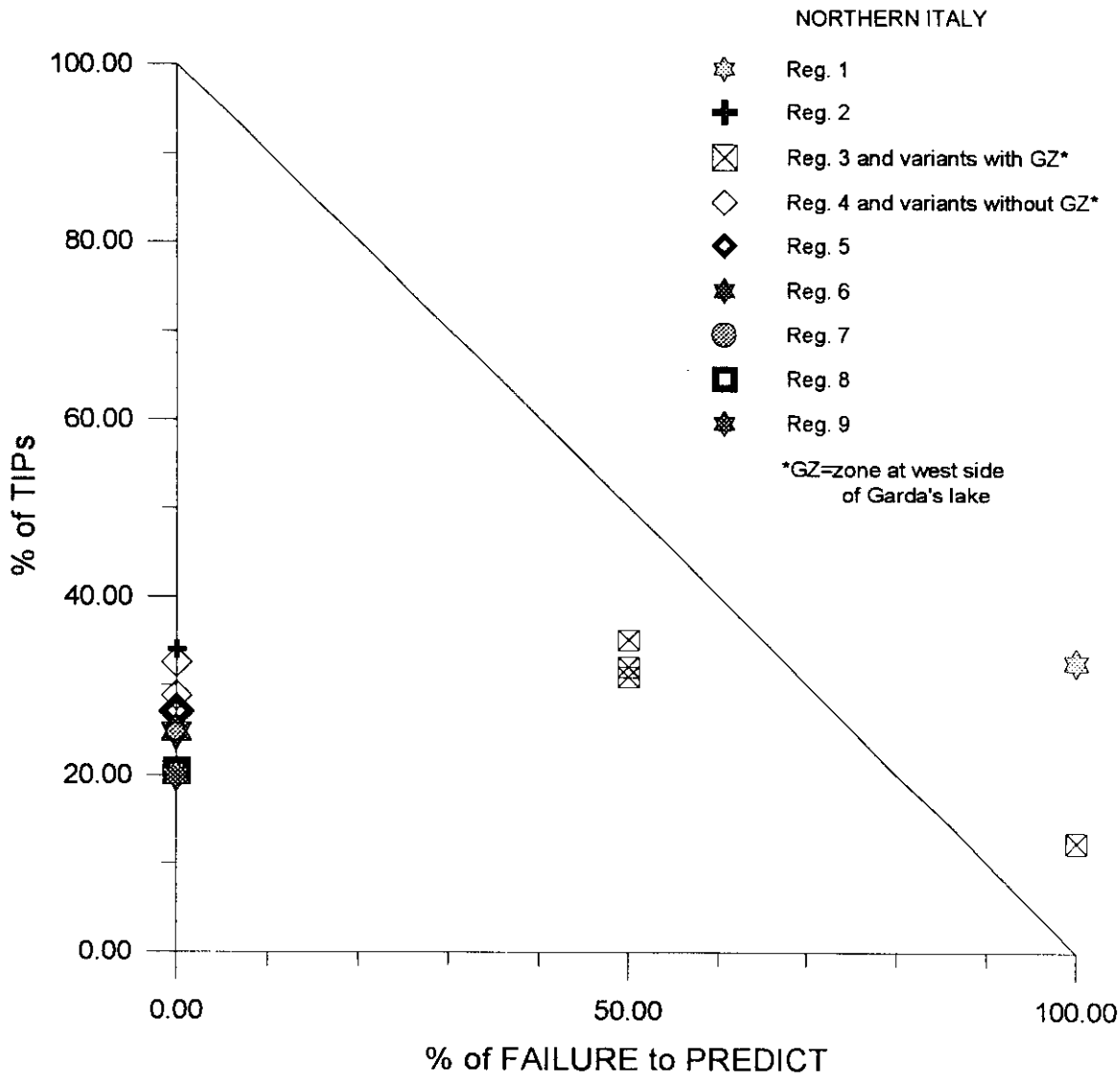
NORTHERN ITALY
Reg. 1
Reg. 2
Reg. 3 and variants with GZ*
Reg. 4 and variants without GZ*
Reg. 5
Reg. 6
Reg. 7
Reg. 8
Reg. 9
*GZ=zone at west side of Garda's lake
100.00
80.00
60.00
40.00
20.00
0.00
% of TIPs
0.00
50.00
100.00
% of FAILURE to PREDICT

fig. 4

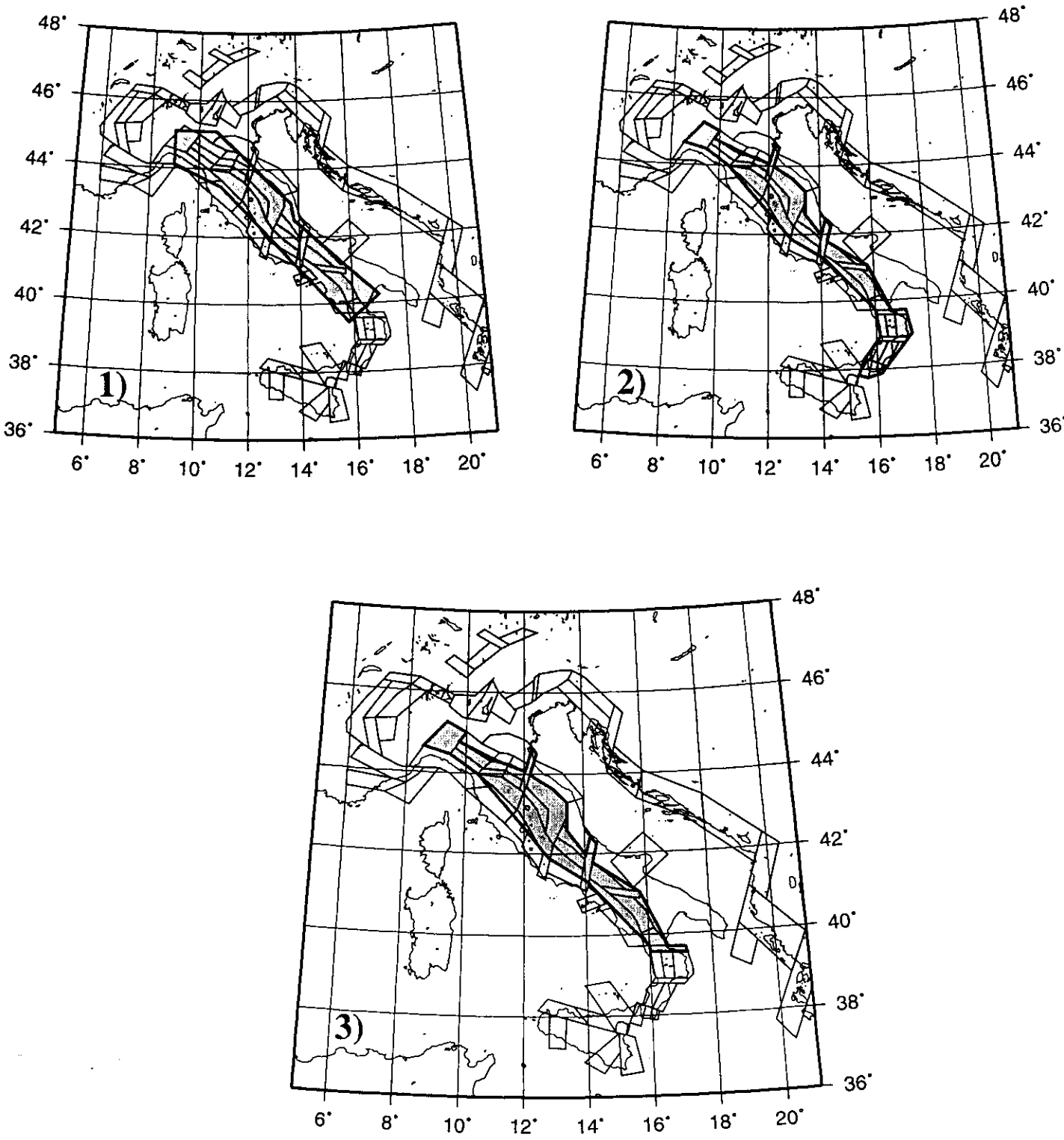

fig. 5

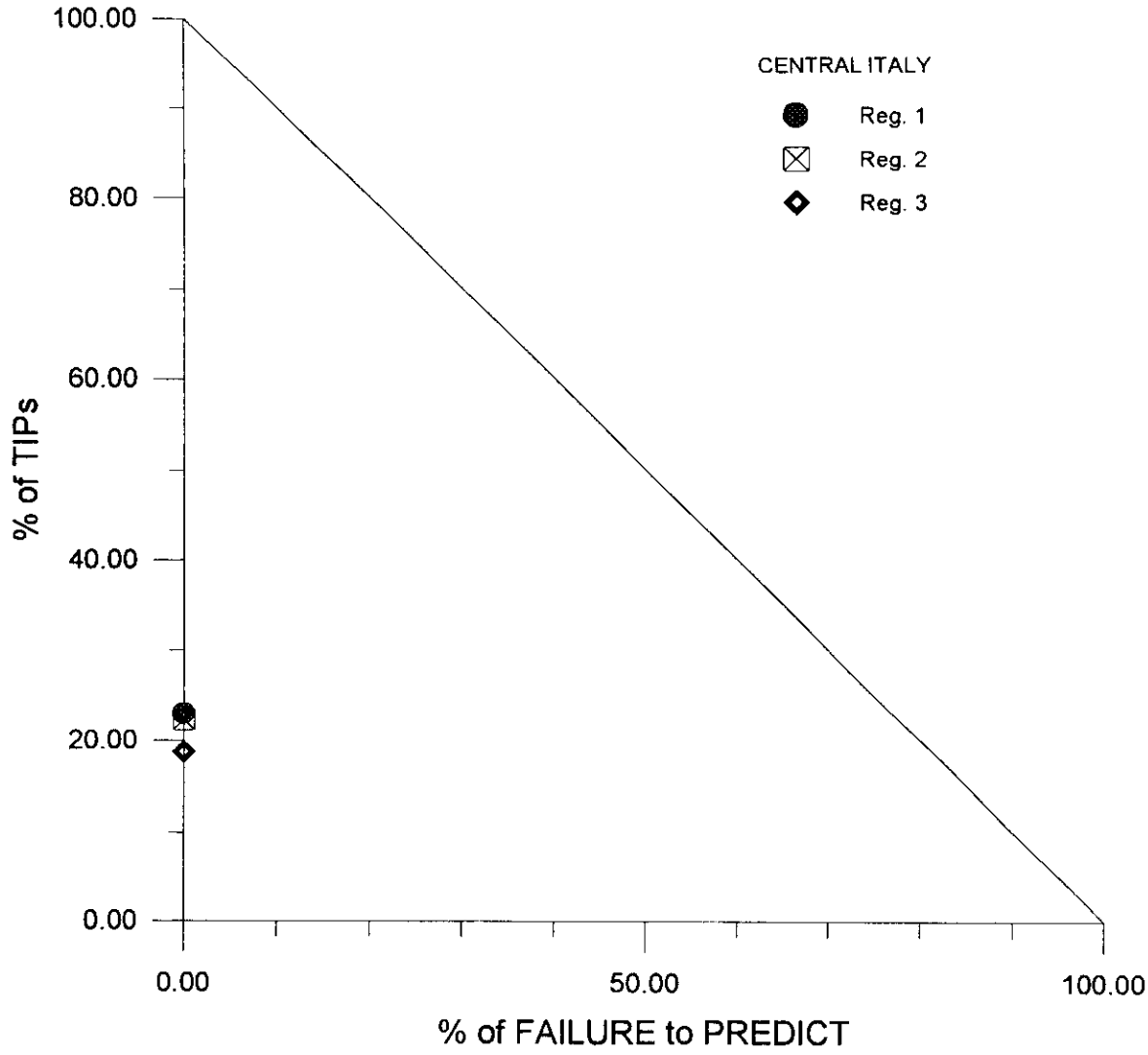
CENTRAL ITALY
Reg. 1
Reg. 2
Reg. 3
100.00
80.00
60.00
40.00
20.00
0.00
% of TIPs
0.00
50.00
100.00
% of FAILURE to PREDICT

fig. 6

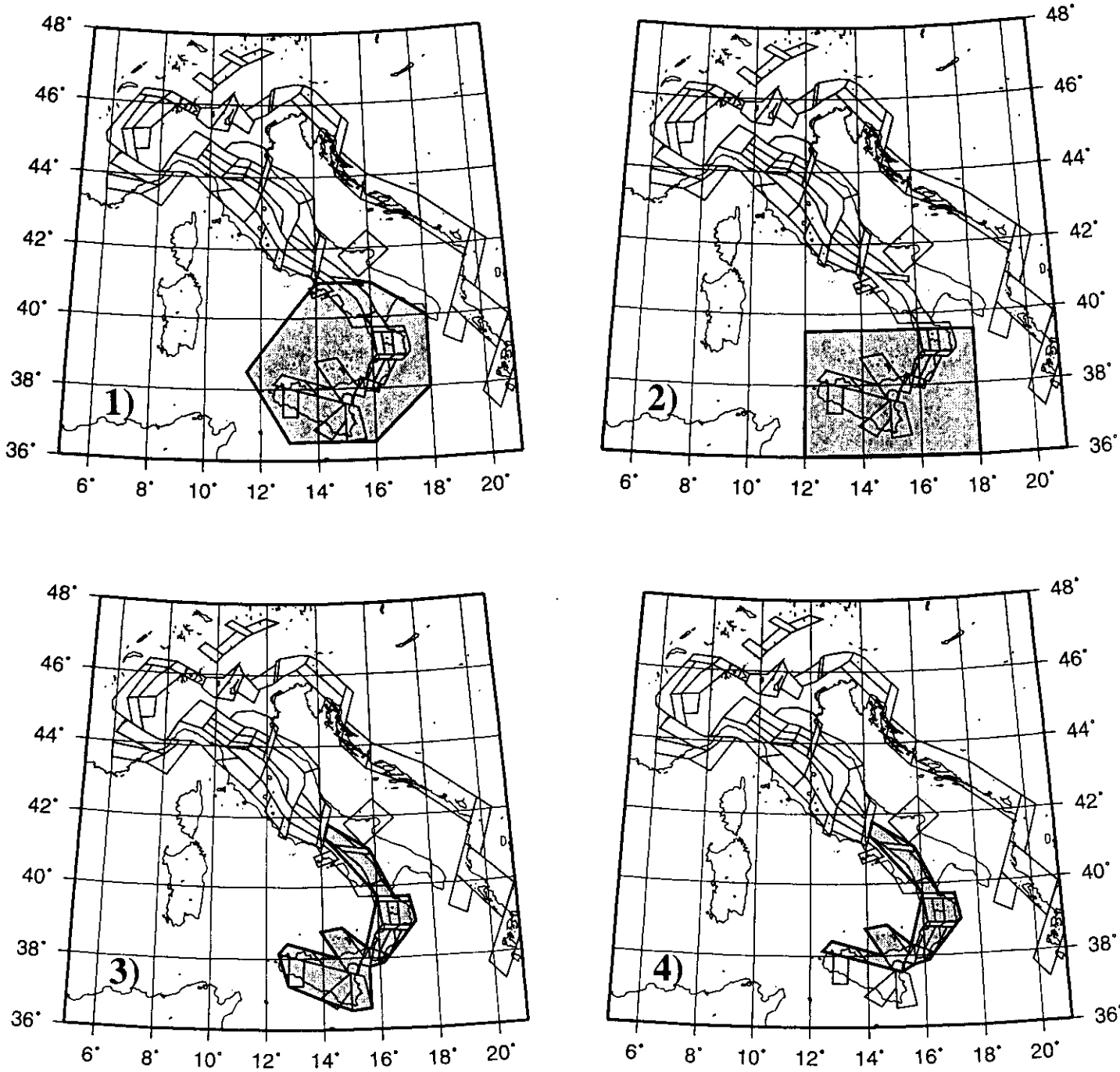

fig. 7

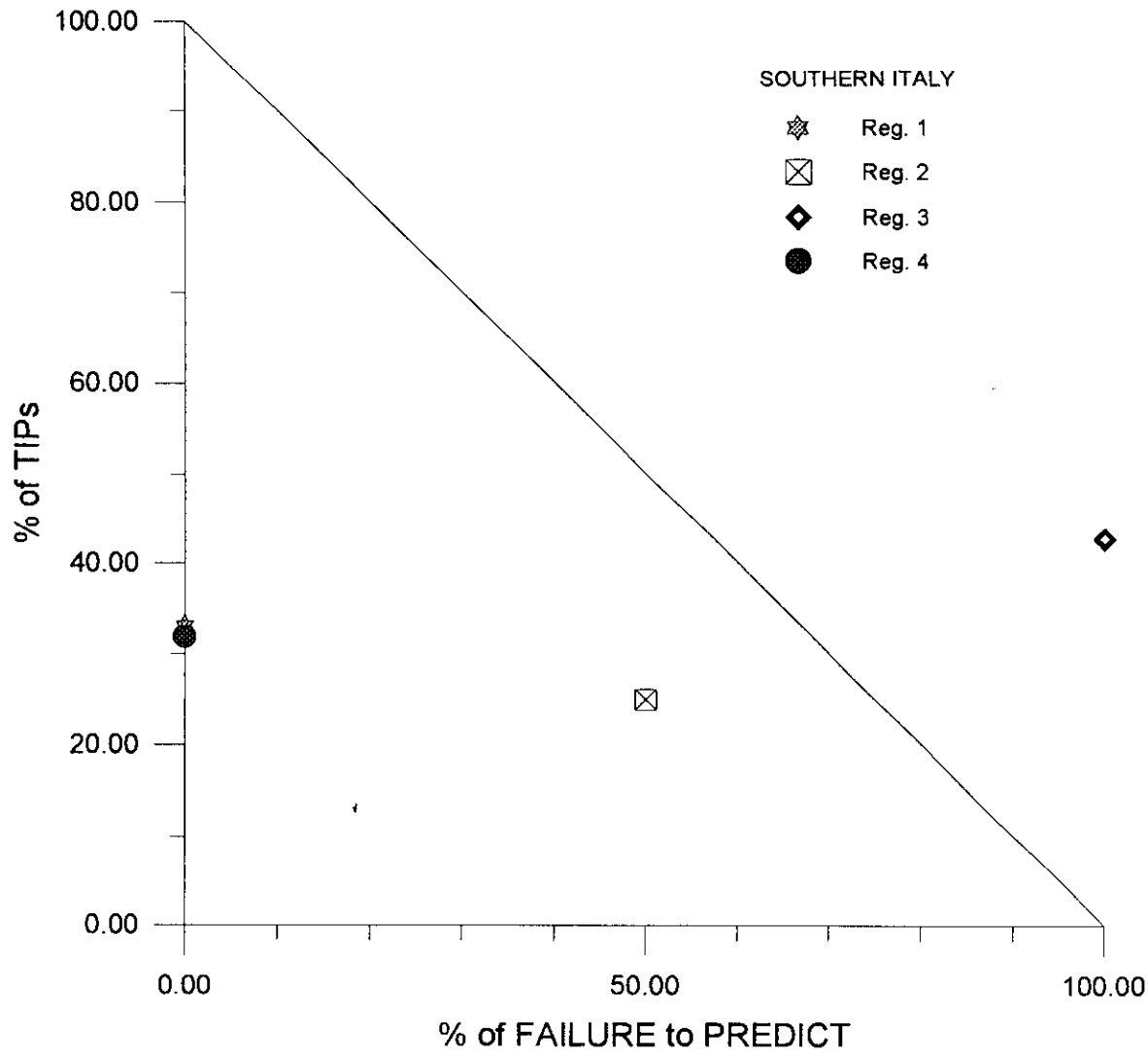
SOUTHERN ITALY
Reg. 1
Reg. 2
Reg. 3
Reg. 4
100.00
80.00
60.00
40.00
20.00
0.00
% of TIPs
0.00
50.00
100.00
% of FAILURE to PREDICT

fig. 8

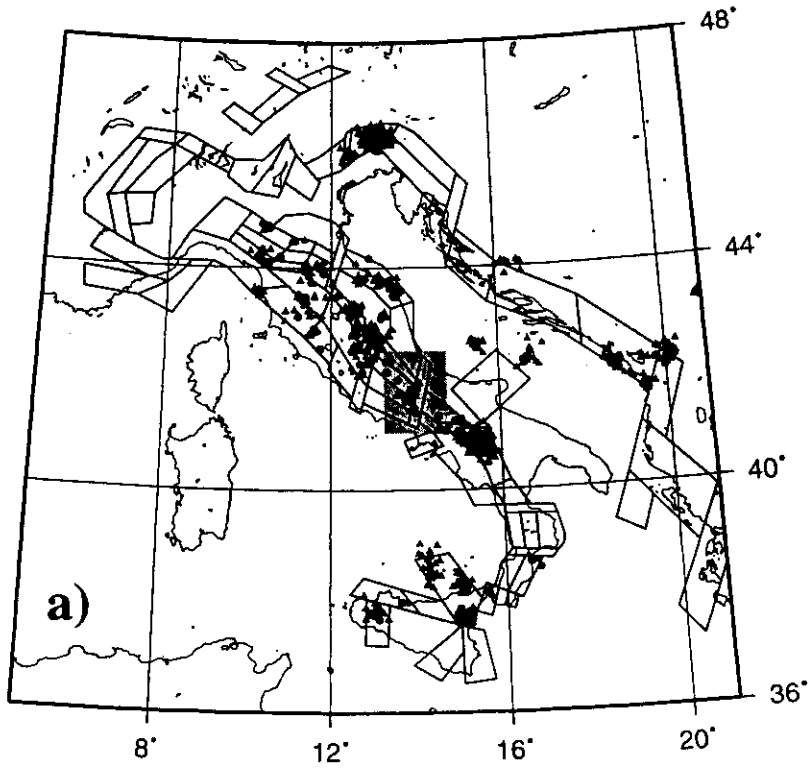

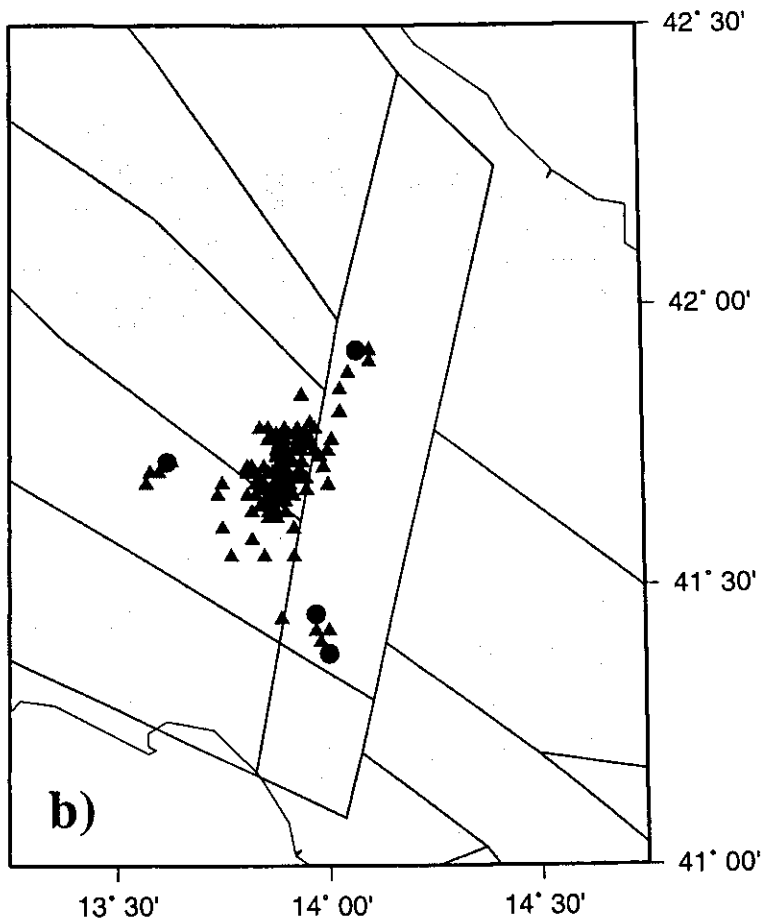

fig. 9

a)

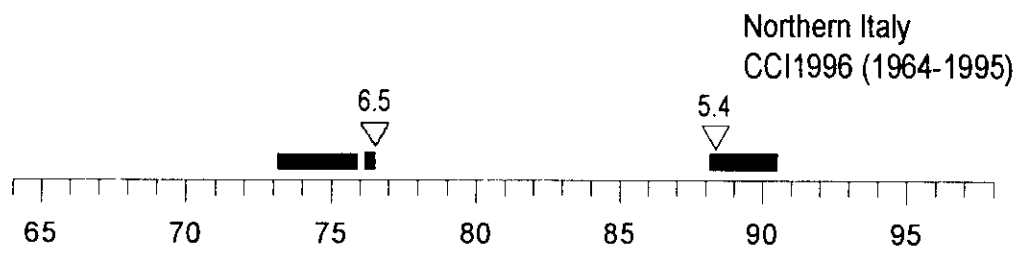
Northern Italy
CCI1996 (1964-1995)
6.5
5.4
65
70
75
80
85
90
95

b)

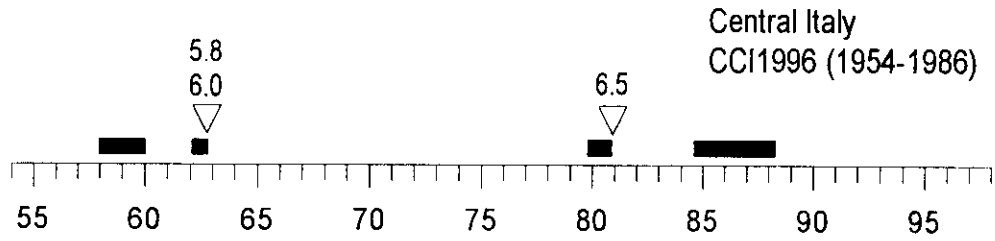
Central Italy
CCI1996 (1954-1986)
5.8
6.0
6.5
55
60
65
70
75
80
85
90
95

c)

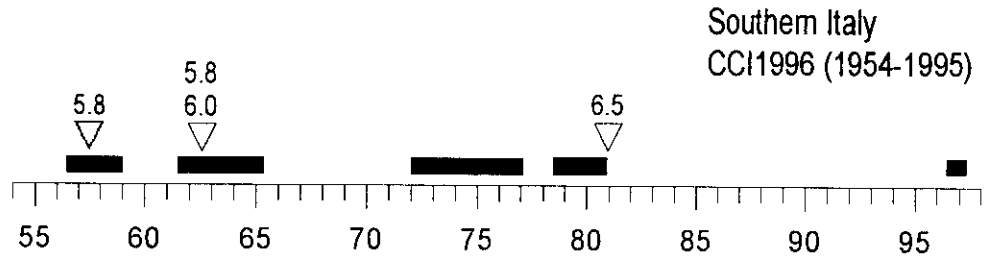
Southern Italy
CCI1996 (1954-1995)
5.8
5.8
6.0
6.5
55
60
65
70
75
80
85
90
95

fig. 10

PAGEOPH, Vol. 134, No. 1 (1990)

0033-4553/90/010079-14$1.50 + 0.20/0

On Intermediate-Term Earthquake Prediction in Central Italy

V. I. KEILIS-BOROK[1,3], I. V. KUZNETSOV[1,3], G. F. PANZA[2], I. M. ROTWAIN[1,3], and G. COSTA[2]

Abstract—The Time of Increased Probability (TIP) for the occurrence of a strong earthquake is determined in Central Italy. This is done with an algorithm that has been successfully applied in other regions of the world (algorithm CN, from the initials of California and Nevada, where the first diagnoses of TIPs were made). The use of normalized functions allows direct application of the orginal algorithm to the new region being studied, without any *ad hoc* adjustment of the parameters.

Retrospective analysis carried on until 1986 shows that TIPs occupy 26 percent of the total time considered and precede four out of five strong earthquakes. Forward monitoring indicates the possible existence of a TIP started in May 1988.

Several tests indicate that the results obtained are quite stable, even when using catalogues from different agencies. Apart from obvious practical interest, this research is essential for the worldwide investigation of self-similarity in the origin of strong earthquakes.

Key words: Seismology, earthquake prediction, self-similarity, algorithm CN, Central Italy.

1. Introduction

The algorithm is described in full detail by GABRIELOV *et al.* (1986) and KEILIS-BOROK *et al.* (1988) and has been applied for the first time to the California-Nevada (CN) region by ALLEN *et al.* (1983). Here, we consider the specific version described by KEILIS-BOROK *et al.* (1988). The algorithm CN is designed to diagnose the Time of Increased Probability of strong earthquake (TIP) from a set of traits of the earthquake's flow. The traits considered are the level of seismic activity (intensity of earthquakes flow), its variation in time, clustering of earthquakes in space and time and their concentration in space.

[1] International Institute of Earthquake Prediction Theory and Mathematical Geophysics, Academy of Sciences of the U.S.S.R., Warshavskoye, 79, K.2, 113556 Moscow, U.S.S.R.

[2] Universita degli Studi di Trieste, Istituto di Geodesia e Geofisica, Via dell'Universita, 7, 34123 Trieste, Italy.

[3] International Center for Earth and Environmental Sciences (ICS), 34100 Trieste Miramar.

Table 1

Function	Definition
SIGMA (t)	SIGMA $(t) = \Sigma\, 10^{\beta(M_i - \alpha)}$ The main shocks with $m_i \le M_i \le M_0 - 0.1$ and origin time $(t - 3$ years$) \le t_i \le t$ are included in summation; $\alpha = 4.5$, $\beta = 1.00$.
$S_{\max}(t)$	$S_{\max}(t) = \max\left\{\frac{S_1}{N_1}, \frac{S_2}{N_2}, \frac{S_3}{N_3}\right\}$, where S_j is calculated as SIGMA(t) for the events with the origin time $(t - j$ years$) \le t_i \le (t - (j-1)$ years$)$, and N_j is the number of earthquakes in the sum.
$Z_{\max}(t)$	$Z_{\max}(t) = \max\left\{\frac{Z_1}{N_1^{2/3}}, \frac{Z_2}{N_2^{2/3}}, \frac{Z_3}{N_3^{2/3}}\right\}$, where Z_j is calculated as S_j with $\beta = 0.5$, and N_j is the same as in the definition of $S_{\max}(t)$.
$N_2(t)$	The number of main shocks with $M \ge m_3$, which occurred in the time interval $(t - 3$ years, $t)$.
$N_3(t)$	The number of main shocks with $M \ge m_2$, which occurred in the time interval $(t - 10$ years, $t - 7$ years$)$.
$K(t)$	$K(t) = K_1 - K_2$, where K_1 is the number of main shocks with $M_1 \ge m_2$ and origin time $(t - 2 \cdot j$ years$) \le t_i \le (t - 2 \cdot (j-1)$ years$)$.
$B_{\max}(t)$	The largest number of aftershocks for the main shocks with $M_i \ge m_0 - 1.9$ and origin time within $((t - 3$ years$), t)$. Aftershocks are counted within a radius of 50 km for the first 2 days after the main shock and for $M > M_0 - 3.6$.
$G(t)$	$G(t) = 1 - P$, where P is the ratio of the number of the main shocks with $M_j \ge m_2$ to the number of the main shocks with $M_j \ge m_1$. Only main shocks with origin time $(t - 1$ year$) \le t_j \le t$ are considered.
$q(t)$	$q(t) = \sum_{j=1}^{6} \max\{0, 6a_2 - n_j\}$, where a_2 is the average annual number of main shocks with $M_1 \ge m_2$, n_j is the number of main shocks with $M_1 \ge m_2$ and origin time $(t - (8+j)$ years$) \le t_1 \le (t - (2+j)$ years$)$

For a given territory the traits are represented by certain functions of time defined in Table 1; these are computed, within a sliding time window, using the earthquakes contained in the catalogues. In the computations the aftershocks are not considered, but the number of aftershocks is included as one of the parameters ($B_{\max}$) characterizing a main shock. All functions depend upon magnitude (see Table 1). The first three functions are evaluated counting each earthquake with a weight proportional to the magnitude, while for the remaining six functions the earthquakes are counted with equal weight, independently of their individual magnitude.

The functions representing the traits are normalized so that these functions can be applied uniformly to territories with different sizes and seismicities. The introduction of normalization is also of obvious interest in connection with the possibility

of identifying self-similarity in the flow of earthquakes. The normalization is obtained by choosing three mangitude ranges, m_1, m_2, m_3. These ranges are defined by the condition that, in the territory analysed, the average annual number of earthquakes with $M \geq m_1$ (or m_2, or m_3) is equal to a constant, a_1 (or a_2, or a_3), common to all territories. In this way the intensities of flows of earthquakes are equalized. The values $a_1 = 3$, $a_2 = 1.4$ and $a_3 = 0.36$ were determined empirically for the California-Nevada territory, and will be used in this paper also.

At each time, within the territory being considered, the flow of the earthquakes is represented by the vector formed with the values of the different functions.

The problem of earthquake prediction can be formulated as follows: given the values of the functions at a given time t, determine whether the time interval $(t, t + \tau)$ belongs to a TIP of a main shock, or of a foreshock with magnitude M greater than a selected magnitude threshold M_0. For each territory the value of M_0 is chosen very close to the magnitude of the event with average return period of 5–7 years. The values of M_0 that have thus far been determined by GABRIELOV *et al.* (1986), DMITRIEVA *et al.* (1990), and KEILIS-BOROK *et al.* (1989) are in the range 4.5–7.5.

In our analysis of the flow of earthquakes, the time axis has been divided into intervals termed D, N and X. Intervals D extend for two years before each strong earthquake ($M \geq M_0$). Intervals X extend for three years after each strong earthquake; intervals of type X can become intervals of type D if a strong earthquake occurs within the three years. The remaining time intervals are termed N.

For a given region, the functions are discretized by defining the thresholds small, medium and large, on the basis of the quantiles levels 1/3 and 2/3. For all discretized functions, we estimate which combinations of the different functions are more typical for intervals D, and which for intervals N. These combinations, named characteristic features, were defined for the first time for California and Nevada by the method of pattern recognition (GELFAND *et al.*, 1976) with the purpose of predicting earthquakes having local magnitude $M_1 \geq 6.4$.

Table 1 shows the list of the selected functions, which are evaluated in the region under consideration. Following the procedure of pattern recognition, features D are defined by the condition that, in general, they occur during time intervals D, and not, during time intervals N. Features N are defined by the opposite condition. Each feature corresponds to a discretized value of the function, or to a combination of such values, for 2 or 3 functions.

The following rule was determined empirically by Keilis-Borok *et al.* (1989): a TIP is declared for one year at the time t if

$$n_D(t) - n_N(t) \geq V = 5 \tag{1}$$

$$\sigma(t) = 10^{-\beta(M_0-\alpha)}\Sigma 10^{\beta(M_i-\alpha)} < E = 4.9, \tag{2}$$

where

$$\beta = 1; \quad \alpha = 5; \quad M_i \geq M_0 - 1.4.$$

Here $n_D(t)$ is the number of characteristic features D that the flow of earthquakes has at the time t, and $n_N(t)$ is the number of the features of opposite kind N. The function $\sigma(t)$ is proportional to the total seismic energy released in the whole region within a period of 3 years before time t, and normalized by the seismic energy of an earthquake of magnitude M_0. The TIP during which a strong earthquake does not occur is defined, in this context, a false alarm. Consecutive TIPs may overlap and therefore give rise to alarm periods longer than one year. TIPs are interrupted if $\sigma(t) > E$, therefore false-alarm durations may be shorter than one year. A strong earthquake that occurs outside the TIPs is termed a "failure to predict".

The algorithm is formulated in a normalized manner; therefore, it can be transferred from one territory to another without additional retrofitting of parameters. In each territory only boundaries and the value of M_0 are defined with some degree of freedom.

The algorithm has been successfully applied to several regions: Central Asia, Caucasus, Western Turkmenia, Kamchatka and Kuril Islands, Eastern-Carpathians, Belgium, Cocos plate, Gulf of California, and Northern-Appalachians (GABRIELOV *et al.*, 1986; DMITRIEVA *et al.*, 1990; KEILIS-BOROK *et al.*, 1989). The results can be summarized as follows: on a worldwide scale, TIPs precede 27 out of 34 strong earthquakes and, in different regions, occupy, on the average, about 24 percent of the time interval analyzed.

For the Italian territory, clustering has been analysed by BOTTARI and NERI (1983). Only earthquake prediction based on clustering has been considered by CAPUTO *et al.* (1983) and CAPUTO (1983). Here we apply the CN algorithm for intermediate-term earthquake prediction in Central Italy.

2. Earthquake Statistics

The algorithm CN has been applied to the catalogues ENEL, CSEM, ING and PFG. In a first step we used the data until 1986, taken from ENEL, CSEM and ING. Events contained in CSEM but not present in ENEL or ING were included in the list of events used in this paper. Furthermore as far as magnitude is concerned M_l (local magnitude) has been used whenever available. If M_l is not available M_s (surface waves magnitude) from CSEM is used; if even M_s is not available we used M_b (body waves magnitude) from CSEM; for the events for which even M_b is not available we used M_d (coda magnitude) from ING. Initially we analysed the whole Italian territory. Tables 2–4 are constructed from ENEL, CSEM and ING and show the distribution of earthquakes versus magnitude and time, for different parts: Northern (lat. 48–45 N), Central (lat. 45–39.5 N) and Southern (lat. 39.5–35 N). The completeness of the catalogue we have constructed for these parts is quite different. For Central Italy it is reasonable to assume that our catalogue is sufficiently complete for magnitude greater than 4.0, after 1950.

Table 2

Distribution of earthquakes in magnitude and time (Northern Italy)

Year	0	Magnitude ≥ 3.0	3.1	3.2	3.3	3.4	3.5	4.0	4.5	5.0	5.5	6.0
1940	10	·	·	·	·	·	·	·	·	·	·	·
1941	1	·	·	·	·	·	·	·	·	·	·	·
1942	8	1	1	1	1	1	1	·	·	·	·	·
1943	21	4	4	4	4	4	4	4	3	·	·	·
1944	2	·	·	·	·	·	·	·	·	·	·	·
1945	3	1	1	1	1	1	1	1	1	·	·	·
1946	3	·	·	·	·	·	·	·	·	·	·	·
1947	10	1	1	1	1	1	1	1	·	·	·	·
1948	15	·	·	·	·	·	·	·	·	·	·	·
1949	29	2	2	2	2	2	2	2	1	·	·	·
1950	6	·	·	·	·	·	·	·	·	·	·	·
1951	8	3	3	3	3	3	3	3	1	·	·	·
1952	8	1	1	1	1	1	1	1	·	·	·	·
1953	2	1	1	1	1	1	1	·	·	·	·	·
1954	11	2	2	2	2	2	2	1	1	·	·	·
1955	15	1	1	1	1	1	1	1	·	·	·	·
1956	7	1	1	1	1	1	1	1	1	·	·	·
1957	10	·	·	·	·	·	·	·	·	·	·	·
1958	9	·	·	·	·	·	·	·	·	·	·	·
1959	17	3	3	3	3	3	3	3	2	·	·	·
1960	41	4	4	4	4	4	4	4	2	·	·	·
1961	17	·	·	·	·	·	·	·	·	·	·	·
1962	7	·	·	·	·	·	·	·	·	·	·	·
1963	16	1	1	1	1	1	1	·	·	·	·	·
1964	30	·	·	·	·	·	·	·	·	·	·	·
1965	18	·	·	·	·	·	·	·	·	·	·	·
1966	30	1	1	1	1	1	1	·	·	·	·	·
1967	25	2	2	2	2	2	1	1	1	·	·	·
1968	30	3	3	3	3	3	3	2	2	·	·	·
1969	17	2	2	2	2	2	2	1	·	·	·	·
1970	13	4	4	4	4	4	4	1	·	·	·	·
1971	29	8	8	8	8	8	7	2	·	·	·	·
1972	18	1	1	1	1	1	1	·	·	·	·	·
1973	14	4	4	4	4	4	3	2	·	·	·	·
1974	14	3	3	3	3	3	3	1	·	·	·	·
1975	7	5	5	5	5	5	4	3	1	·	·	·
1976	628	174	174	174	174	174	154	61	21	11	5	3
1977	117	30	30	30	30	30	18	8	2	1	1	·
1978	56	26	26	26	26	23	19	6	1	·	·	·
1979	62	20	20	20	20	19	17	6	3	·	·	·
1980	62	12	12	12	12	9	8	4	1	1	·	·
1981	45	17	17	17	17	12	10	3	1	·	·	·
1982	54	15	15	15	15	12	10	2	·	·	·	·
1983	67	19	19	19	19	17	12	7	3	·	·	·
1984	59	18	18	18	18	17	15	3	1	·	·	·
1985	61	11	11	11	11	9	6	1	·	·	·	·
1986	151	34	29	24	20	16	12	4	2	·	·	·
1987	155	29	18	11	9	4	4	2	·	·	·	·
1988	182	23	20	15	9	7	6	3	2	1	·	·
1989	109	7	6	3	3	3	3	·	·	·	·	·

Table 3

Distribution of earthquakes in magnitude and time (Central Italy)

Year	Magnitude ≥ 0	0.3	3.1	3.2	3.3	3.4	3.5	4.0	4.5	5.0	5.5	6.0
1940	107	6	6	6	6	6	6	6	2	·	·	·
1941	191	4	4	4	4	4	4	4	2	1	·	·
1942	59	·	·	·	·	·	·	·	·	·	·	·
1943	52	5	5	5	5	5	5	4	2	·	·	·
1944	2	2	2	2	·	·	·	·	·	·	·	·
1945	7	4	4	4	4	4	4	4	2	1	·	·
1946	9	2	2	2	2	2	2	2	·	·	·	·
1947	40	6	6	6	5	5	5	5	3	1	·	·
1948	45	7	7	7	6	6	6	6	5	1	·	·
1949	54	4	4	4	3	3	3	2	·	·	·	·
1950	52	5	5	5	5	5	5	4	3	1	·	·
1951	34	10	10	10	10	10	10	10	4	1	·	·
1952	17	8	8	8	8	8	8	6	·	·	·	·
1953	26	9	9	9	9	9	7	4	·	·	·	·
1954	17	4	4	4	4	4	4	2	2	·	·	·
1955	49	12	12	12	10	10	10	6	2	1	·	·
1956	96	17	17	17	16	16	16	10	4	1	·	·
1957	105	21	21	21	19	19	19	12	5	·	·	·
1958	61	6	6	6	3	3	3	3	1	1	·	·
1959	89	6	6	6	6	6	6	5	3	1	1	·
1960	82	21	21	19	17	13	10	3	·	·	·	·
1961	74	26	26	26	25	25	25	16	9	·	·	·
1962	83	28	28	27	26	25	24	16	6	4	3	1
1963	137	48	48	43	39	35	32	17	6	4	2	·
1964	86	18	18	18	14	14	14	10	4	1	·	·
1965	69	35	35	34	34	32	29	15	4	·	·	·
1966	63	16	16	16	10	9	9	6	·	·	·	·
1967	56	19	19	17	15	15	14	11	5	1	1	·
1968	60	29	29	27	24	21	16	9	1	·	·	·
1969	71	32	32	27	26	24	24	12	3	·	·	·
1970	113	39	39	37	34	32	26	13	1	·	·	·
1971	329	80	74	68	60	57	50	21	6	1	·	·
1972	355	183	144	129	112	76	52	25	5	2	·	·
1973	165	31	30	27	25	22	20	13	1	·	·	·
1974	208	74	67	61	53	50	44	16	3	1	·	·
1975	104	32	29	28	25	18	13	4	2	·	·	·
1976	137	61	49	49	41	39	36	14	5	2	·	·
1977	211	89	56	55	42	39	34	17	3	·	·	·
1978	108	81	66	65	46	45	38	14	5	·	·	·
1979	465	234	142	142	91	88	75	19	5	2	1	·
1980	745	234	213	185	159	141	120	60	24	6	1	1
1981	283	116	86	67	58	54	46	14	4	·	·	·
1982	185	95	83	74	68	57	49	18	5	1	·	·
1983	88	64	56	46	41	31	29	10	4	2	1	·
1984	211	143	134	127	107	98	84	33	8	4	3	·
1985	120	79	71	58	53	43	36	10	2	2	·	·
1986	1247	193	154	120	92	67	57	17	4	·	·	·
1987	879	106	85	64	53	43	34	13	2	·	·	·
1988	971	66	49	44	36	30	22	8	2	1	·	·
1989	634	21	16	15	13	11	7	2	·	·	·	·

Table 4

Distribution of earthquakes in magnitude and time (Southern Italy)

Year	Magnitude ≥ 0	3.0	3.1	3.2	3.3	3.4	3.5	4.0	4.5	5.0	5.5	6.0
1940	7	2	2	2	2	2	2	2	2	.	.	.
1941	20	1	1	1	1	1	1	1	1	1	1	1
1942	5	1	1	1	1	1	1	1	.	.	.	.
1943	3	1	1	1	1	1	1	1	.	.	.	.
1944	.	.	.	.	.	.	.	.	.	.	.	.
1945	1	.	.	.	.	.	.	.	.	.	.	.
1946	6	.	.	.	.	.	.	.	.	.	.	.
1947	67	.	.	.	.	.	.	.	.	.	.	.
1948	7	.	.	.	.	.	.	.	.	.	.	.
1949	41	1	1	1	1	1	1	1	1	1	1	.
1950	41	5	5	5	5	5	5	3	1	1	.	.
1951	4	.	.	.	.	.	.	.	.	.	.	.
1952	22	5	5	5	5	5	4	1	.	.	.	.
1953	8	3	3	3	3	3	3	1	.	.	.	.
1954	26	5	5	5	5	5	5	4	2	1	.	.
1955	38	1	1	1	1	1	1	.	.	.	.	.
1956	4	2	2	2	2	2	2	1	.	.	.	.
1957	18	3	3	3	3	3	3	2	2	2	1	.
1958	7	.	.	.	.	.	.	.	.	.	.	.
1959	17	3	3	3	2	2	2	1	1	1	1	.
1960	12	2	2	2	2	2	2	.	.	.	.	.
1961	7	5	5	4	4	2	1	1	1	1	.	.
1962	6	.	.	.	.	.	.	.	.	.	.	.
1963	9	1	1	1	1	1	1	1	.	.	.	.
1964	2	.	.	.	.	.	.	.	.	.	.	.
1965	7	2	2	2	2	2	2	2	1	.	.	.
1966	5	.	.	.	.	.	.	.	.	.	.	.
1967	7	4	4	4	4	3	3	3	3	1	.	.
1968	177	144	144	137	124	101	94	44	15	6	5	1
1969	22	5	5	5	5	5	5	1	.	.	.	.
1970	16	2	2	2	1	1	1	1	1	.	.	.
1971	21	4	4	4	4	4	4	3	1	.	.	.
1972	23	1	1	1	1	1	1	1	.	.	.	.
1973	10	1	1	1	1	1	1	1	1	.	.	.
1974	40	20	19	19	18	16	15	7	1	.	.	.
1975	12	4	4	4	4	4	3	1	.	.	.	.
1976	29	14	13	13	12	12	12	6	.	.	.	.
1977	28	17	16	16	15	15	15	8	3	1	.	.
1978	153	86	72	72	61	61	55	18	3	2	2	.
1979	107	54	34	34	23	23	21	6	1	1	.	.
1980	82	56	55	52	50	47	39	14	4	3	1	.
1981	36	30	27	27	26	25	21	14	5	1	.	.
1982	37	18	14	14	14	13	11	1	.	.	.	.
1983	13	13	13	13	13	13	13	7	3	1	1	1
1985	17	14	14	13	13	13	11	8	2	.	.	.
1986	288	80	64	47	34	22	14	1	.	.	.	.
1987	208	26	18	15	8	5	4	2	1	.	.	.
1988	375	15	12	11	6	4	3	.	.	.	.	.
1989	302	12	9	7	6	5	4	.	.	.	.	.

For the Northern and Southern parts a sufficient degree of completeness can be seen only after 1976. Our definition of sufficient completeness is justified by the fact that all functions, with the exception of $B_{\max}(t)$, depend upon events with magnitude greater than m_1. This threshold, on the basis of the flow of earthquakes, deduced from catalogues ENEL, CSEM, ING, has been estimated to be equal to 4.4. The function $B_{\max}(t)$ depends on events with magnitude greater than $M_0 - 3.6$. In its definition, therefore, it is also necessary to use events with relatively small magnitudes.

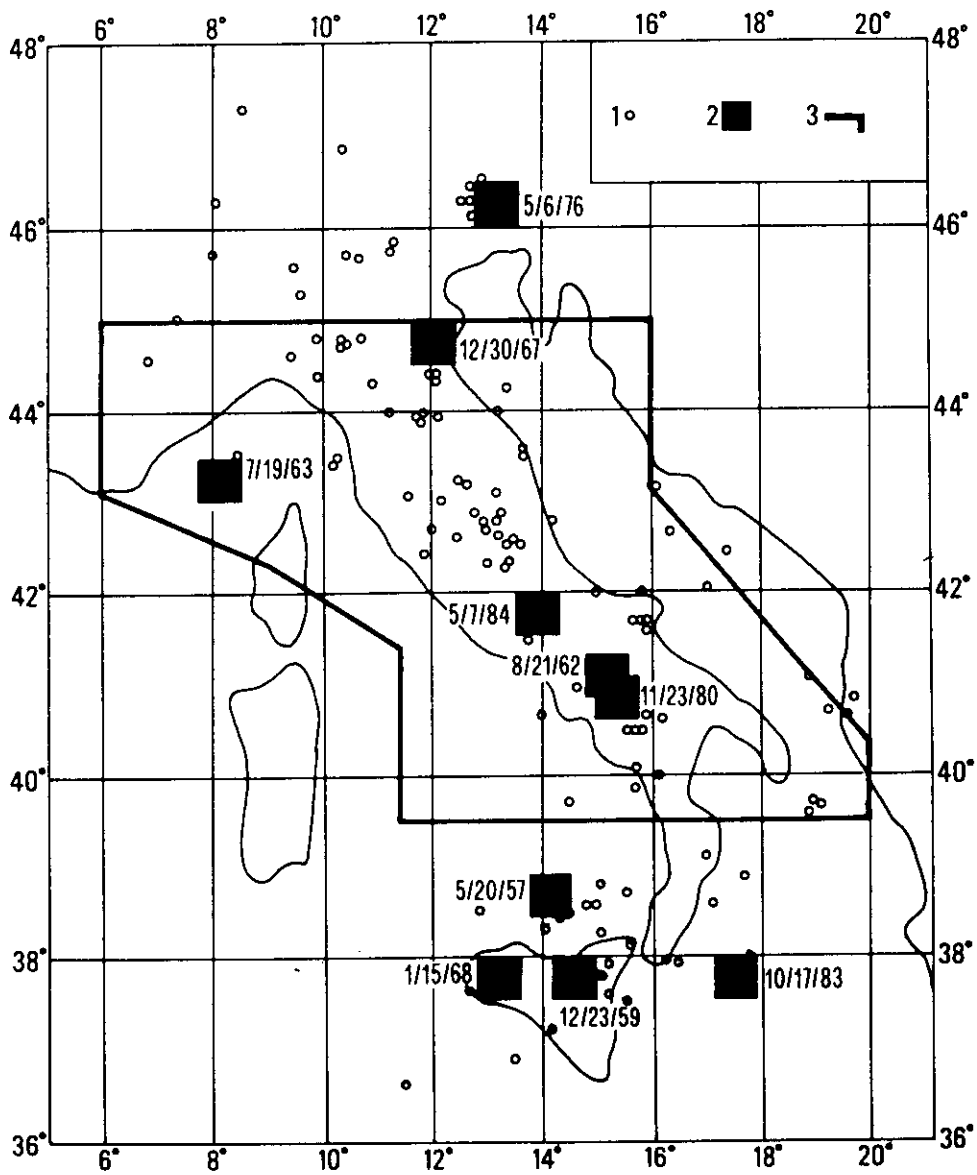

Figure 1
Epicenters of earthquakes recorded in the period 1950–1985 [9, 10, 11]; 1—epicenters of earthquakes with $M \geq 4.5$; 2—epicenters of earthquakes with $M \geq 5.6$ identified by their date of occurrence; 3—boundary of selected region (Central Italy).

On the basis of this preliminary analysis we decided to test the algorithm for Central Italy. The boundaries of the territory considered are shown in Figure 1 as thick solid lines and have been drawn on the basis of the spatial distribution of epicenters, and the scheme of morphostructural zonation (CAPUTO *et al.*, 1980). The region chosen includes the zone along which there is interaction between different lithospheric blocks (Figure 2) as outlined by surface wave dispersion analysis

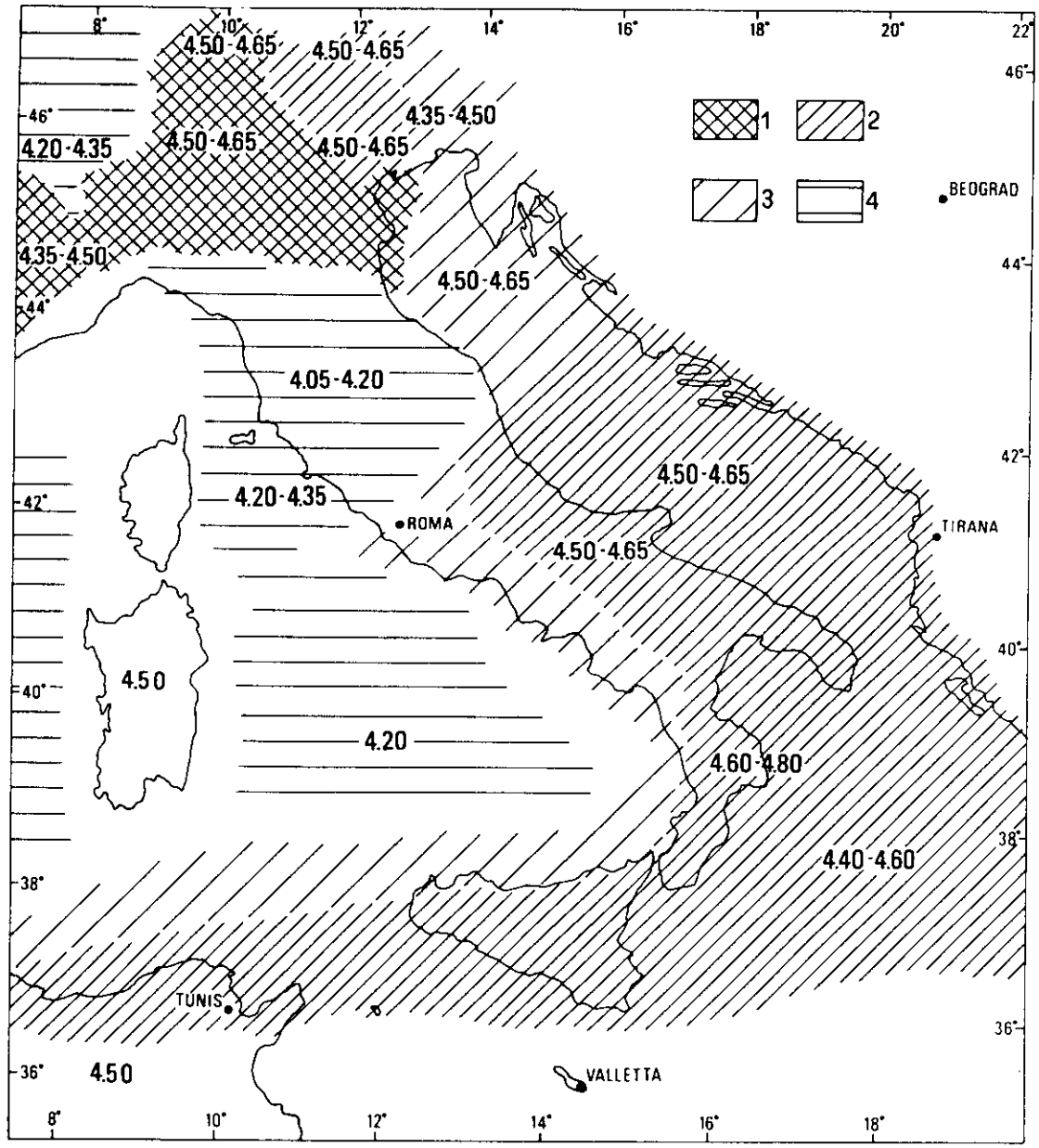

Figure 2

Schematic regionalization of the elastic properties of the lithospheric sub-Moho layer, the 'lid', as deduced from surface waves dispersion analysis (CALCAGNILE and PANZA, 1981): 1—lid thickness not exceeding 105 km; 2—lid thickness not exceeding 75 km; 3—lid thickness not exceeding 45 km; 4—lid thickness not exceeding 15 km. The three digits numbers indicate the average *S*-wave velocity in the lid.

(CALCAGNILE and PANZA, 1981). Catalogues ENEL and ING contain useful information only for longitudes less than 19 E. The extension to 20 E has been made using CSEM for the time interval 1976–1988.

Before 1971, magnitude was determined only for a fraction of the earthquakes with $M < 4$. The approximate number of all earthquakes listed up to 1971 is about the same as for listed earthquakes with $M \geq 3$ after 1971. Accordingly, in this study, we have used all earthquakes that are listed before 1971, and earthquakes with a magnitude greater than or equal to 3 thereafter.

We consider only earthquakes with focal depth $H < 100$ km, and we define as strong earthquakes the events with $M \geq 5.6$. In other words we choose the threshold $M_0 = 5.6$. The list of such events is given in Table 5. This magnitude threshold is chosen because earthquakes with $M \geq 5.6$ have an average return period of about 6 years (see Table 6), as in most of the regions considered in previous studies. Since events n.1 and n.2 of Table 5 have the same coordinates and occurred on the same day they cannot be considered separately in our analysis. Therefore the number of strong earthquakes to be actually predicted reduces to five.

Table 5

Strong earthquakes in Central Italy, $M \geq 5.6$, 1950–1989

No.	Date	$\phi°$, N	$\lambda°$, E	H	Magnitude			
					M_l	M_d	M_b	M_s
1	21. 8.1962	41.13	15.12	40	5.8	—	—	—
2	21. 8.1962	41.13	15.12	40	6.0	—	—	—
3	19. 7.1963	43.15	8.08	29	5.6	—	—	—
4	30.12.1967	44.80	12.05	35	5.8	—	—	—
5	23.11.1980	40.86	15.33	18	6.5	—	6.28	6.7
6	7. 5.1984	41.76	13.89	16	—	5.4	5.43	5.7

Table 6

Average return period of strong earthquakes (Central Italy)

M ≥	5.0	5.1	5.2	5.3	5.4	5.5	5.6	5.7	5.8	5.9	6.0
Years	1.1	2	2	2.3	2.5	3.5	5.7	7	9	9	17

3. Diagnosis of TIPs

As allowed by the normalization, algorithm *CN* is applied without any change in the numerical parameters, with the purpose of testing the general validity of the results obtained in other parts of the world. In fact, a proper change in the parameters can lead to better predictions—actually better data fitting—in each region, but this requires that we assume different physical processes for the

Table 7

Strong earthquakes and TIPs for Central Italy ($V = 5$, $E = 4.9$)

Start of TIP	Strong earthquake Date	M	End of false alarm	Duration of TIP, months
1. 1.1958			1. 1.1959	12
1.11.1961	21. 8.1962	5.8; 6.0		10
22. 8.1962	19. 7.1963	5.6		11
	30.12.1967	5.8		failure to predict
1. 3.1972			1. 5.1975	38
1.11.1979	23.11.1980	6.5		13
1. 3.1984	7. 5.1984	5.7		2
8. 5.1984			1.11.1986	30
1. 5.1988				>15

occurrence of the earthquakes in different regions.

Aftershocks are identified by the algorithm described by KEILIS-BOROK *et al.* (1980). The choice of $M_0 = 5.6$ and the discretization of functions is made on the basis of the information contained in the catalogues ENEL, CSEM, and ING up to 1986.

TIPs diagnosed in such a way are compared with strong earthquakes ($M \geq M_0$) in Table 7 and in Figure 3a. TIPs occupy 26 percent of the total time interval

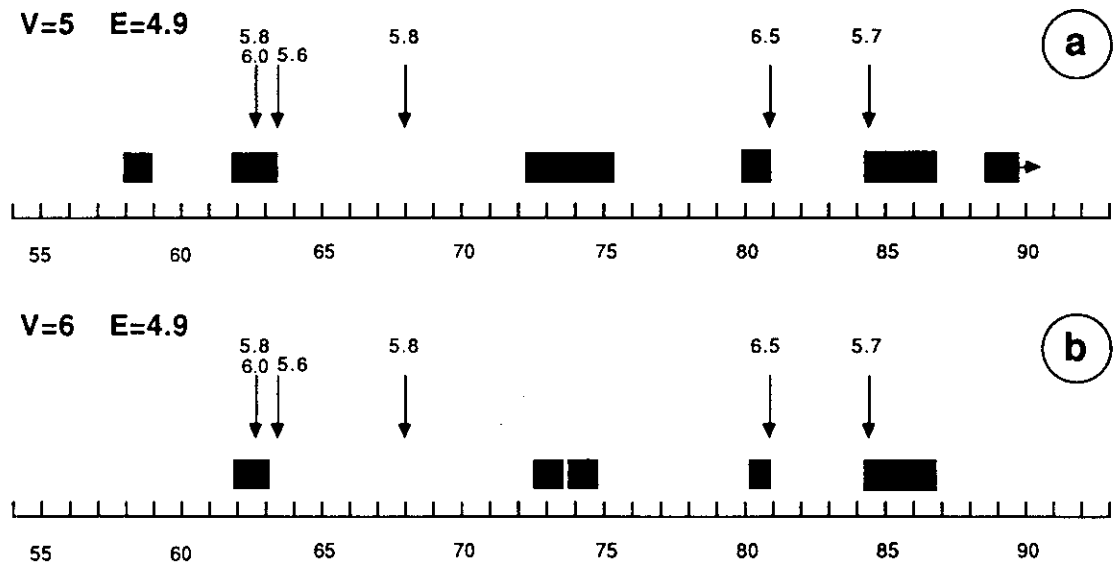

Figure 3

Part a). Results of the diagnosis of TIPs for Central Italy as deduced from catalogues ENEL, ING, CSEM; $M_0 = 5.6$, $E = 4.9$, $V = 5$; Part b). Results of the diagnosis of TIPs for Central Italy as deduced from catalogues ENEL, ING, CSEM; $M_0 = 5.6$, $E = 4.9$, $V = 6$; the time of occurrence of a strong earthquake is indicated by an arrow and a number above giving its magnitude; TIP is indicated by black rectangle.

considered (1954–1986) and precede 4 out of 5 strong earthquakes. The value reached by the function $\sigma(t)$ after the last strong earthquake (May 7, 1984, $M = 5.7$) is not sufficient to interrupt the TIP. This gives rise to a false alarm. If V is increased from 5 to 6 the total duration of TIPs is reduced by about 17 percent with an additional failure to predict (Figure 3b). Even if we observe 3 false alarms, i.e. TIPs not followed by strong earthquakes, the forward monitoring of TIPs may give very useful practical information.

4. *Forward Monitoring*

Forward monitoring, utilizing the available data which describe the seismic activity until August 1989 (ING and CSEM), shows that TIPs occupy 30 percent of the total time interval (1954–1989) and that there is a current TIP started on May 1988. The current TIP is not identified if the threshold V is increased to 6.

5. *Stability*

To test the stability of the results shown in Figure 3, the procedure has been repeated using catalogues PFG and ING. In this case there are only four strong earthquakes ($M \geq 5.6$) since in PFG and ING the events of December 30, 1967 and May 7, 1984 have magnitude 5.4. TIPs, shown in Figures 4a and 4b, occupy 32 and

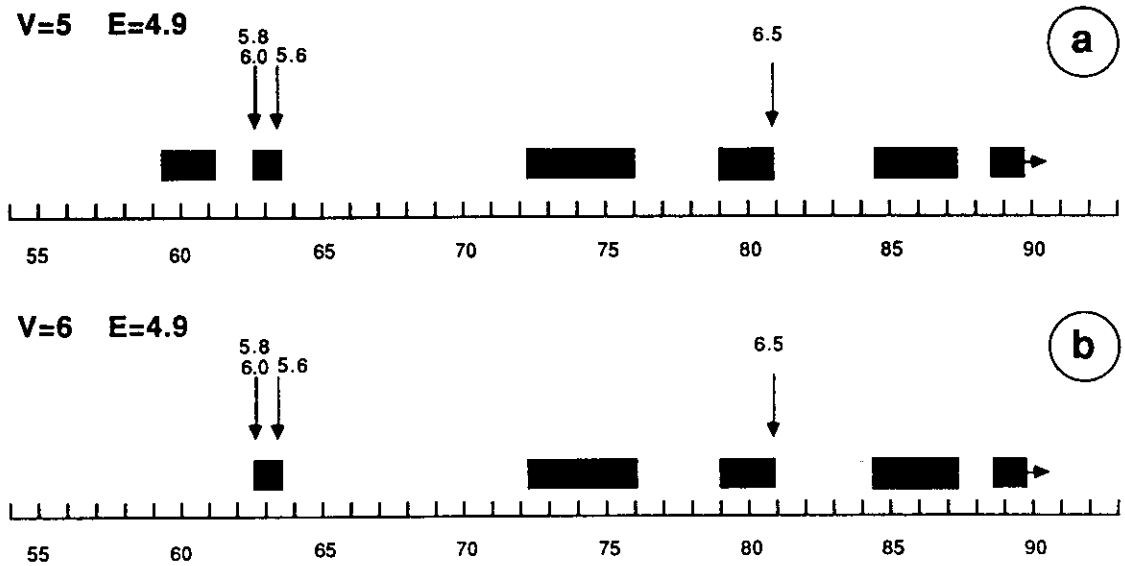

Figure 4

Part a). Results of the diagnosis of TIPs for Central Italy as deduced from catalogues PFG and ING $M_0 = 5.6$, $E = 4.9$, $V = 5$; Part b). Results of the diagnosis of TIPs for Central Italy as deduced from catalogues PFG and ING $M_0 = 5.6$, $E = 4.9$, $V = 6$; the time of occurrence of a strong earthquake is indicated by an arrow and a number above giving its magnitude; TIP is indicated by black rectangle.

27 percent of the total time interval (1954–1989) for $V = 5$ and $V = 6$, respectively. The overall picture shown in Figure 4 is not significantly different from that contained in Figure 3. The main differences are the failure to predict the event of August 21, 1962 when catalog PFG and ING are used, and the absence of a current TIP when catalogs ENEL, CSEM and ING are used with the threshold $V = 6$.

The false alarms in the time intervals 1972–1975 and 1984–1986 have some peculiar aspects. In fact, the first could be associated with the event with magnitude 5.4 which occurred, within the considered area, in October 1974. The assumption for this magnitude value of an underestimate of 0.2 units will lead to the prediction of the event, with a significant reduction of the duration of the subsequent false alarm over the entire period of observation (1954–1989). The second false alarm may be connected with the event of magnitude 5.6 which occurred in Thessaly, Greece, on April 30, 1985. From this it is evident how critical the selection of the area is within which TIPS are sought. Therefore we are now investigating the possibility of using other variants of regionalization based on geological and geophysical interpretations. This is made even more necessary by the existence of a possible current TIP, declared on the basis of traits which are characterizing the seismicity of a zone near the eastern border of the region we have defined as Central Italy. The features are based on B_{max}, whose high value is associated with the 5.4 magnitude earthquake of April 26, 1988 with epicentral coordinates 42.31 N and 16.59 E.

Acknowledgments

This research was partly carried out within the framework of the Pilot Activities of the International Center for Earth and Environmental Sciences (ICS), Trieste Miramar. Partial financial support was given by CNR-Gruppo Nazionale per la Difesa dai Terremoti, contract n.88.01067.54.

We are grateful to Fred Schwab for his comments on revising this manuscript.

REFERENCES

ALLEN, C., HUTTON, K., KEILIS-BOROK, V. I., KNOPOFF, L., KOSOBOKOV, V. G., KUZNETSOV, I. V., and ROTWAIN, I. M. (1983), *Selfsimilar Premonitory Seismicity Patterns*, Abstract, XVIII Congress of IUGG, Hamburg.

BOTTARI, A., and NERI, G. (1983), *Some Statistical Properties of a Sequence of Historical Calabro-Peloration Earthquakes*, J. Geophys. Res. *88*, 1209–1212.

CALCAGNILE, G., and PANZA, G. F. (1981), *The Main Characteristics of the Lithosphere-Asthenosphere System in Italy and Surrounding Regions*, Pure Appl. Geophys. *119*, 865–879.

CAPUTO, M., KEILIS-BOROK, V. I., OFICEROVA, E. N., RANZMAN, E. Ya., ROTWAIN, I. M., and SOLOVIEV, A. A. (1980), *Pattern Recognition of Earthquakes Prone Areas in Italy*, Phys. Earth Planet. Interiors *21*, 305–320.

CAPUTO, M., CONSOLE, R., GABRIELOV, A. M., KEILIS-BOROK, V. I., and SIDORENKO, T. V. (1983), *Long-term Premonitory Seismicity Patterns in Italy*, Geophys. J. R. Astr. Soc. *75*, 71–75.

CAPUTO, M. (1983), *The Occurrence of Large Earthquakes in South Italy*, Tectonophysics *99*, 73–83.

CSEM, *European-Mediterranean Hypocenters Data File 1976–1988* (CSEM, Strasbourg 1989).

DMITRIEVA, O. E., ROTWAIN, I. M., KEILIS-BOROK, V. I., and DE BECKER, M. (1990), *Premonitory Seismicity Patterns in a Platform Region (Ardennes-Rhenish and Brabant Massives, Lower Rhone Graben), 1989*, Computational Seismology *23*, (in press).

ENEL, *Catalogue of Earthquakes of Italy, Years 1000–1980* (Publication ENEL, Roma 1980).

GABRIELOV, A. M., DMITRIEVA, O. E., KEILIS-BOROK, V. I., KOSOBOKOV, V. G., KUZNETSOV, I. V., LEVSHINA, T. A., MIRZOEV, K. M., MOLCHAN, G. M., NEGMATULLAEV, S. Kh., PISARENKO, V. F., PROZOROV, A. G., RINEHART, W., ROTWAIN, I. M., SHEBALIN, P. N., SHNIRMAN, M. G., and SCHREIDER, S. Yu., *Algorithms of Long-Term Earthquakes' Prediction*, International School for Research Oriented to Earthquake Prediction-Algorithms, Software and Data Handling (Lima, Peru, September 1986).

GELFAND, I. M., GUBERMAN, Sh. A., KEILIS-BOROK, V. I., KNOPOFF, L., PRESS, F., RANZMAN, E. Ya., ROTWAIN, I. M., and SADOVSKY, A. M. (1976), *Pattern Recognition Applied to Earthquake Epicenters in California*, Phys. Earth. Planet. Int. *11*, 227–283.

ING, *Seismological Reports 1981–1988* (ING, Rome 1982–1989).

KEILIS-BOROK, V. I., KNOPOFF, L., and ROTWAIN, I. M. (1980), *Bursts of Aftershocks, Long-Term Precursors of Strong Earthquakes*, Nature *283* (5744), 259–263.

KEILIS-BOROK, V. I., KNOPOFF, L., ROTWAIN I. M., and ALLEN, C. R. (1988), *Intermediate-term Prediction of Occurrence Times of Strong Earthquakes*, Nature *335* (6192), 690–694.

KEILIS-BOROK, V. I., and ROTWAIN, I. M. (1989), *Diagnostics of TIPs of Strong Earthquakes in Northern Appalachians*, Computational Seismology *22*, 18–23.

PFG, *Catalogo dei terremoti italiani dall'anno 1000 al 1980* (ed. Postpischl, D.) (CNR-P. F. Geodinamica, 1985).

(Received January 12, 1989, revised September 12, 1989, accepted January 30, 1990)

PAGEOPH, Vol. 147, No. 1 (1996) 0033-4553/96/010119-12$1.50 + 0.20/0

Seismotectonic Models and CN Algorithm: The Case of Italy

GIOVANNI COSTA,[1,2] IVANKA OROZOVA-STANISHKOVA,[1,2]
GIULIANO FRANCESCO PANZA[1,2] and IRINA M. ROTWAIN[3]

Abstract—The CN algorithm is utilized here both for the intermediate term earthquake prediction and to validate the seismotectonic model of the Italian territory. Using the results of the analysis, made through the CN algorithm and taking into account the seismotectonic model, three main areas, one for Northern Italy, one for Central Italy and one for Southern Italy, are defined. Two transition areas between the three main areas are delineated. The earthquakes which occurred in these two areas contribute to the precursor phenomena identified by the CN algorithm in each main area.

Key words: Earthquakes prediction, seismotectonics, seismicity.

1. Introduction

The analysis of the Time of Increased Probability (TIP) of a strong earthquake with magnitude greater than, or equal to a given threshold M_0, based on the algorithm CN, makes use of normalized functions, which describe the seismicity pattern of the analyzed area. Therefore the original algorithm, developed for the California-Nevada region, can be directly used, without any adjustment, in areas with different size and level of seismicity.

It has been shown by COSTA *et al.* (1995) that a regionalization, supported by seismological and tectonic arguments, leads to the reduction of the alarm duration (TIP) and of the failures to predict, and increases the stability of the algorithm. Therefore, the CN algorithm permits to deal with the development of modern regional geodynamic models, involving relationships between the key structural features which control the seismicity, and the selection of the optimal causative fault system for prediction purposes (RUNDKVIST and ROTWAIN, 1994).

The algorithm CN is described in full detail by GABRIELOV *et al.* (1986) and KEILIS-BOROK and ROTWAIN (1990). An application to Central Italy is given by

[1]Dipartimento Scienze della Terra, Università degli Studi di Trieste, via E. Weiss 4, 34127 Trieste, Italy.

[2]International Center for Theoretical Physics-ICTP, 34100 Trieste Miramar, Italy.

[3]International Institute of Earthquake Prediction Theory and Mathematical Geophysics, Academy of Sciences of the U.S.S.R., Warshavskoye, 79, K.2, 113556, Moscow, U.S.S.R.

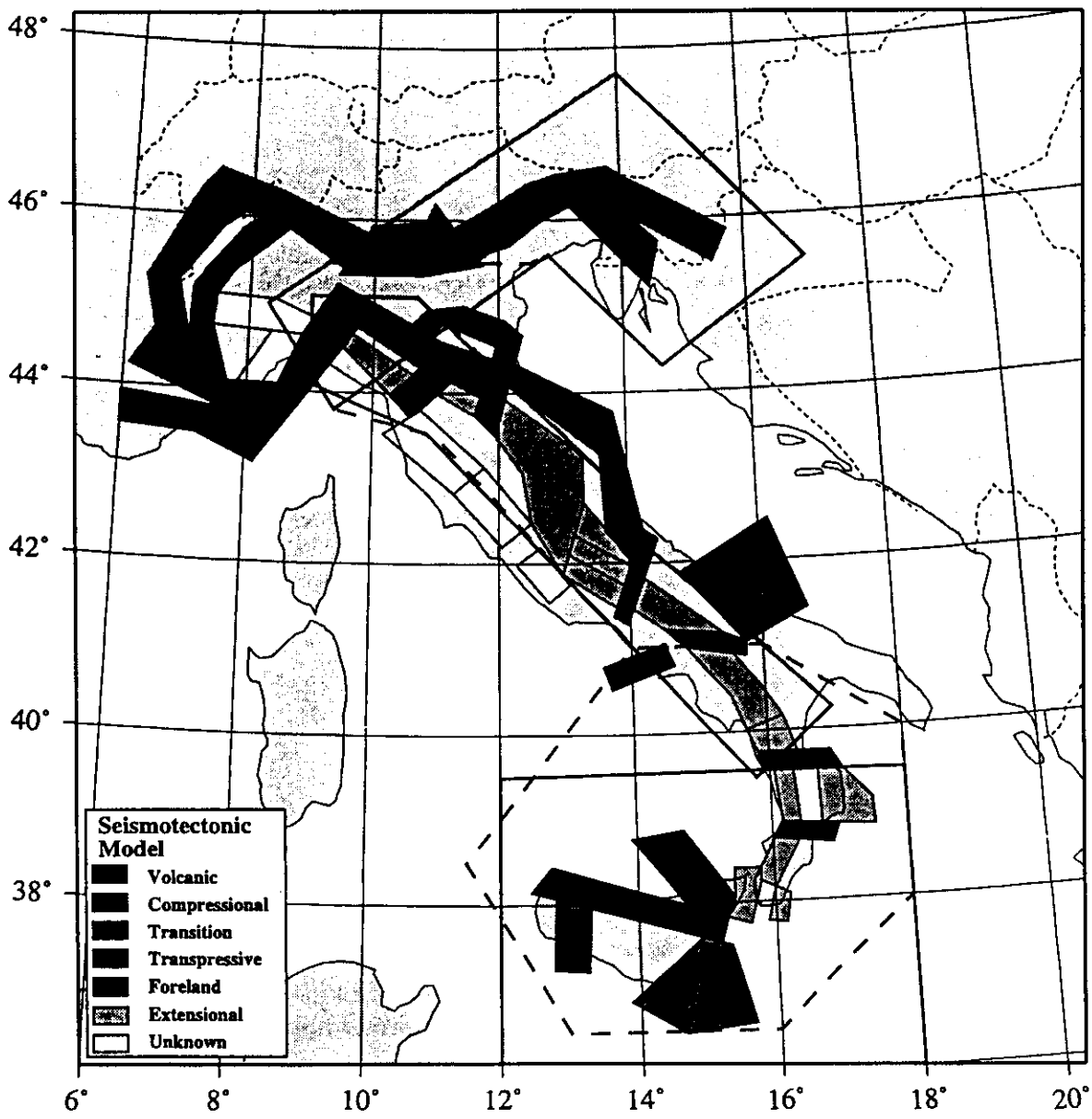

Figure 1
Seismotectonic model of Italy (PATACCA *et al.*, 1990) and regionalization into three main and two transition areas.

KEILIS-BOROK *et al.* (1990), where the borders of the studied area are defined simply according to the completeness of the used catalogue. The analysis of the seismicity and seismotectonic considerations permit the definition of a more detailed regionalization of Central Italy and the testing of the stability of the method (COSTA *et al.*, 1995).

In the present study the analysis is extended to the whole Italian territory. Using the seismotectonic model of Italy (PATACCA *et al.*, 1990) and the spatial distribution of the epicenters (Fig. 1), the country is divided into three main areas (Fig. 2).

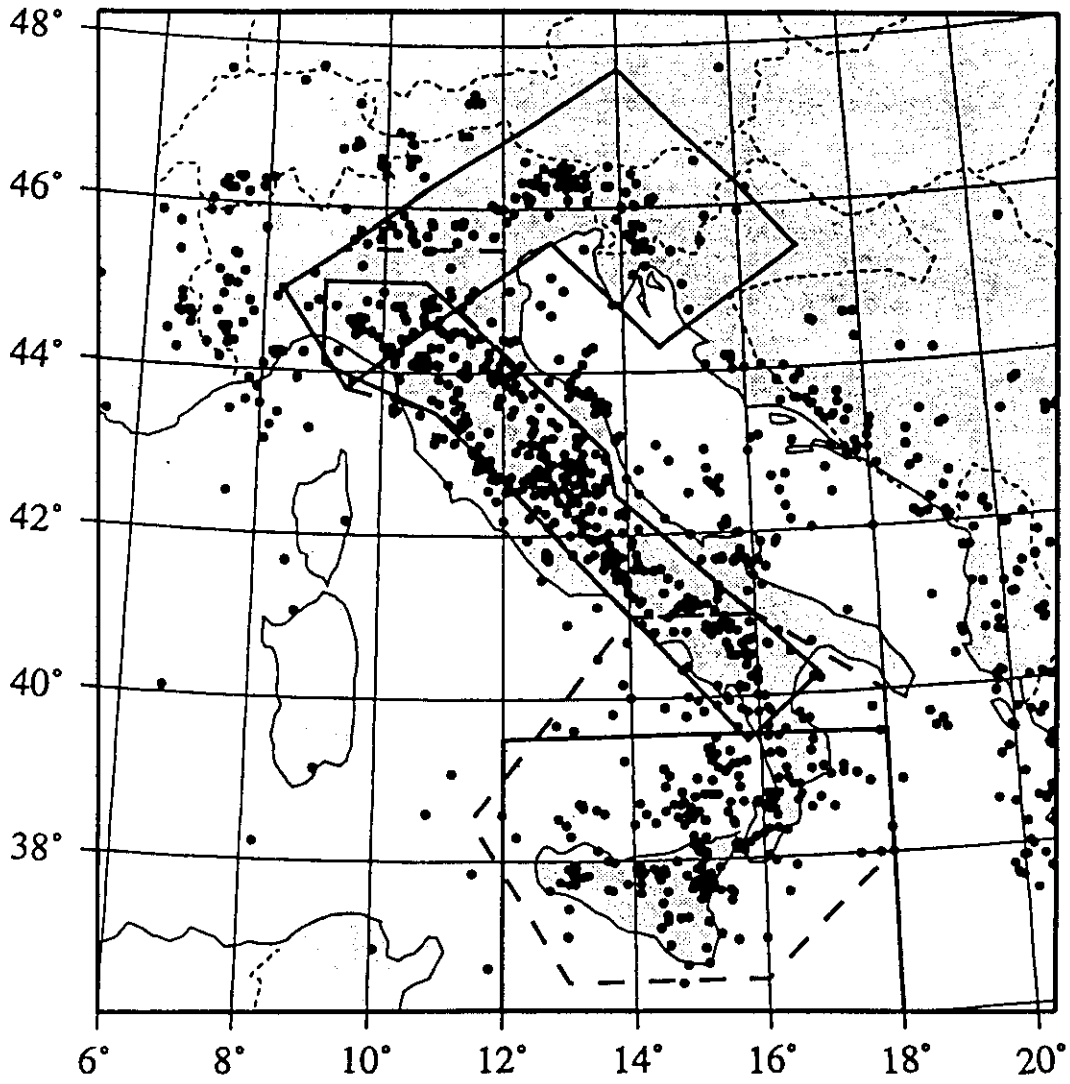

Figure 2
Seismicity map ($M \geq 4.0$) and boundaries of the three main areas in Italy. Dashed line marks variants of the regionalization.

Each of them is characterized by a dominant seismotectonic behavior, with varying seismicity pattern, therefore the appropriate M_0 is used in each area.

The catalogue used routinely for the application of the CN algorithm in Italy has been compiled as follows: for the period 1900–1979 it is taken the PFG (POSTPISCHL, 1985) and since 1980 it is continued with the ING (Istituto Nazionale di Geofisica, 1994) catalogue. This catalogue hereafter is referred as PFGING. M_I (magnitude from intensity), M_d (duration magnitude) and M_L (local magnitude) are available in this catalogue.

2. Geodynamic Outline

The Italian territory can be divided into three main tectonics areas (Northern, Central, and Southern Italy) with different types of recent motion (PATACCA and

SCANDONE, 1989; DAL PIAZ and POLINO, 1989). Each of these main areas is subdivided into several smaller seismogenic zones with different seismotectonic characteristics and behavior (Fig. 1).

The first area, Northern Italy (north of 44°N), is characterized by the presence of the Alpine arc, which is generally uplifting (MUELLER, 1982). The eastern part of the area (Friuli), where one of the branches of the Southern Alps turns to the south along the Adriatic Sea (Dinaric Alps), the western part of the area, and the areas of contact between the Southern Alps and the Northern Apennines are characterized by compression (DAL PIAZ and POLINO, 1989). In the Friuli zone some westerly strike-slip motion is also present (PAVONI *et al.*, 1992). Therefore, in Northern Italy the majority of the seismogenic zones are compressive or transpressive (Fig. 1).

In Central italy two arcs of tectonic shortening, the North-Central Apennines and the Calabrian arc, meet. According to PATACCA and SCANDONE (1989) the deformation in this area has been strictly controlled by the sinking of the foreland lithosphere beneath the mountain chain peninsula and not directly by the collision between Europe and Africa. This hypothesis is strongly supported by surface waves dispersion measurements (CALCAGNILE and PANZA, 1981; PANZA *et al.*, 1982; SUHADOLC and PANZA, 1988), and other more recent investigations (DELLA VEDOVA *et al.*, 1991; MARSON *et al.*, 1995). The North-Central Apennines arc can be divided into two main structures, parallel to its axis: the first one is a zone of compression, and the second one is a zone of extension (Fig. 1). These two main structures are crossed by few transfer zones. Previous studies (COSTA *et al.*, 1991, 1995), have shown that the zones of extension and compression in Central Italy should not be jointly considered in the regionalization.

According to PATACCA *et al.* (1990), the 41°N parallel divides the Apennines chain in two completely different tectonic domains, and this line is proposed to separate Central from Southern Italy. The division of the Apennines into two major arcs may be related to the different sinking of the foreland lithosphere in the Northern Apennines and in the Calibrian arc (MARSON *et al.*, 1995). The passive subduction of the Po-Adriatic-Ionic lithosphere, caused by gravitational sinking, appears as a reasonable mechanism to explain contemporaneous geodynamic events such as mountain building in the Apennines and the extension in the Tyrrhenian area.

Southern Italy is characterized by very complex tectonics and different seismotectonic zones with extensive, transfer, foreland and volcanic character, can be recognized. The complexity here is even increased by the presence of several intermediate and deep focus earthquakes (CAPUTO *et al.*, 1970), related to the Calabrian arc (Eastern Sicily, Calabria). This arc, which is the most important tectonic structure in Southern Italy, is an old subduction zone, where the deep-focus earthquakes are related to the existence of a lithospheric slab which may represent, in its deepest parts, the remnant of the Adriatic lithosphere which subducted

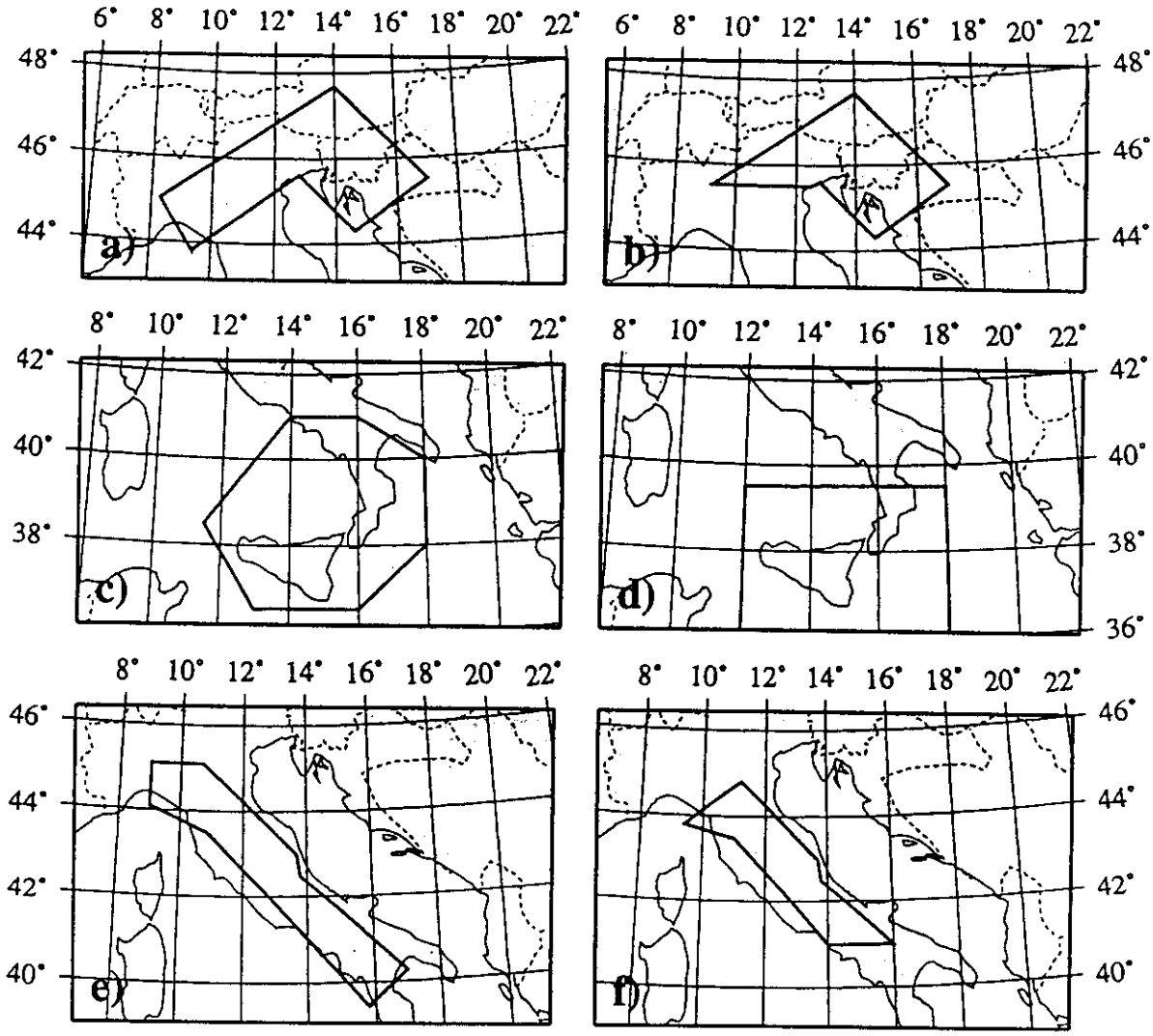

Figure 3
Different regionalizations, considered in the present study: a) first variant considered in Northern Italy (area 1); b) second variant considered in Northern Italy (area 2); c) first variant considered in Southern Italy (area 1); d) second variant considered in Southern Italy (area 2); e) Central Italy regionalization according to COSTA *et al.* (1995) (area 1); f) second regionalization considered in Central Italy (area 2).

Corsica-Sardinia before the opening of the Tyrrhenian Sea (PATACCA and SCANDONE, 1989).

3. *Regionalization*

To minimize the spatial uncertainty, the area in which a strong earthquake must be predicted, should be as small as possible, but there are two rules that limit its minimum dimensions: 1) the border of the area must be drawn following to the extent possible the minima in seismic activity; 2) the annual number of earthquakes with magnitude greater or equal to the completeness threshold of the catalogue must be greater or equal to 3.

Table 1

Earthquake catalogues used in Northern Italy

Catalog	Period	Magnitude	Priority
PFGING	1000–1992	M_I, M_d, M_L	M_L, M_d, M_I
ALPOR	1000–1985	M_I, M_L	M_L, M_I
NEIC	1900–1992	m_b, M_s, M_L	M_L, M_s, m_b
Final	1900–1992	$M_{(ALPOR)}$, $M_{(PFGING)}$, $M_{(NEIC)}$	MAX

Note:
The priority M_1, M_2, M_3 indicates that the magnitude M_1 has been used whenever available. If M_1 is not available, M_2 has been used, etc. MAX = Max(M_1, M_2, M_3).

The borders between the three main areas: Northern, Central and Southern, described in Section 2, are not sharply defined and they can be better represented by a transition domain. In fact, as we will see, the division of the Italian territory into three main areas, separated by two transition areas, seems to be consistent with the indications given concerning the properties of seismicity by the CN algorithm. A synoptic representation of the different areas is given in Figure 2, while the shapes of the two variants of each main area are given in Figure 3.

3.1. Northern Italy

The Alpine arc, the most important tectonic feature in Northern Italy, is crossed by different political borders and consequently the catalogue PFGING is fairly incomplete for our purposes. To fill in the gap it was necessary to add the information contained in two other catalogues: ALPOR (1987) and NEIC (1992). ALPOR is the catalogue of the Eastern Alps, compiled at the Osservatorio Geofisico Sperimentale, Trieste, Italy. In this catalogue two magnitudes are reported: M_I and M_L. NEIC is the catalogue of the National Earthquake Information Center (NEIC, USGS, Denver, USA). In this catalogue the body wave magnitude, m_b, the surface wave magnitudes, M_S, and M_L are reported.

The catalogue which we used in the application of the CN algorithm to Northern Italy is obtained merging ALPOR, PFGING and NEIC. Taking into account the uncertainties, which are intrinsic in the three different catalogues considered, the events differing in origin time by less than 1 minute and in epicentral location by less than 0.5°, both in latitude and longitude, are considered the same event. The priority in the choice of the magnitude to be used in the further processing is given in Table 1. The aftershocks are eliminated, using the criteria given by KEILIS-BOROK *et al.* (1980), and only the events with magnitude greater than, or equal to 3 have been used.

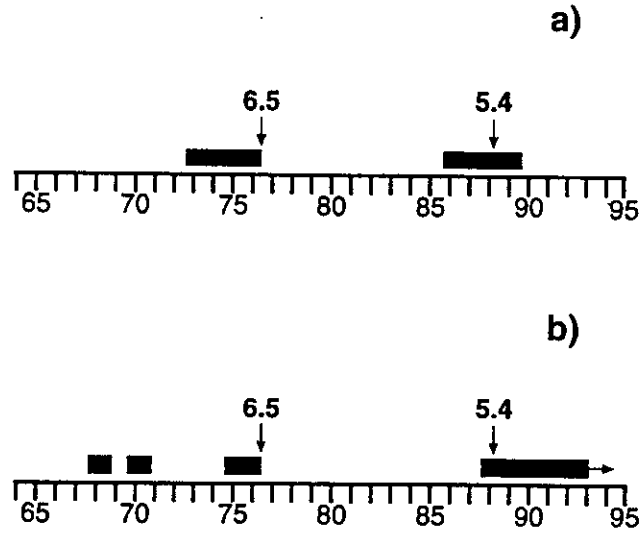

Figure 4
Results of the CN analysis in Northern Italy: a) area 1; b) area 2. The arrows indicate earthquakes with $M \geq M_0$, TIPs are marked by black rectangles.

According to the standards used in the CN algorithm (COSTA *et al.*, 1995), the magnitude threshold for the definition of the strong earthquakes is chosen to be $M_0 = 5.4$. In the present study the period 1960–1992 is analyzed because of the significant incompleteness of the catalogue before 1960. In the region, only two strong earthquakes occurred during the last 30 years ($M = 6.5$, May 6, 1976 and $M = 5.4$, January 2, 1988). The $M = 6.0$ September 15, 1976 event is a strong aftershock, identified as Related Strong Earthquake by VOROBIEVA and PANZA (1993), and therefore it is not a target of the CN algorithm.

There are two important tectonic features in Northern Italy: the intersection of the Alps and the Dinarides in Friuli and the intersection of the Alps and the Apennines in Liguria. Because of the complexity of the region, it is rather difficult to define the appropriate borders of the area to be considered for the purposes of the CN algorithm. To solve this problem, an hypothesis has been formulated that the stress, responsible for earthquake occurrence, "propagates" along a major fault or tectonic structure and "accumulates" at the edges of this structure, and/or in the areas of intersection with other important faults or tectonic structures. Therefore, for the purposes of earthquake prediction, the events concentrated at the edges, or in the areas of intersections with other structures, of a given tectonic structure cannot be considered independent and should be all contained in the same area. In the present study, the Alpine arc is considered as the structure along which the tectonic stress propagates, and the events concentrated on both of its edges, western and eastern, are assumed to be correlated, and therefore included in the same area.

The seismogenic region, thus defined, is shown in Figure 3a. The two strong events are predicted and the TIP duration is 27% of the total time (see Fig. 4a). There is only one false alarm after the strong earthquake of 1988.

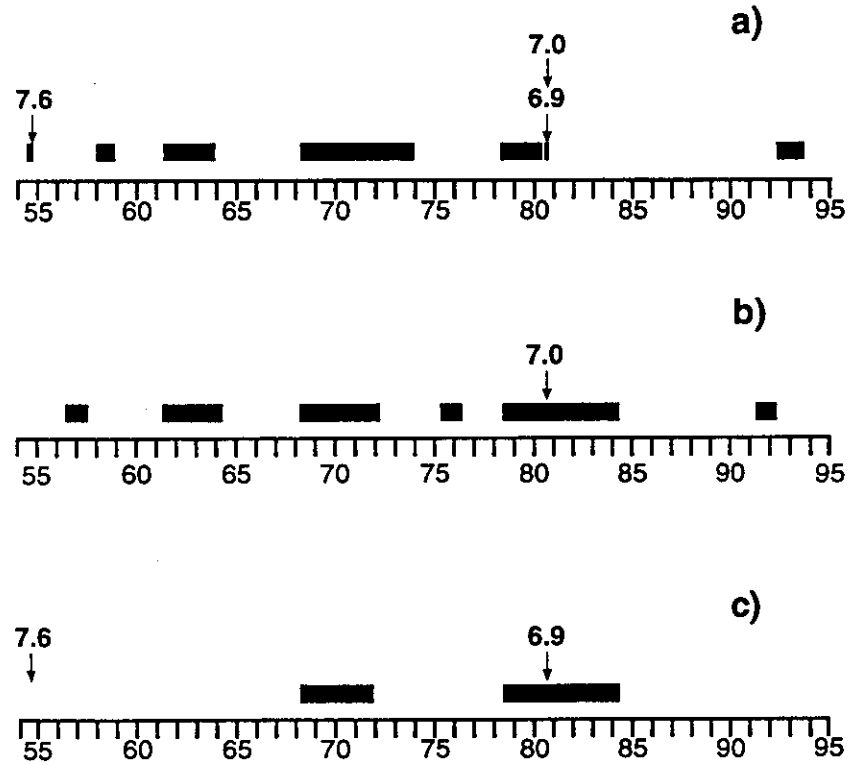

Figure 5
Results of the CN analysis in Southern Italy: a) area 1; b) area 1, considering only the shallow events; c) area 2. The arrows indicate earthquakes with $M \geq M_0$, TIPs are marked by black rectangles. The magnitude 6.9 is referred to an intermediate-depth earthquake in the Tyrrhenian Sea, while the magnitude 7 (taken from the PFGING catalogue) corresponds to the Irpinia, 1980, earthquake.

In order to test the hypothesis that the earthquakes, concentrated on the edges of a tectonic structure or in the areas of intersection with other structures, cannot be neglected for the purposes of earthquake prediction, a second regionalization (Fig. 3b), which includes only the compressive domains in the Eastern Alps (Fig. 1) is considered. The two strong events are predicted (Fig. 4b), but the TIP duration increases to 34% of the total time, and there are three false alarms.

3.2. Southern Italy

If we take the magnitude priority MAX (see note of Table 1) the utilized catalogue, PFGING, can be considered complete in this part of Italy only after 1950, and for magnitudes over three. The magnitude threshold in the definition of the strong earthquakes has been chosen as $M_0 = 6.5$.

Following the idea of PATACCA *et al.* (1990), that the 41°N parallel divides the Apennines into two completely different tectonic domains, for Southern Italy the area shown in Figure 3c has been delineated. The results of the CN algorithm applied to this area are reported in Figure 5a. All three strong earthquakes ($M = 7.6$, November 23, 1954, $M = 7.0$ November 23, and $M = 6.9$, November 24,

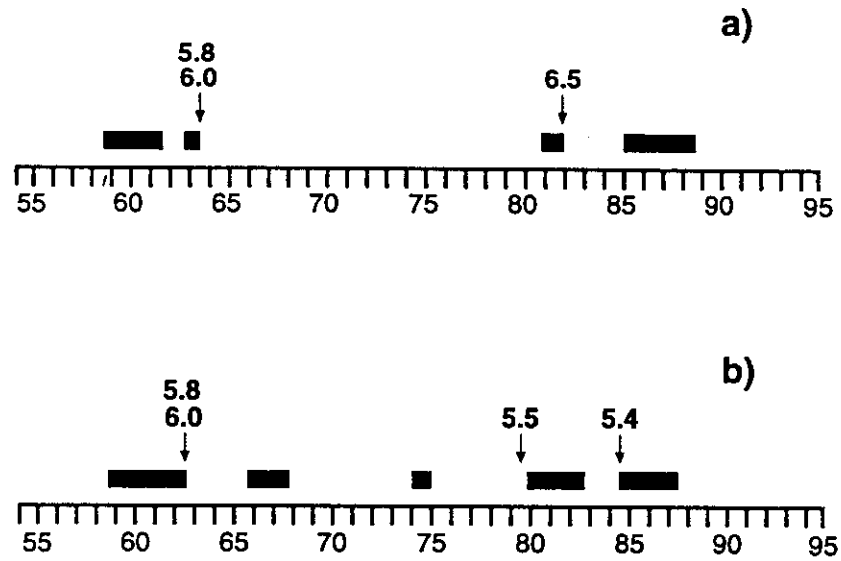

Figure 6
Results of the CN analysis in Central Italy: a) area 1; b) area 2. The arrows indicate earthquakes with $M \geq M_0$, TIPs are marked by black rectangles.

both in 1980) are predicted and the duration of TIP is 33% of the total time. There are five false alarms.

To study the influence of the relevant deep seismicity we consider only the shallow earthquakes and thus the only strong event to be predicted is the $M = 7.0$, November 23, 1980 earthquake. The diagnosis of the CN algorithm is given in Figure 5b. The strong event is predicted, but the duration of TIP increases up to 44% of the total time and there are six false alarms. This result indicates that the shallow and the deep seismicity in this area are not independent, in contrast with observations in other parts of the world (KEILIS-BOROK and ROTWAIN, 1990).

As a second test, according to the regionalization for Central Italy proposed by COSTA *et al.* (1995), the northern border of Southern Italy is traced along the 39.5° parallel (Fig. 3d). In this area the two strong earthquakes to be predicted are the $M = 7.6$, November 23, 1954 and the $M = 6.9$, November 23, 1980 events. The 1980 earthquake is predicted with a TIP duration lasting for 25% of the total time; the 1954, $M = 7.6$, event is a failure to predict and there are two false alarms (Fig. 5c).

3.3. Central Italy

The CN algorithm initially has been applied to Central Italy (KEILIS-BOROK *et al.*, 1990; COSTA *et al.*, 1995), because the catalogue PFGING is rather complete here. In the present study, utilizing the regionalization shown in Figure 3e, given by COSTA *et al.* (1995), we extend the analysis through the end of 1994 (Fig. 6a).

The definition of the areas in Northern and Southern Italy makes necessary a revision of the regionalization of Central Italy. In fact, the regionalizations for

Table 2

Final results

	Northern Italy		Southern Italy			Central Italy	
	Area 1	Area 2	Area 1	Area 1*	Area 2	Area 1	Area 2
Events	2	2	3	1	2	3	4
Predicted	2	2	3	1	1	3	3
False alarms	1	2	5	6	2	2	4
Failures to predict	0	0	0	0	1	0	1
% of TIPs	27	34	33	44	25	23	38

*Only shallow events.

Northern and Southern Italy, proposed in the present study, contain some zones (see Fig. 2), previously included in Central Italy (COSTA *et al.*, 1995). The new regionalization for this area is presented in Figure 3f. Four strong earthquakes occurred in the area: $M = 5.8$ and $M = 6.0$, both on August 21, 1962, $M = 5.5$, September 19, 1979 and $M = 5.4$, May 7, 1984. As can be seen from Figure 6b, three of the four strong earthquakes are predicted by the CN algorithm, while the 1979 event is a failure to predict; there are four false alarms and the TIPs increase, with respect to the previous study (COSTA *et al.*, 1995), from 30% to 38% of the total time.

Only the crustal earthquakes which occurred in Central Italy are used to obtain the results shown in Figure 6. According to the model proposed by MARSON *et al.* (1995), few intermediate and deep earthquakes belong to Central Italy and should be considered when using the CN algorithm. However, their inclusion in the data set does not affect the results, and this is not surprising since the number of these events and their size are small.

4. Conclusions

Three main areas in Italy (Northern, Central and Southern, each having a distinct seismicity pattern) have been analyzed in the present study, utilizing the CN algorithm. The separation among them is not marked by sharp boundaries, and on the basis of different zonations, it is possible to identify intersection areas, which can be assigned to either bordering main areas. The TIPs duration decreases in each main area when the intersection areas are included in it (Table 2). On the basis of these results, one can conclude that the fault systems belonging to the domains of intersection are involved in the generation of strong earthquakes in the bordering main areas and, therefore, for the purpose of earthquake prediction, they must be considered together with the faulting system of the main areas.

In Southern Italy, where numerous, intermediate and deep focus events occur, all the earthquakes (shallow, intermediate and deep focus) should be used for the purposes of intermediate-term earthquake prediction.

HABERMANN and CREAMER (1994) analyzed M8 (KEILIS-BOROK and KOSOBOKOV, 1986), a prediction algorithm similar to CN, and suggested that the algorithm preferentially identifies TIPs during periods of systematically increased magnitudes. The systematic increase of magnitudes has the same effect of changes in the completeness of the catalogue used in the prediction. The analysis of the completeness of the PFGING catalogue, made by MOLCHAN *et al.* (1995), allows us to state that the TIPs, diagnosed by the CN algorithm, cannot be obviously associated with the changes in the completeness level of the catalogue.

Acknowledgments

The authors are very grateful to Professor V. I. Keilis-Borok for stimulating discussions. One of the authors (I. Rotwain) thanks ICTP for financial support for her stay in Trieste during which a large part of this work has been done. We acknowledge financial support from MURST (40% and 60%) funds, CNR-Gruppo Nazionale per la difesa dai Terremoti contracts nos. 92.02867.54 and 93.02492.54 and INTAS 94-232 contract.

REFERENCES

ALPOR. (1987), *Catalogue of the Eastern Alps*, Osservatorio Geofisico Sperimentale, Trieste, Italy (computer file).

CALCAGNILE, G., and PANZA, G. F. (1981), *The Main Characteristics of the Lithosphere-astenosphere System in Italy and Surroundings Regions*, Pure and Appl. Geophys. *119*, 865–879.

CAPUTO, M. G., PANZA, G. F., and POSTPISCHL, D. (1970), *Deep Structure of the Mediterranian Basin*, J. Geophys. Res. *75*, 4919–4923.

COSTA, G., PANZA, G. F., and ROTWAIN, I. M. (1991), *Time of increased probability for earthquakes with $M > 5.6$ in Central Italy*. Proceedings of International Conference on Earthquake Predictions: State-of-the Art. Strasbourg, France, 15–18 October.

COSTA, G., PANZA, G. F., and ROTWAIN, I. M. (1995), *Stability of Premonitory Seismicity Pattern and Intermediate-term Earthquake Prediction in Central Italy*, Pure and Appl. Geophys. *145*, 259–275.

DAL PIAZ, G. V., and POLINO, R., *Evolution of the Alpine Tethys*. In *The Lithosphere in Italy* (eds. Boriani, A., Bonafede, M., Piccardo, G. B., and Vai, G. B.) (Academia Nazionale de Lincei, Atti dei Convegni Lincei, 80, Roma 1989) pp. 93–109.

DELLA VEDOVA, B., MARSON, I., PANZA, G. F., and SUHADOLC, P. (1991), *Upper Mantle Properties of the Tuscan-Tyrrhenian Area: A Key for Understanding the Recent Tectonic Evolution of the Italian Region*, Tectonophysics *195*, 311–318.

GABRIELOV, A. M., DMITRIEVA, O. E., KEILIS-BOROK, V. I., KOSOBOKOV, V. G., KUZNETSOV, I. V., LEVSHINA, T. A., MIRZOEV, K. M., MOLCHAN, G. M., NEGMATULLAEV, S. Kh., PISARENKO, V. F., PROZOROV, A. G., RINEHART, W., ROTWAIN, I. M., SHEBALIN, P. N., SHNIRMAN, M. G., and SCHREIDER, S. Yu. (1986), *Algorithms of Long-Term Earthquakes' Predictions*. International School for Research Oriented to Earthquake Prediction-Algorithms, Software and Data Handling, Lima, Perù.

HABERMANN, R. E., and CREAMER, F. (1994), *Catalogue Errors and the M8 Earthquake Prediction Algorithm*, Bull. Seismol. Soc. Am. *84*, 1551–1559.

ING. (1995), *Seismological Reports 1980–1995.* Istituto Nazionale di Geofisica, Roma, Italy (computer file).

KAGAN, Y. Y., and KNOPOFF, L. (1981), *Stochastic Synthesis of Earthquake Catalogs*, Geophys. J. R. Astr. Soc. *86*, 303–320.

KEILIS-BOROK, V. I., KNOPOFF, L., and ROTWAIN, I. (1980), *Bursts of Aftershocks, Long-term Precursors of Strong Earthquakes*, Nature *283*, 259–263.

KEILIS-BOROK, V. I., and KOSOBOKOV, V. S. (1986), *Time of Increased Probability for the Great Earthquake of the World*, Computational Seismology *19*, 48–57.

KEILIS-BOROK, V. I., KUZNETSOV, I. V., PANZA, G. F., ROTWAIN, I. M., and COSTA, G. (1990), *On Intermediate-term Earthquake Prediction in Central Italy*, Pure and Appl. Geophys. *134*, 79–92.

KEILIS-BOROK, V. I., and ROTWAIN, I. (1990), *Diagnosis of Time of Increased Probability of Strong Earthquakes in Different Regions of the World: Algorithm CN*, Phys. Earth Planet. Inter. *61*, 57–72.

MARSON, I., PANZA, G. F., and SUHADOLC, P. (1995), *Crust and Upper Mantle Models along the Active Tyrrhenian Rim*, Terra Nova *7*, 348–357.

MOLCHAN, G. M., KRONROD, T. L., and DMITRIEVA, O. E. (1995), *Statistical Analysis of Seismicity and Hazard Estimation for Italy (Mixed Approach)*, ICTP, IAEA, UNESCO, Internal Report, IC/95/27, 85 pp. Trieste, Italy.

MUELLER, S., *Deep structure and recent dynamics in the Alps.* In *Mountain Building Process* (ed. K. J. Hsu) (Academic Press 1982) pp. 181–199.

NEIC. (1992), *Worldwide earthquake catalogue*, National Earthquake Information Center (NEIC), USGS, Denver, Colorado, U.S.A. (computer file).

PANZA, G. F., MUELLER, S., CALCAGNILE, G., and KNOPOFF, L. (1982), *Delineation of the North Central Italian Upper Mantle Anomaly*, Nature *296*, 238–239.

PATACCA, E., and SCANDONE, P., *Post-Tortonian mountain building in the Apennines. The role of the passive sinking of a relic lithospheric slab.* In *The Lithosphere in Italy* (eds. Boriani, A., Bonafede, M., Piccardo, G. B., and Vai, G. B.) (Academia Nazionale dei Lincei, Atti dei Convegni Lincei, 80, Roma 1989) pp. 157–176.

PATACCA, E., SATORI R., and SCANDONE, P. (1990), *Tyrrhenian Basin and Apenninic Arcs: Kinematic Relation since Late Tortonian Times*, Mem. Soc. Geol. It. *45*, 425–451.

PAVONI, N., AHJOS, T., FREEMAN, R., GREGERSEN, S., LANGER, H., LEYDECKER, G., ROTH, Ph., SUHADOLC, P., and USKI, M., *Seismicity and focal mechanisms.* In *A Continent Revealed—The European Geotraverse: Atlas of Compiled Data* (eds. Freeman, R. and Mueller, S.) (Cambridge University Press, Cambridge 1992) pp. 14–19.

PFG (1985), *Catalogo dei terremoti italiani dall'anno 1000 al 1980* (ed. Postpischl, D.), CNR-P. F. Geodinamica.

RUNDKVIST, D. V., and ROTWAIN, I. M. (1994), *Present-day Geodynamics and Seismicity of Asia Minor*, Computation of Seismology *27*, 201–245.

SUHADOLC, P., and PANZA, G. F. (1988), *The European-African Collision and its Effects on the Lithospheric-astenosphere System*, Tectonophysics *146*, 59–66.

VOROBIEVA, I. A., and PANZA, G. F. (1993), *Prediction of Occurrence of Related Strong Earthquakes in Italy*, Pure and Appl. Geophys. *141*, 25–41.

(Received July 14, 1995, accepted November 6, 1995)

PAGEOPH, Vol. 145, No. 2 (1995) 0033-4553/95/020259-17$1.50 + 0.20/0

Stability of Premonitory Seismicity Pattern and Intermediate-term Earthquake Prediction in Central Italy

G. COSTA,[1,2] G. F. PANZA[1,2] and I. M. ROTWAIN[3]

Abstract—The algorithm CN makes use of normalized functions. Therefore the original algorithm, developed for the California-Nevada region, can be directly applied, without adjustment of the parameters, to the determination of the Time of Increased Probability (TIP) of strong earthquakes for Central Italy. The prediction is applied to the events with magnitude $M \geq M_0 = 5.6$, which in Central Italy have a return period of about six years. The routinely available digital earthquake bulletins of the Istituto Nazionale di Geofisica (ING), Rome, permits continuous monitoring. Here we extend to November 1994 the first study made by Keilis-Borok *et al.* (1990b). On the basis of the combined analysis of seismicity and seismotectonic, we formulate a new regionalization, which reduces the total alarm time and the failures to predict, and narrows the spatial uncertainty of the prediction with respect to the results of KEILIS-BOROK *et al.* (1990b).

The premonitory pattern is stable when the key parameters of the CN algorithm and the duration of the learning period are changed, and when different earthquake catalogues are used.

The anlysis of the period 1904–1940, for which $M_0 = 6$, allows us to identify self-similar properties between the two periods, in spite of the considerably higher seismicity level of the earlier time interval compared with the recent one.

Key words: Seismicity, earthquake prediction, seismotectonic, regionalization, Italy.

1. Introduction

The algorithm CN, described in full detail by GABRIELOV *et al.* (1986), KEILIS-BOROK *et al.* (1988) and KEILIS-BOROK *et al.* (1990a), has been applied to Central Italy for the first time by KEILIS-BOROK *et al.* (1990b). CN is designed to define the Time of Increased Probability (TIP) of strong earthquakes. For this purpose the traits considered are the level of seismic activity, its variation in time, clustering of the earthquakes in space and time, and their concentration in space.

[1] Istituto di Geodesia e Geofisica, Università degli Studi di Trieste, via dell'Università 7, 34123 Trieste, Italy.

[2] International Center for Theoretical Physics, ICTP, 34100 Trieste Miramar, Italy.

[3] International Institute of Earthquake Prediction Theory and Mathematical Geophysics, Academy of Sciences of Russia, Warshavskoye, 79, K.2, 113556, Moscow, Russia.

Table 1

Functions used in the algorithm CN

$SIGMA(T)$	$SIGMA(t) = \sum 10^{\beta(M_i - \alpha)}$; the main shocks with $m_i \leq M_i \leq -0.1$ and origin time ($t - 3$ years) $\leq t_i \leq t$ are included in the summation; $\alpha = 4.5$, $\beta = 100$.
$S_{max}(t)$	$S_{max}(t) = \max\{S_1/N_1, S_2/N_2, S_3/N_3\}$ where S_j is calculated as $SIGMA(t)$ for the events with the origin time ($t - j$ years) $\leq t_i \leq (t - (j-1)$ years), and N_j is the number of earthquakes in the sum.
$Z_{max}(t)$	$Z_{max}(t) = \max\{Z_1/N_1^{2/3}, Z_2/N_2^{2/3}, Z_3/N_3^{2/3}\}$ where Z_j is calculated as S_j, but with $\beta = 0.5$ and N_j is the number of earthquakes in the sum.
$N_2(t)$	Number of main shocks with $M \geq m_3$, which occurred in the time interval ($t - 3$ years, t).
$N_3(t)$	Number of main shocks with $M \geq m_2$, which occurred in the time interval ($t - 10$ years, $t - 7$ years).
$K(t)$	$K(t) = K_1 - K_2$, where K_i is the number of main shocks with $M_i \geq m_2$ and origin time ($t - 2j$ years) $\leq t_i \leq (t - 2(j-1)$ years).
$B_{max}(t)$	Maximum number of aftershocks for each main shock, counted within a radius of 50 km for the first 2 days after the main shock and for $M > M_0 - 3.6$.
$G(t)$	$G(t) = 1 - P$, where P is the ratio among the number of the main shocks with $M_j \geq m_2$ ($m_2 > m_1$) and the number of the main shocks with $M_j \geq m_1$. Only main shocks with origin time t_j in the interval ($t - 1$ year) $\leq t_j \leq t$ are considered.
$q(t)$	$q(t) = \sum_{j=1}^{6} \max\{0, 6a_2 - n_j\}$, where a_2 is the average annual number of main shocks with $M_j \geq m_2$, n_j is the number of main shocks with $M_j \geq m_2$ and origin time ($t - (8+j)$ years) $\leq t_i \leq (t - (2+j)$ years).

The functions which describe the traits for a given territory are defined in Table 1. These functions are normalized so that they can be applied to different territories, with different seismicity, without *ad hoc* adjustment. The normalization is obtained by choosing the three magnitude thresholds, m_1, m_2 and m_3, satisfying the condition that, in the territory under study, the average annual number of events with $M \geq m_i$ is equal to the constants, a_i, common to all seismically active territories.

The flow of the earthquakes is represented, at each time t, by the vector formed by the values of the different functions at time t. The value of the minimum magnitude of the events to be predicted (strong earthquakes), M_0, satisfies in general two simultaneous conditions: 1) to correspond to events with a return period of about six years; 2) to be as close as possible to a minimum in the histogram Magnitude-Number of events (Fig. 1). Condition 1 is introduced accordingly with the criteria used for the California-Nevada region; and condition 2 is introduced to minimize the effect of the threshold introduced by the choice of M_0. We will refer to those conditions as "CN rule."

In the CN analysis of the flow of earthquakes, the time axis is divided into three intervals: D (dangerous), N (nondangerous) and X (undetermined). The D intervals extend for two years before each strong event ($M \geq M_0$). Intervals X extend for

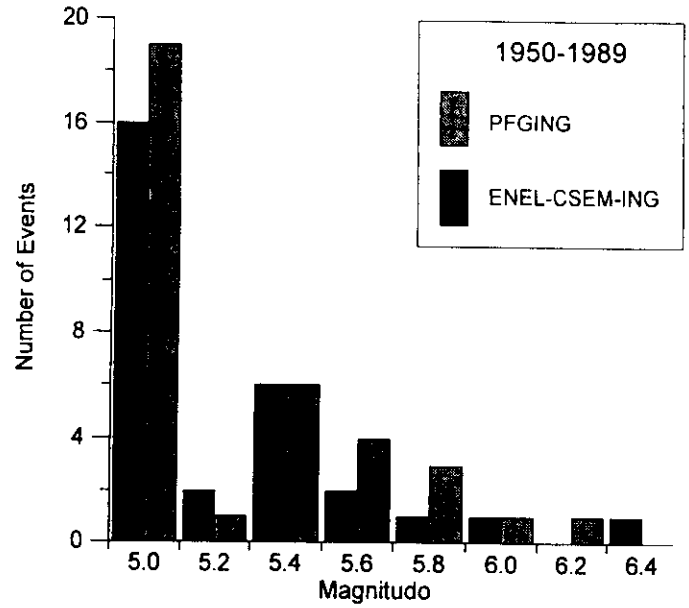

Figure 1
Histogram Magnitude-Number of events, with step 0.2 in magnitude, in the years 1950–1989 for the new regionalization proposed in this paper.

three years after each strong event; if a strong earthquake occurs within three years, the X period becomes a D period. The remaining time intervals are N intervals.

The functions defined in Table 1 are discretized by defining the thresholds as small, medium and large, on the basis of the quantile levels 1/3 and 2/3. We then estimate the combinations of the different discretized functions which are more typical for intervals D, and for intervals N. Following the procedure of pattern recognition, features D are defined by the condition that in general they occur during the intervals D and not during the intervals N. Features N are defined by the reverse condition. Each feature corresponds to a discretized value of the function, or to a combination of such values, for two or three functions.

A TIP is declared at the time t for one year if

$$n_{D(t)} - n_{N(t)} \geq V = 5$$

$$\sigma(t) = 10^{-\beta(M_0 - \alpha)} \sum 10^{\beta(M_i - \alpha)} < E = 4.9 \qquad (1)$$

where

$$\beta = 1; \quad \alpha = 0.5$$

$n_{D(t)}$ is the number of characteristic features D which the flow of earthquakes has at time t; $n_{N(t)}$ is the number of features N; in each main shock's area, $\sigma(t)$ is a function proportional to the total number of earthquakes, with magnitude M_i, occurring within a period of three years before time t.

Consecutive TIPs may overlap and induce an alarm period exceeding one year. The TIP can be interrupted if $\sigma(t) > E$, in which case the TIP can be shorter than one year. If during a TIP we have no strong event we have a "false alarm," if we have a strong event outside the TIP we have a "failure to predict."

All the constants and the definition of D and N features appearing in the algorithm CN are determined from the retrospective analysis of the California-Nevada seismicity (KEILIS-BOROK *et al.*, 1990a).

2. Tectonics and Regionalization

Central Italy is characterized by the presence of two arcs, the north-central Apennines and the Calabrian arc, of tectonic shortening. Starting from their present-day structure and analyzing the time-space evolution of the thrust belt-fore-deep-foreland system, PATACCA *et al.* (1990) reached the conclusion that the deformation has been strictly controlled by the dipping of the foreland lithosphere sinking beneath the mountain chain peninsula and not directly by the collision between Europe and Africa. This hypothesis is strongly supported by surface waves dispersion measurements (CALCAGNILE and PANZA, 1981; PANZA *et al.*, 1982; SUHADOLC and PANZA, 1988; DELLA VEDOVA *et al.*, 1991), and more recent investigations which combine different geophysical data sets regarding aeromagnetic and gravity anomalies with the available structural information concerning the lithosphere-asthenosphere system (MARSON *et al.*, 1994).

The arc present in the north-central Apennines can be divided in two main structures parallel to his axis: one is an area of compression, and the second is a zone of extension (Fig. 2). These two main structures are crossed by a few transfer zones.

The passive subduction of the Po-Adriatic-Ionian lithosphere by gravitational sinking appears as a reasonable mechanism to explain contemporaneous geodynamic events such as mountain building in the Apennines and extension in the Tyrrhenian area. The partition of the Apennines into two major arcs may be related to the differential sinking of the foreland lithosphere in the Northern Apennines and in the Calabrian Arc.

The regionalization is a very important factor in producing a useful prediction, minimizing the spatial uncertainty. The area in which a strong earthquake must be predicted must be the smallest possible, but there are some limitations to its minimum dimensions: 1) the borders of the area must not cross continuous seismotectonic zones, at least the ones easily identifiable, and, 2) the annual number of earthquakes must be ≥ 3 for the magnitude for which the catalogue is completed.

The regionalization used by KEILIS-BOROK *et al.* (1990b) (Fig. 3), based only on the boundaries and completeness of ENEL catalogue, covers an area of about 6.3×10^5 km^2 and allows us to obtain overall satisfactory results, but without negligible false alarms and failures to predict (Fig. 4).

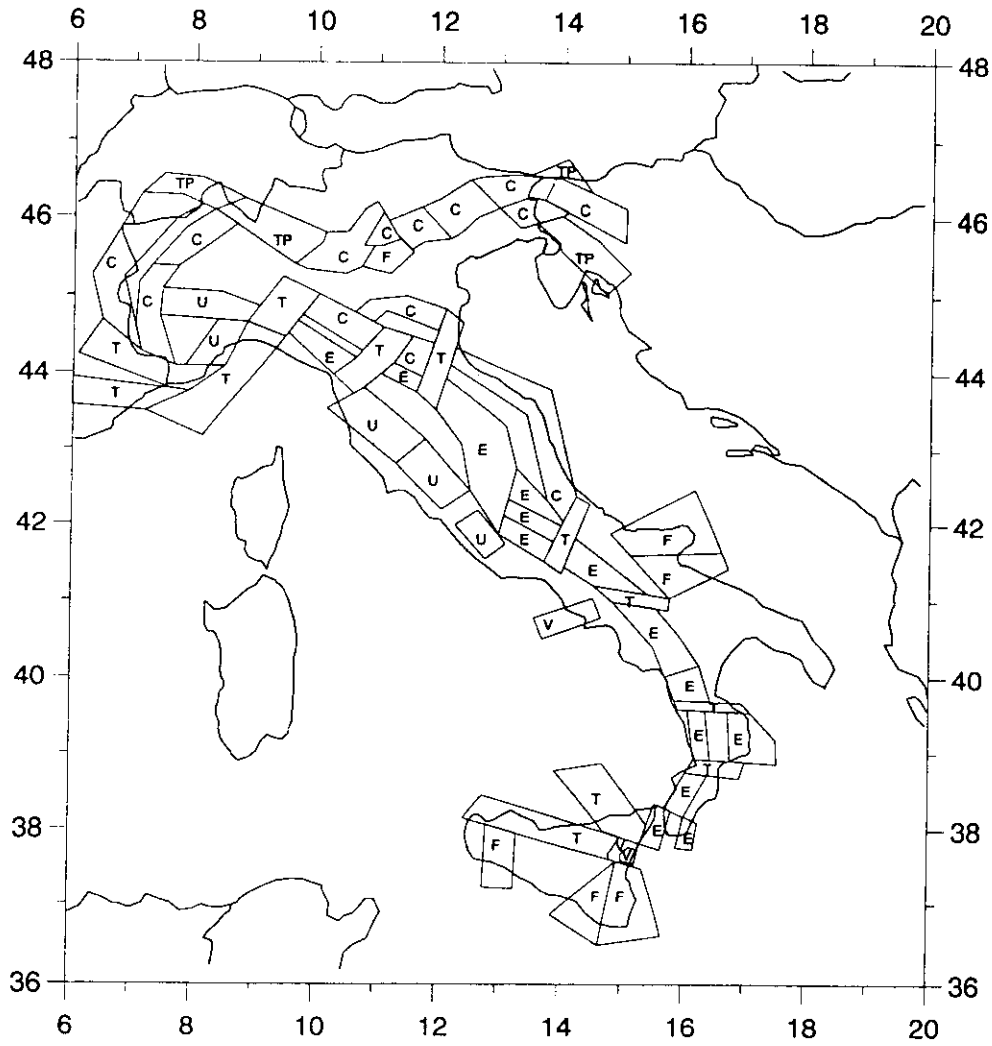

Figure 2
Seismotectonic map of PATACCA *et al.* (1990): *E*) extension areas, *C*) compressional areas, *T*) transition areas, *F*) areas of fracture in foreland zone, *TP*) transpressive areas, *V*) volcanic areas, and *U*) undefined areas.

The analysis of the occurrence, just before the TIPs, of the events with a magnitude greater than the minimum magnitude, m_1, used in the definition of the functions in the CN algorithm, reveals that in all the three-year time intervals which immediately precede the TIPs, it is possible to identify three distinct seismically active areas: the Apennines, the Ancona zone and the Gargano region (compare Fig. 5 with Fig. 6). The seismicity along the Apennines is present during all TIPs, while the events along the eastern border of the Adriatic microplate in the Ancona zone and in the Gargano region, occur only before the false alarms (Figs. 6c,d). This may suggest that the earthquakes along the Apennines are independent from the seismicity of the other two areas (Ancona zone and Gargano region) and that the events in the Ancona zone and in the Gargano region are associated with dynamic processes of the lithospheric blocks, which are different than those

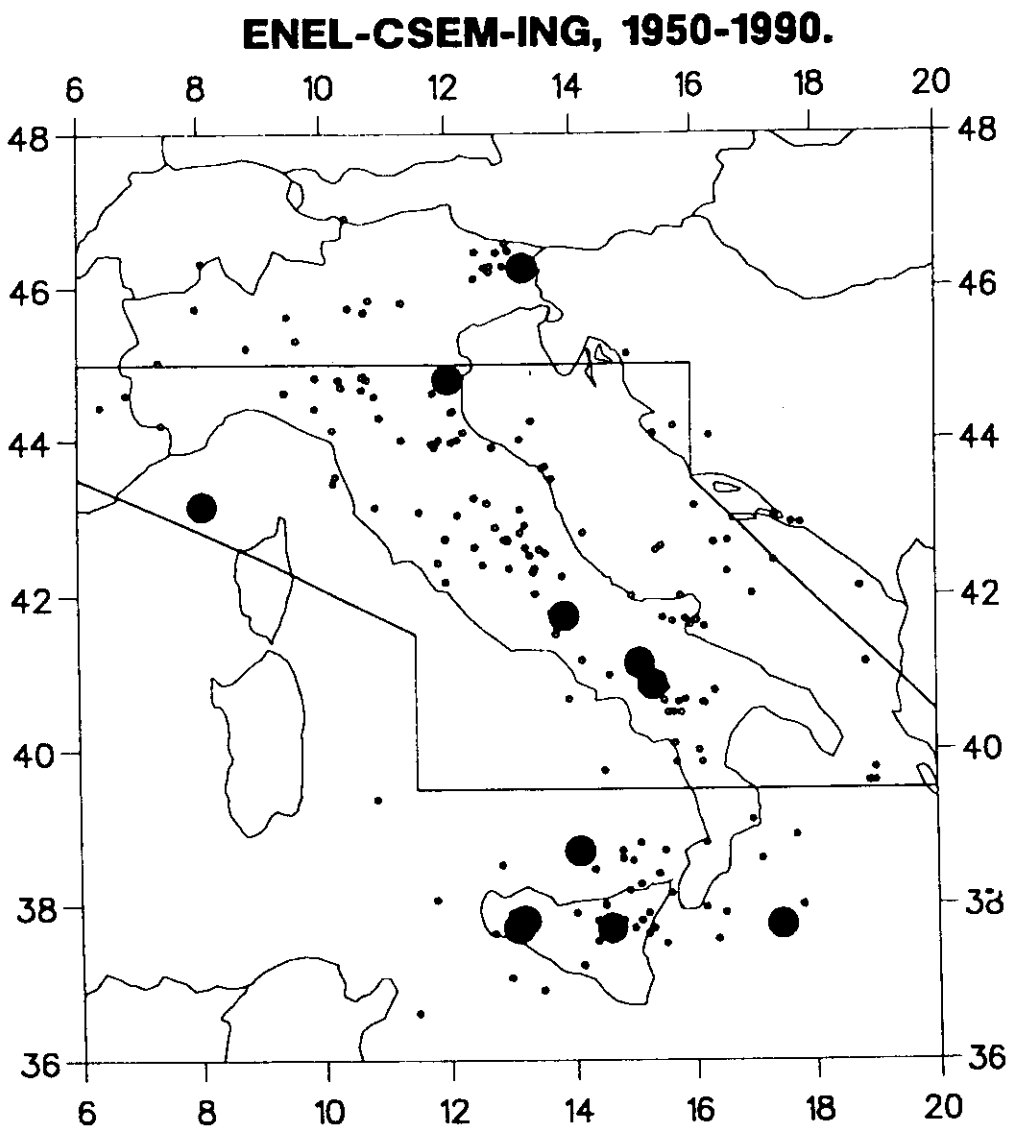

Figure 3

Epicenters recorded in the period 1950–1990; small dots indicate events with magnitude $M \geq 4.4$; large dots indicate events with magnitude $M \geq M_0 = 5.6$; the poligon indicates the boundaries of the regionalization proposed by KEILIS-BOROK *et al.* (1990b).

characterizing the Apennines. The events in the Ancona zone and in the Gargano region can be correlated with the seismicity of the eastern border of the Adriatic microplate (compare Fig. 5 with Fig. 6).

The map of the main shocks in Italy, obtained from the PFG-ING catalogue, shows that there are two maxima in the number of events in the Apennines (Umbria and Lazio) and, in general, a very large number of events along the Apennines from Liguria to Campania (Fig. 7a); this area can be separated from the other seismic regions in Italy. The map of the events with $M \geq m_1 = 4.4$, shown in Fig. 7c, indicates that the earthquakes in the Ancona and Gargano regions can be separated from the events located in the Apennines. The tectonic map by PATACCA

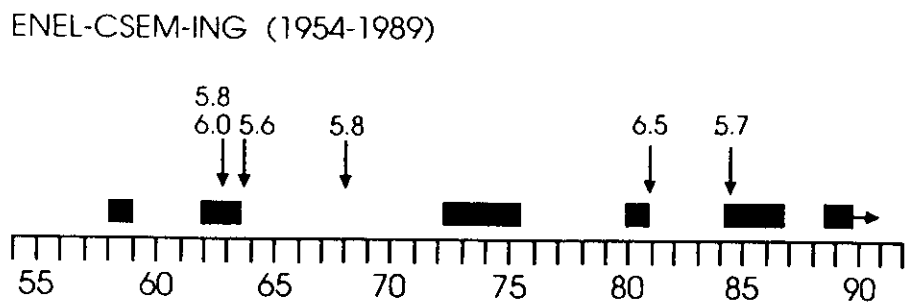

Figure 4
Results of the diagnosis of TIPs, for the regionalization of Figure 2, as deduced from the catalogue ENEL-CSEM-ING; $M_0 = 5.6$. The time of occurence of a strong earthquake is indicated by an arrow and the number above it gives the magnitude; TIPs are indicated by block rectangles (KEILIS-BOROK. *et al.*, 1990b).

et al. (1990) illustrates two nearly parallel NW-SE elongated active areas (Fig. 7b) in the Central Apennines (Toscana, Umbria, Marche). The alignment near the Adriatic Sea is in a compressive state, while the other, more westerly, has an extensional character. The Gargano region has, on the other hand, exhibited a tectonic behavior characterized by the coexistence of mechanisms of dip-slip, oblique-slip, and strike-slip type (PATACCA *et al.*, 1990).

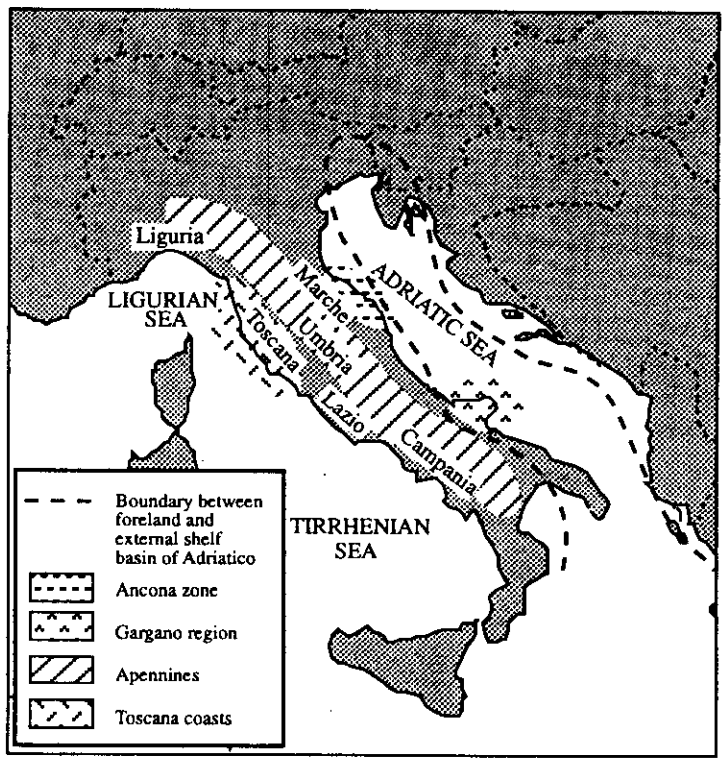

Figure 5
Map showing the boundary between foreland and external shelf basin of Adriatic after HORVARTH and CHANNEL (1976) and other geographical references, mentioned in the text.

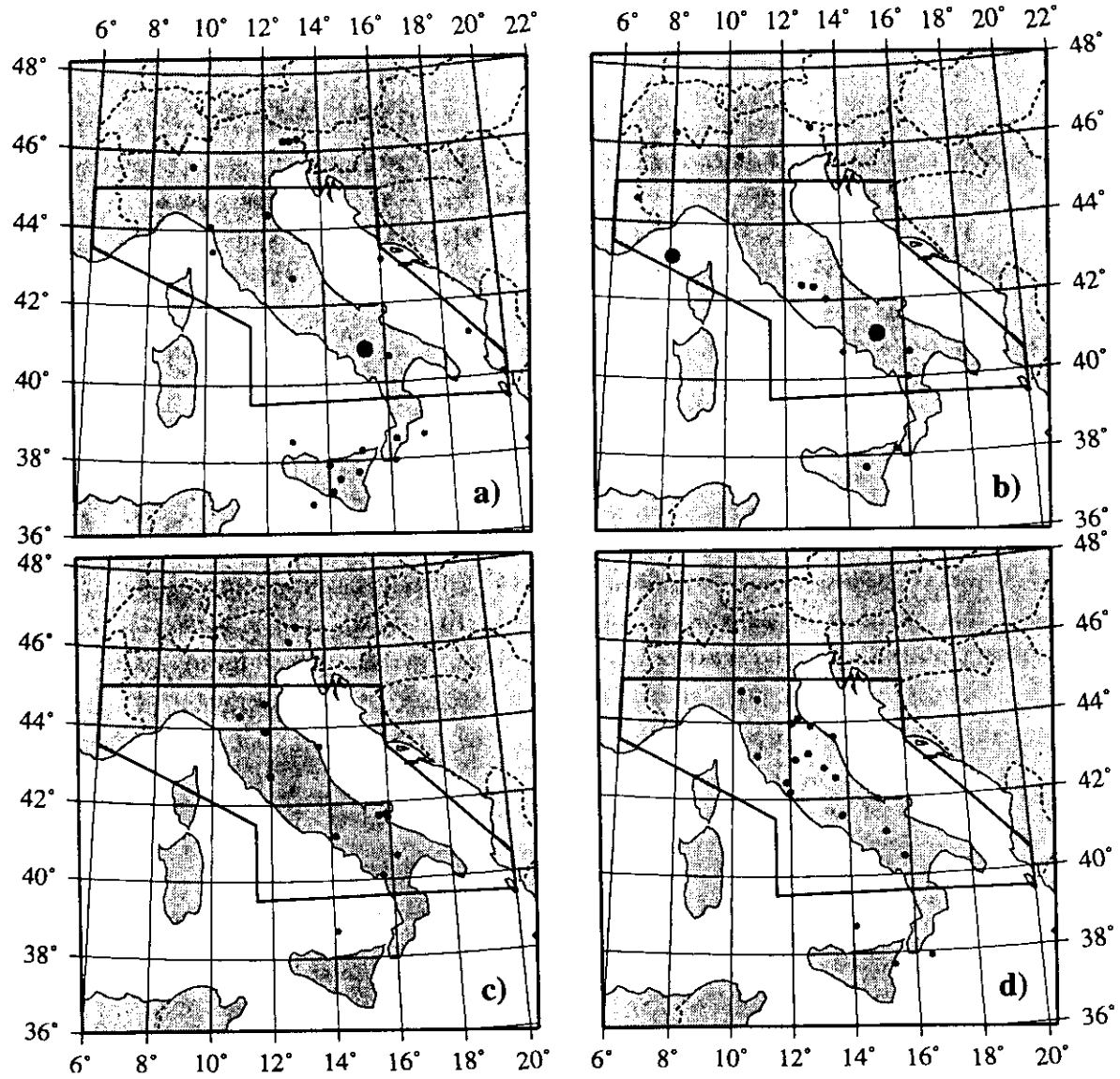

Figure 6
Main shocks (small dots) with $M \geq m_1 = 4.4$ for three years before the TIP, and strong earthquake (large dot). The polygon indicates the boundaries of the regionalization. Only the events inside the PFG polygon are considered; a) the TIP started in 1979; b) the TIP started in 1961; c) the TIP started in 1958; d) the TIP started in 1972.

Taking into account these seismotectonic features, and mainly considering the analysis of the occurrence, just before the TIPs, of the events with a magnitude greater than the minimum magnitude used in the definition of the functions, a new rough regionalization is proposed, which does not cut very active regions and includes the seismicity maxima present in the Apennines and the extensional areas oriented NW-SE, and excludes the Ancona zone and the Gargano region (Fig. 7b). The Ligurian Sea, Tyrrhenian Sea and the coasts of Toscana are excluded, since the very low seismicity in these areas does not occur in the periods just before the TIPs (Fig. 6), and therefore does not influence the functions used by the CN algorithm.

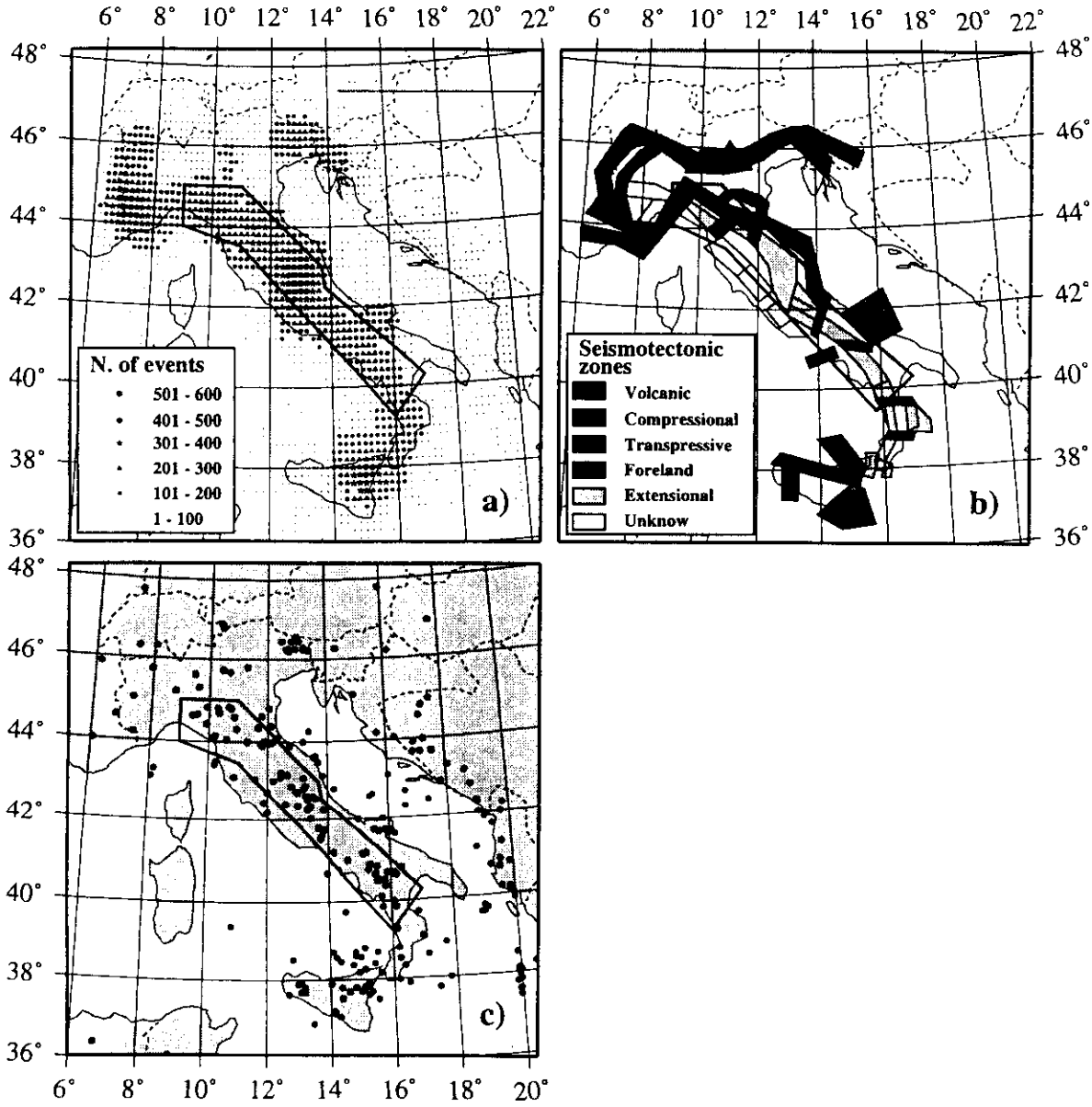

Figure 7

New regionalization for the diagnosis of TIPs superimposed to: a) map of seismicity. In the map it is represented by the total number of earthquakes, smoothed within a 0.6° diameter circle. Each smoothing circle is centered on the knots of a grid of 0.2° × 0.2°. It has been used as the main shocks catalogue from 1000 to 1990 from the PFG-ING catalogue, using the criteria proposed by KEILIS-BOROK *et al.* (1980) for the aftershock identification; b) seismotectonic map of Patacca; c) main events with magnitude $M \geq 4.4$. Catalogue ENEL-CSEM-ING.

The borders deliberately only roughly follow the main seismotectonic features, since we are interested here in describing the results of a first-order refinement of regionalization. A more detailed regionalization, made following the borders of each seismogenetic zone and taking into account their character, will be the subject of a forthcoming paper.

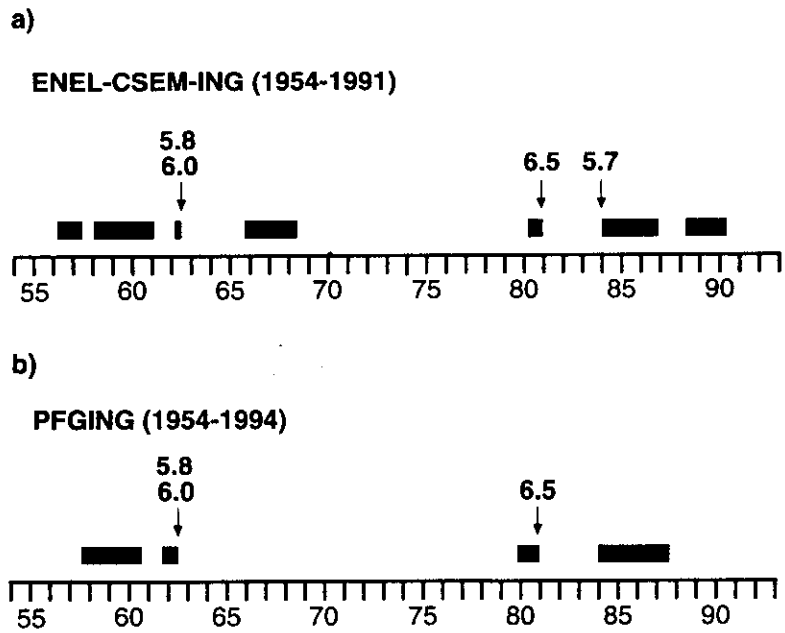

Figure 8

Results of the diagnosis of TIPs for the new regionalization. The time of occurrence of a strong earthquake is indicated by an arrow and the number above it gives the magnitude; TIPs are indicated by block rectangles, a) catalogue ENEL-CSEM-ING, $M_0 = 5.6$; b) catalogue PFG-ING, $M_0 = 5.6$.

The area of the new regionalization is only about the 15% of the one used by KEILIS-BOROK *et al.* (1990b), consequently, the number of earthquakes is significantly reduced. The repetition of the analysis made by KEILIS-BOROK *et al.* (1990b), using the new regionalization and the catalogue ENEL-CSEM-ING, allows us to predict the four strong events with a total alarm period of about 32% of the total time with no failure to predict (Fig. 8a).

In global application, the CN algorithm places about 80% of the strong earthquakes into the alarms occupying 20–40% of the space-time considered (KEILIS-BOROK *et al.*, 1990b). The predictive power of this algorithm is of course stronger than those figures since the expectation time (the volume of alarm until the strong earthquake) is much shorter, around 10 to 20%.

The statistical significance is established strictly to date only for one component of CN algorithm, namely the abnormal clustering used as an independent precursor in different formalizations. The statistical significance of the algorithm CN as a whole is being tested by forward prediction but no final conclusions are reached, and, among others, the forward prediction in Central Italy, performed using the new regionalization proposed in this paper, is a base test for the statistical significance of the algorithm CN.

3. Stability

The test of the stability of the premonitory seismicity pattern and of the feasibility of the prediction has been carried out with respect to changes: 1) in

catalogues, 2) in regionalization, 3) in the length of the learning period, and 4) in the thresholds for the rules to declare a TIP.

A new catalogue (PFG-ING) has been prepared. For the period 1900–1979, the new catalogue is formed by the PFG catalogue, which is the revised version of the ENEL catalogue; from 1980, the ING catalogue has been used. The magnitude M_l (local magnitude) has been considered whenever available; if M_l is not available, the values M_1 (magnitude from intensity), in the PFG catalogue, and M_d (duration magnitude), in the ING catalogue, have been applied.

The learning period, which must extend at least twenty years and have a balanced number of N and D periods, is the period in which the catalogue is analyzed in order to define the values of the thresholds m_1, m_2, m_3 and the values of the functions in the periods immediately before a strong earthquake (D periods) and in the periods without strong earthquakes (N periods). The stability of the premonitory pattern has been successfully tested using two different learning periods, 1954–1980 and 1954–1986. Since within the time interval 1980–1986 there is only one D period, the stability of the results is mainly relevant with respect to changes of m_1, m_2, m_3. The properties that must be satisfied by the learning periods do not permit to consider other larger differences in the time interval employed.

The differences which are present in the available catalogues are quite significant, as can be seen from Figure 1; for example, in the catalogue ENEL-CSEM-ING there are four strong earthquakes with $M \geq 5.6$, while in the PFG-ING catalogue there are only three earthquakes with $M \geq 5.6$. Since the histogram Magnitude-Number of events for the PFG-ING catalogue has a minimum slightly less than $M = 5.4$, and the events with a magnitude above this threshold have a return period of about six years, the analysis is made using the value of $M_0 = 5.4$ also. The results of the processing of both catalogues, for the two different regionalizations and for two different values of M_0, are reported in Table 2. The results are satisfactory and stable, mainly when the regionalization which takes into account seismotectonic considerations is used. In particular, using the PFG-ING catalogue all strong events are predicted and the total alarm occupies about 23% of the total time, a percentage significantly less than the one obtained with the analysis performed with the ENEL-CSEM-ING catalogue (Fig. 8b). The results of the stability analysis confirm that the revision of the ENEL catalogue produced a higher quality data file: the PFG catalogue.

In general, the number of predictable failures is zero or one, and the total alarm time is less than 35% of the total time. In only two cases (variants 4 and 5 in Table 2) is there a large number of failures to predict. In these two cases the catalogue used is the PFG-ING and the regionalization is the one based only on catalogue boundaries and completeness.

The thresholds for the rules to declare a TIP are given by equations (1). The value of the parameters E and V obtained empirically in the California-Nevada region, and subsequently used with success in other regions of the world, are

Table 2

Results of the stability tests of the premonitory seismicity pattern. The old regionalization is the one proposed by KEILIS-BOROK et al. (1990b) and the new is the regionalization proposed in this paper. The old catalogue is the ENEL-CSEM-ING and the new catalogue is the PFG-ING. A is the number of events to be predicted, B is the number of failures to predict, C is the percent of total time occupied by alarms, D is the number of false alarms.

	M_0		Regionalization		Learning period		Catalogue used for learning		Catalogue used for analysis		Threshold parameters		Results			
N°	5.4	5.6	old	new	1954 1980	1954 1986	old	new	old	new	*V*	*E*	*A*	*B*	*C*	*D*
1		X	X			X	X		X		5	4.9	6	1	26.0	5
2		X	X			X		X	X		5	4.9	6	1	33.3	4
3		X	X			X	X			X	5	4.9	4	1	29.6	4
4		X	X			X		X		X	5	4.9	4	3	27.4	4
5	X	X	X		X			X		X	5	4.9	8	4	26.9	2
6	X			X	X			X		X	5	4.9	5	1	37.4	3
7	X			X		X		X		X	5	4.9	5	1	31.9	3
8		X		X	X			X		X	5	4.9	3	0	23.7	2
9		X		X		X		X	X		5	4.9	4	0	31.5	5
10		X		X		X		X		X	5	4.9	3	0	23.3	2

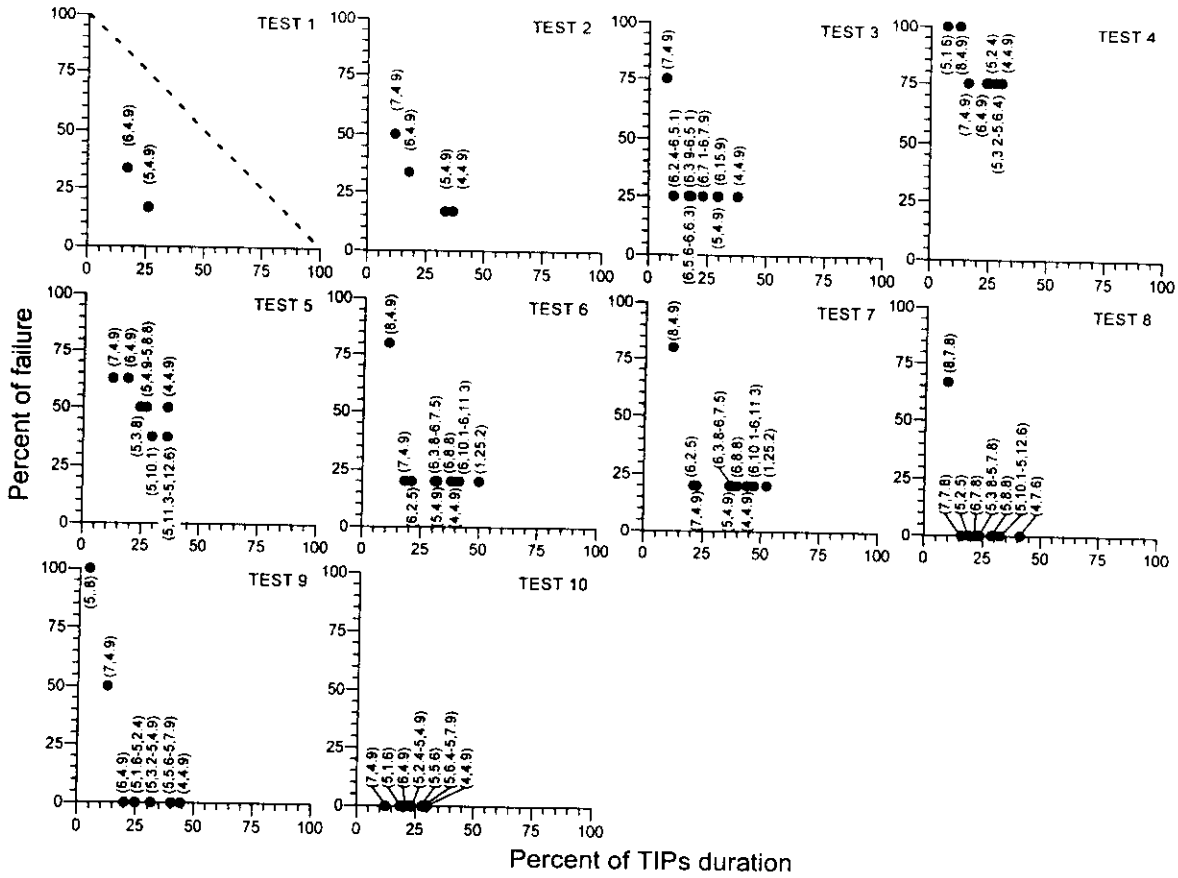

Figure 9

Diagrams [percent of failures to predict] – [percent of TIPs] duration obtained varying the parameters V and E in the tests of Table 5. Between brackets the values of V and E are given in the order. In each test, random results are represented by points outside the triangle (0, 0), (100, 0) (0, 100) shown, for example, in TEST 1 as gray area.

$E = 4.9$ and $V = 5$, as shown in Table 2 (KEILIS-BOROK *et al.*, 1990a). To test the stability of the premonitory pattern, the values of E and V have been changed with respect to the default values. The results obtained changing these two values, for all the variants given in Table 2, are shown in Figure 9. The results are very stable even for variations of E and V in a rather large range. The stability is lost only for extreme values of the two parameters. Figure 9 supplies a measure of the non-randomness of the different predictions: in each test random results are represented by points outside the triangle (0, 0), (100, 0), (0, 100), shown, for example in TEST 1 as gray area. For instance random results are obtained in test 4 with $V = 5$, $E = 1.6$ and with $V = 8$, $E = 4.9$, and test 9 with $V = 5$, $E = 0.8$.

4. *Period 1904–1940*

The analysis of the PFG catalogue reveals that information, sufficiently complete for the use of the algorithm CN, is contained also in the period 1904–1940,

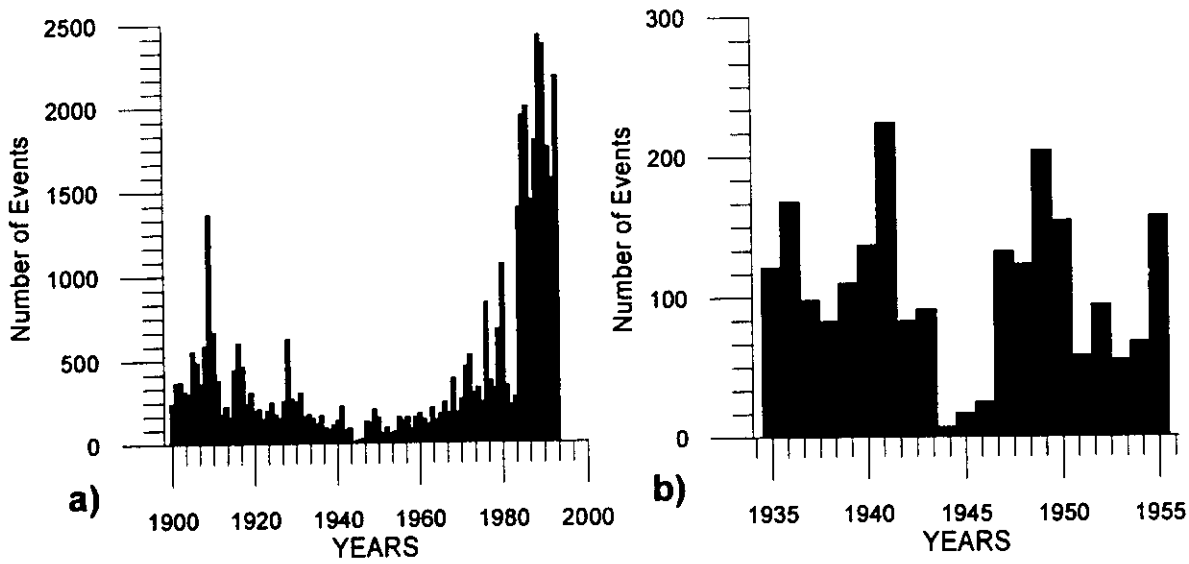

Figure 10
Histogram Magnitude – Number of events in the years: a) 1900–1994; b) 1935–1955.

the incompleteness of the catalogue in the period 1941–1953 being strongly correlated with World War 2 (Fig. 10). Therefore the algorithm CN has been applied to the period 1904–1940, using the same time interval as learning period. The seismicity in this time interval is higher than in the period 1954–1991 and therefore the magnitude, M_0, corresponding to events with a return period of about

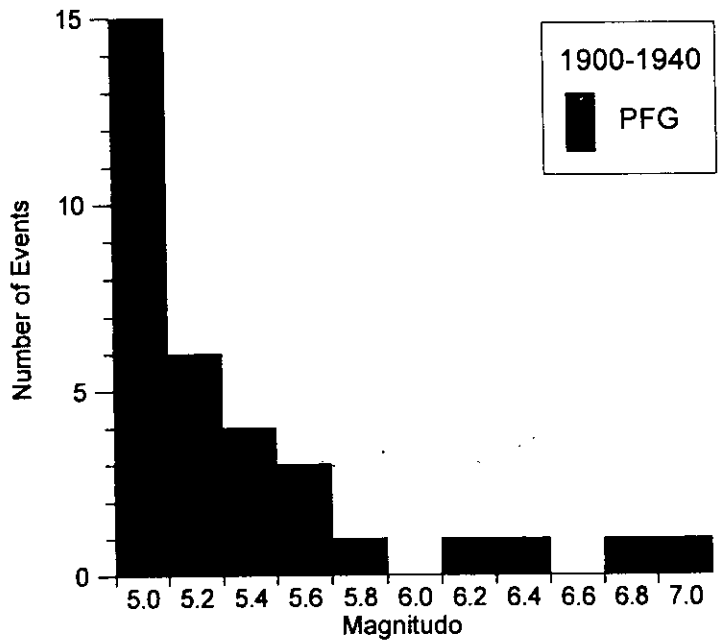

Figure 11
Histogram Magnitude – Number of events, with step of 0.2 in magnitude, in the years 1900–1940 for the new regionalization proposed in the paper. Catalogue PFG.

Table 3

Results obtained from the analysis of two different periods, 1904-1940 and 1954-1990, characterized by different seismicity levels. A is the number of events to be predicted, B is the number of failures to predict, C is the percent of total time occupied by alarms, D is the number of false alarms

	M_0		Learning period		Analysis period		Threshold parameters		Results			
			1904	1954	1904	1954						
N°	5.6	6.0	1940	1980	1940	1990	*V*	*E*	*A*	*B*	*C*	*D*
1		X	X		X		5	4.7	3	1	38.0	7
2		X	X			X	5	4.7	2	1	33.6	5
3	X			X		X	5	4.9	3	0	23.7	2
4	X		X		X		5	3.1	7	4	22.3	5
5	X			X	X		5	3.1	7	3	40.0	8
6	X		X			X	5	4.9	3	2	16.1	2

six years and to a minimum in the histogram Number of events – Magnitude, i.e., the M_0 satisfying the CN rule, is around 6.0 (Fig. 11).

The results obtained for $M_0 = 6.0$ are reported in Table 3, variant 1. The number of strong events is three; two of them are predicted, and the alarm occupies about 38.0% of the total time (Fig. 12). If, breaking the CN rule, the value of M_0 is decreased to 5.6, equal to the threshold M_0 used for the period with lower

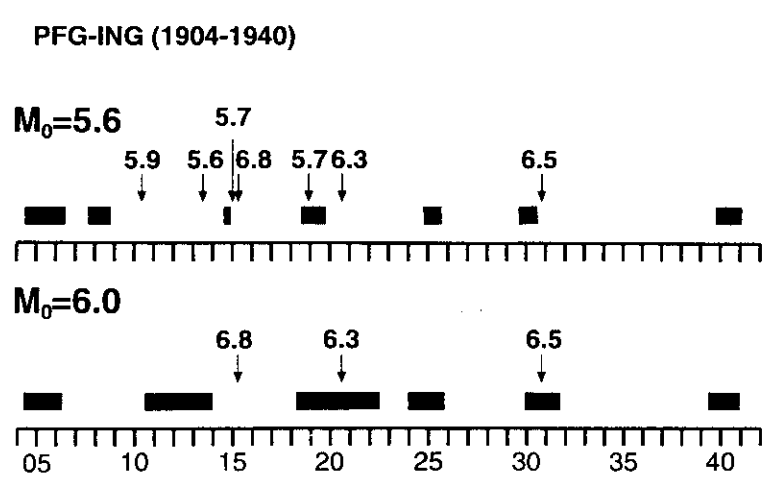

Figure 12

Results, based on catalogues PFG-ING, of the diagnosis of TIPs for the new regionalization; and for two different thresholds M_0. The time of occurrence of a strong earthquake is indicated by an arrow and the number above it gives the magnitude; TIPs are indicated by block rectangles.

seismicity 1950–1994, the number of strong events becomes seven and the performance of the algorithm is very poor: three events are predicted, and the alarm duriation is equal to 22.3% of the total time (variant 4, Table 3).

Even if the level of seismicity in the time interval 1904–1940 is considerably higher than in the period 1954–1994, the good results of the diagnosis of TIPs for each interval separately indicate that self-similarity characterizes the seismicity of the two periods.

5. Conclusion

A significant reduction of the spatial uncertainty in the identification of a TIP has been obtained using a regionalization based not only on catalogue completeness but also on seismotectonic evidences. The use of such regionalization, in general, increases the stability of the premonitory pattern. All the stability tests demonstrate that the CN algorithm in Central Italy produces very stable results.

Our research suggests use of the catalogue PFG-ING, the new regionalization, and the threshold $M_0 = 5.6$, for the routine forward monitoring, which satisfies the condition of having a return period approaching six years.

The analysis of the period 1904–1940 shows that even when the catalogue completeness threshold corresponds to a magnitude as high as 4.0, the CN algorithm still supplies useful information. The comparison of the results obtained during the periods 1904–1940 and 1954–1994 supplies further evidence favoring the existence of self-similarity in the occurrence of earthquakes (e.g., KAGAN and KNOPOFF, 1981).

Acknowledgments

The authors are very grateful to Prof. V. I. Keilis-Borok, Drs. A. Gabrielov and S. Schreider for stimulating discussions. One of the authors, (I. M. Rotwain), thanks ICTP for financial support for her stay in Trieste, during which a large part of this work was undertaken. We acknowledge financial support from MURST (40% and 60%) funds, CNR-Gruppo Nazionale per la difesa dai Terremoti contracts nos. 91.02539.54, 92.02867.54 and NATO linkage grants SA. 12-2-02 (ENVIRLG 931206) and SA. 12-5-02 (CN. SUPPL 94880).

REFERENCES

DELLA VEDOVA, B., MARSON, I., PANZA, G. F., and SUHADOLC, P. (1991), *Upper Mantle Properties of the Tuscan-Tyrrhenian Area: A Key for Understanding the Recent Tectonic Evolution of the Italian Region*, Tectonophys. *195*, 311–318.

CALCAGNILE, G., and PANZA, G. F. (1981), *The Main Characteristics of the Lithosphere-astenosphere System in Italy and Surrounding Regions*, Pure and Appl. Geophys. 119, 865–879.

CSEM, *European-Mediterranean Hypo-centers Data File* 1976–1988 (Csem, Strasbourg 1989).

ENEL, *Catalogue of Earthquake of Italy, Years 1000–1980* (Publication ENEL, Roma 1980).

GABRIELOV, A. M., DMITRIEVA, O. E., KEILIS-BOROK, V. I., KOSOBOKOV, V. G., KUZNETSOV, I. V., LEVSHINA, T. A., MIRZOEV, K. M., MOLCHAN, G. M., NEGMATULLAEV, S. Kh., PISARENKO, V. F., PROZOROV, A. G., RINEHART, W., ROTWAIN, I. M., SHLBALIN, P. N., SHNIRMAN, M. G., and SCHREIDER, S. Yu (1986), *Algorithms of Long-term Earthquakes' Prediction*, International School for Research Oriented to Earthquake Prediction-algorithms, Software and Data Handling (Lima, Peru, 1986).

HORVATH, F., and CHANNEL, J. E. T. (1976), *Further evidence relevant to the African/Adriatic promotory as a paleogeographic premise for Alpine orogency*, International Symposium on the Structural History of the Mediterranean Basins, Split (Yugoslavia) 25–29 October 1976 (eds. Biju-Duval, B. and Montadert, L.) (EDITIONS TECHNIP, Paris 1977), pp. 133–142.

ING, *Seismological Reports 1980–1991* (ING, Roma 1982–1991).

KAGAN, Y. Y., and KNOPOFF, L. (1981), *Stochastic Synthesis of Earthquake Catalogs* Geophys. J. R. Astr. Soc. *86*, 303–320.

KEILIS-BOROK, V. I., KNOPOFF, L., and ROTWAIN, I. M. (1980), *Burst of Aftershocks, Long-term Precursors of Strong Earthquakes*, Nature *283* (5744), 259–263.

KEILIS-BOROK, V. I., KNOPOFF, L., ROTWAIN, I., and ALLEN, C. R. (1988), *Intermediate-term Prediction of Occurence Times of Strong Earthquakes*, Nature *335* (6192), 690–694.

KEILIS-BOROK, V. I., and ROTWAIN, I. (1990a), *Diagnosis of Time of Increased Probability of Strong Earthquakes in Different Regions of the World: Algorithm CN*, Phys. Earth Planet. Inter. *61*, 57–72.

KEILIS-BOROK, V. I., KUZNETSOV, I. V., PANZA, G. F., ROTWAIN, I. M., and COSTA, G. (1990b), *On Intermediate-term Earthquake Prediction in Central Italy*, Pure Appl. Gesphys. *134*, 79–92.

MARSON, I., PANZA, G. F., and SUHADOLC, P. (1994), *Crust and Upper Mantle Models along the Active Tyrrhenian Rim*, Terra Nova, in press.

PANZA, G. F., MUELLER, S., CALCAGNILE, G., and KNOPOFF, L. (1982), *Delineation of the North Central Italian Upper Mantle Anomaly*, Nature *296*, 238–239.

PATACCA, E., SARTORI R., and SCANDONE, P. (1990), *Tyrrhenian Basin and Apenninic Arcs: Kinematic Relation since Late Tortonian Times*, Mem. Soc. Geol. It. *45*, 425–451.

PFG, *Catalogo dei terremoti italiani dall'anno 1000 al 1980* (ed. Postpischl, D.) (CNR-P.F. Geodinamica 1985).

SUHADOLC, P., and PANZA, G. F. (1988), *The European-African Collision and its Effects on the Lithosphere-asthenosphere System*, Tectonophys. *146*, 59–66.

(Received May 16, 1994, accepted January 5, 1995)

8.

Seismic Input Modelling for Zoning and Microzoning

G. F. Panza, F. Vaccari, G. Costa, P. Suhadolc, and D. Fäh

The strong influence of lateral heterogeneities and of source properties on the spatial distribution of ground motion indicates that the traditional methods require an alternative when earthquake records are not available. The computation of broad-band synthetic seismograms makes it possible, as required by a realistic modelling, to take source and propagation effects into account, fully utilizing the large amount of geological, geophysical and geotechnical data, already available. For recent earthquakes, where strong motion observations are available, it is possible to validate the modelling by comparing the synthetic seismograms with the experimental records. The realistic modelling of the seismic input has been applied to a first-order seismic zoning of the whole territory of several countries. Even though it falls in the domain of the deterministic approaches, the method is suitable to be used in new integrated procedures which combine probabilistic and deterministic approaches and allow us to minimize the present drawbacks which characterise them when they are considered separately. Detailed modelling of the ground motion for realistic heterogeneous media (up to 10 Hz) can be immediately used in the design of new seismo-resistant constructions and in the reinforcement of existing buildings, without having to wait for a strong earthquake to occur. The discrepancies between the ground responses computed with standard methods and the results of our detailed modelling cannot be ignored when formulating building codes and retrofitting the built environment.

1. INTRODUCTION

The guidelines of the United Nations sponsored International Decade for Natural Disaster Reduction (IDNDR), for the drawing up of pre-catastrophe plans of action, have led to the consolidation of the idea that zoning can and must be used as a means of prevention in areas that have not yet been hit by disaster but are potentially prone to it. The optimisation of techniques

(GFP,FV,GC,PS) Univ. di Trieste - Dip. di Scienze della Terra, via Weiss 1, I-34127 Trieste, Italy
(GFP,FV,GC,PS) ICTP, SAND Group, P.O.Box 586, I-34100 Trieste, Italy
(FV) CNR - Gruppo Nazionale per la Difesa dai Terremoti, via Nizza 128, I-00198 Roma, Italy
(DF) Institut für Geophysik - ETH Hönggerberg Zürich - CH-8093 Switzerland

©Earthquake Spectra, Volume 12, No. 3, August 1996

aimed at prevention will be one of the basic themes of the development of seismic zoning in the 21st century.

The first scientific and technical methods developed for zoning were deterministic and based on the observation that damage distribution is often correlated to the spatial distribution and the physical properties of the underlying terrain and rocks. The 1970s saw the beginning of the construction of probabilistic seismic zoning maps on a national, regional and urban (microzoning) scale. In the 1990s these instruments for the mitigation of seismic hazard are coming to prevail over deterministic cartography.

The most controversial question in the definition of standards to be used in the evaluation of seismic hazard may be formulated as follows: should probabilistic or deterministic criteria and methods be used? At the current level of development in the modelling of seismogenesis and of seismic wave propagation the best policy for the future is to combine the advantages offered by both methods, using integrated approaches (e.g. Reiter, 1990). In this way, among others, we have the main advantage of making possible the extension of seismic zoning to long periods, a period band up to now almost totally ignored by all methods, but that is acquiring a continuously increasing importance, due to the widespread existence in the built environment of special objects, with relatively long free periods.

Studies carried out following the most recent strong earthquakes (e.g. the 1985 Michoacan earthquake) have proved to be important sources of basic knowledge and have acted as catalysts for the use of zoning in seismic risk management. The impetus for this has come essentially from politicians and administrators particularly interested in rapid reconstruction according to criteria which reduce the probability of a repetition of disasters. These post-earthquake studies have led to the conclusion that the destruction caused by an earthquake is the result of the interaction of three complex systems: 1) the solid earth system, made up of a) the seismic source, b) the propagation of the seismic waves, c) the geometry and physical conditions of the local geology; 2) the anthropised system, whose most important feature in this context is the quality of constructions (buildings, bridges, dams, pipelines, etc.); 3) the social, economic and political system, which governs the use and development of a settlement before it is struck by an earthquake.

The most recent results have shown that in an anthropised area it is now technically possible to identify zones in which, by virtue of physical parameters of source, propagation and local conditions, the most serious damage can be predicted. Actual examples of this capability, closely linked to the ability to calculate realistic synthetic seismograms, are illustrated in Section 2.4.

With the knowledge acquired to date, a drastic change is required in the orientation of zoning, that must no longer be considered a post-disaster activity. It is necessary to proceed to pre-disaster surveys that can be usefully employed to mitigate the effects of the next earthquake, using all available technologies. As clearly indicated by the recent events in Los Angeles (1994) and Kobe (1995) we cannot confine ourselves to using what has been learned from a catastrophe in the area in which it took place, we must be able to take preventive steps, extending, in a scientifically-acceptable way, results obtained to areas in which no direct experience has yet been

gained. An opportunity is offered in this direction by the scientific community's ability to make realistic simulations of the behaviour of the solid earth system through the computation of increasingly realistic synthetic seismograms, with a broad frequency content. Thus seismic zoning can use scientific data banks, integrated in an expert system, by means of which it is possible not only to identify the safest and most suitable areas for urban development, taking into account the complex interaction between the solid earth system, the environmental system and the social, economic and political system, but also to define the seismic input that is going to affect a given building. The construction of an integrated expert system will make it possible to tackle the problem at its widest level of generality and to maintain the dynamic updating of zoning models, made necessary by the acquisition of new data and the development of new model-building methods.

2. DETERMINISTIC ZONING USING SYNTHETIC SEISMOGRAMS

The procedure for the deterministic seismic zoning developed by Costa et al. (1992, 1993) represents one of the new and most advanced approaches and can, at the same time, be used as a starting point for the development of an integrated approach that will combine the advantages of the probabilistic and of the deterministic methods, thus minimising their drawbacks.

Synthetic seismograms are constructed to model ground motion at the sites of interest, using the knowledge of the physical process of earthquake generation and wave propagation in realistic media. In first-order zoning a database of seismograms covering the area of interest (at a regional scale) is computed, taking into account the effects of lateral heterogeneities in a rough way. Synthetic seismograms are efficiently generated by the modal summation technique (Panza, 1985; Florsch et al., 1991), so it becomes possible to perform detailed parametric analyses at reasonable costs. For example, different source and structural models can be taken into account in order to create a wide range of possible scenarios from which to extract essential information for decision making. In this sense, an efficient technique, based on the analytical computation of partial derivatives, is currently under development.

Once the parametric analysis is performed and the gross features of the seismic hazard are defined, a more detailed modelling of ground motion, which can take into account the local geological and geotechnical conditions at a specific site of interest, is possible using the hybrid approach which combines, for the description of wave propagation in anelastic heterogeneous media, the modal summation with finite differences techniques (Fäh et al., 1990; Fäh, 1992). This deterministic modelling goes well beyond the conventional deterministic approach taken in hazard analyses - in which only a simple wave attenuation relation is invoked - in that it includes full waveform modelling.

2.1. FIRST-ORDER ZONING OF THE ITALIAN TERRITORY

Starting from the available information on the Earth's structure, seismic sources and the level of seismicity of the investigated area, it is possible to estimate the maximum ground

acceleration, velocity and displacement in a given frequency band (AMAX, VMAX and DMAX respectively) or any other parameter relevant to seismic engineering, which can be extracted from the computed theoretical signals. This procedure allows us to obtain a realistic estimate of the seismic hazard also in those areas for which scarce (or no) historical or instrumental information is available, and to perform the relevant parametric analyses.

To reduce the amount of computations the seismic sources can be grouped into homogeneous seismogenic areas, and for each group the representative focal mechanism can be kept constant. The scalar seismic moment associated with each source is determined from the analysis of the maximum magnitude observed in the epicentral area. The flow-chart of the procedure is shown in Figure 2.1.

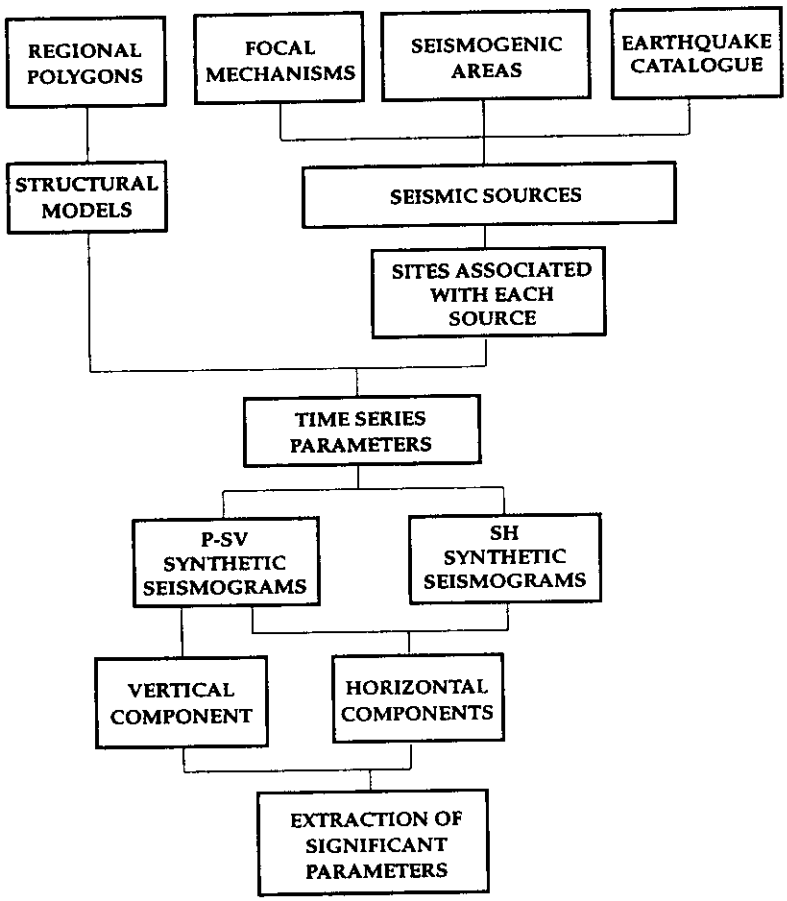

Figure 2.1 Flow chart describing the procedure for the first-order zoning of a territory (after Costa et al., 1993).

2.1.1. Synthetic models

The detailed description of the input data used in the procedure shown in Figure 2.1 is given by Costa et al. (1993) and Panza and Vaccari (1994). The NT file prepared by GNDT (Stucchi et al., 1993) and the ING (1980-1991) seismological reports are used for the definition of seismicity. The smoothed magnitude distribution for the cells belonging to the seismogenic zones defined by GNDT (1992) is given in Figure 2.2.

The synthetic signals are computed for an upper frequency limit of 1 Hz, and the point-source approximation is still acceptable. This is justified by practical considerations, since, for instance, several-story buildings might have a peak response in the frequency range around 1 Hz (e.g. Manos and Demosthenous, 1992) and by the fact that modern seismic design approaches and technologies, like seismic isolation, tend to lower the free oscillation frequencies of buildings.

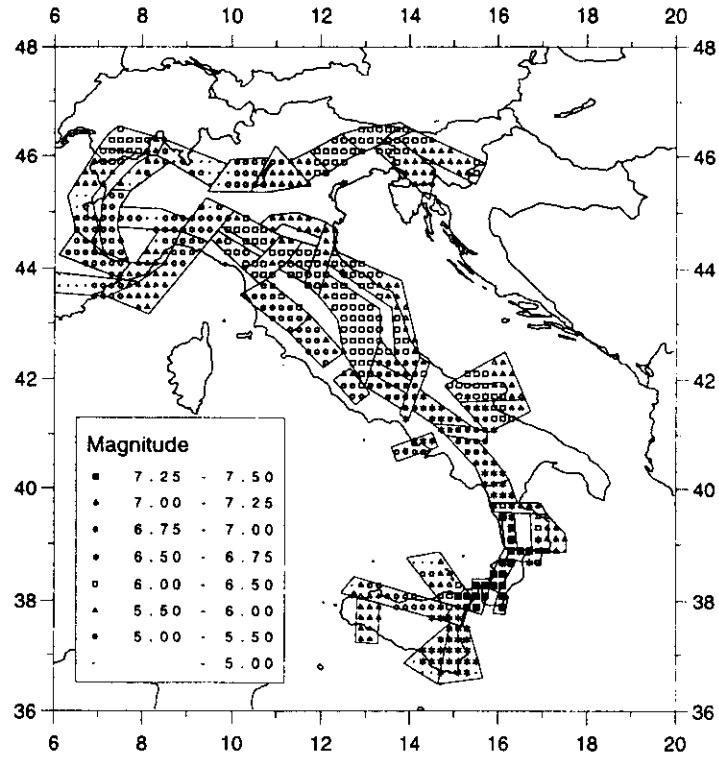

Figure 2.2 Smoothed magnitude distribution (Panza et al., 1990) for the cells belonging to the seismogenic zones defined by GNDT (1992).

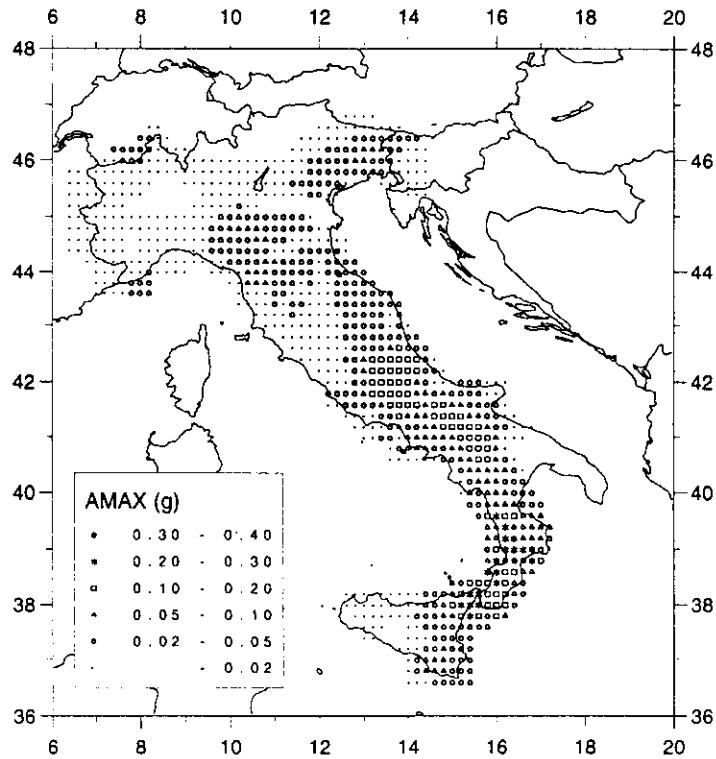

Figure 2.3a Horizontal AMAX (expressed in fractions of g, acceleration of gravity) distribution for Italy, obtained as a result of the application of the procedure described in Figure 2.1. Maximum frequency 1 Hz.

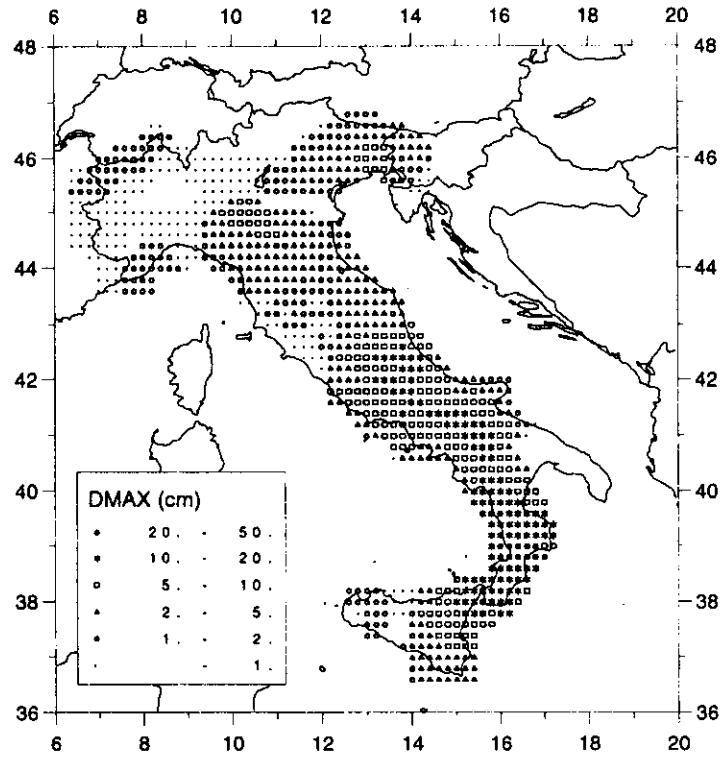

Figure 2.3b Horizontal DMAX distribution for Italy, obtained as a result of the application of the procedure described in Figure 2.1. Maximum frequency 1 Hz.

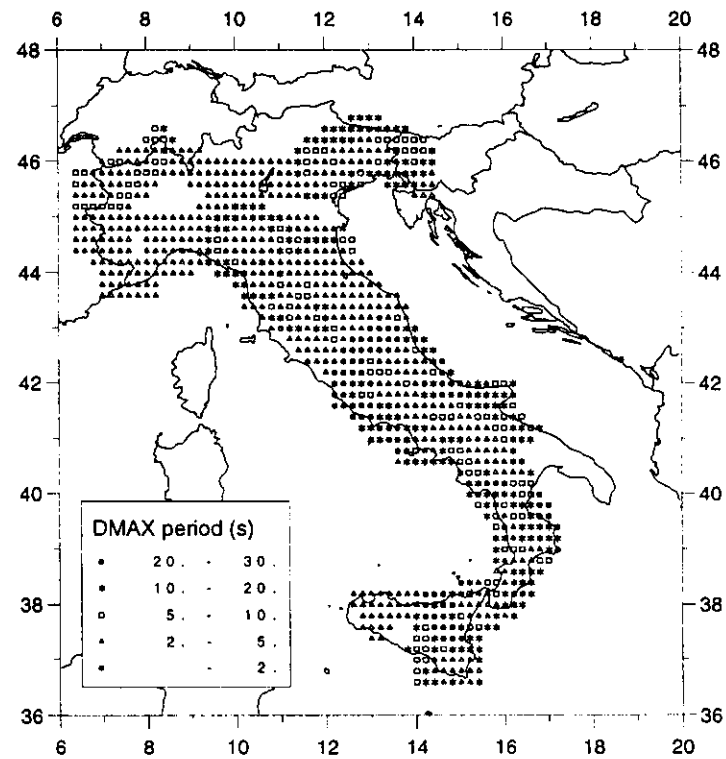

Figure 2.3c Periods, in seconds, characterised by the maximum amplitude, determined from the spectral analysis of the signals from which the DMAX values of Figure 2.3b have been derived.

P-SV (radial and vertical components) and SH (transverse component) synthetic seismograms are computed for a point-source with seismic moment of 10^{-7} Nm. The amplitudes are then properly scaled to a finite dimension source according to the (smoothed) magnitude (to be conservative we have assumed that all magnitude values given in the NT file are M_s) associated with the cell of the source, using the moment-magnitude relation given by Kanamori (1977) and the spectral scaling law proposed by Gusev (1983).

Among the parameters representative of the strong ground motion we have, for the moment, focused our attention on the maximum ground acceleration and displacement (AMAX and DMAX) in the considered range of frequencies (i.e. for frequencies up to 1 Hz). Since we compute the complete time series we are not limited to this choice, and it is also possible to consider other parameters, like Arias intensity (Arias, 1970) or other integral quantities that can be of interest in earthquake engineering or engineering seismology. Since recordings of many different sources are associated to each site, different maps can be produced. If one single value is to be plotted on a map (e.g. Figure 2.3), then only the maximum value of the analysed parameter is considered (e.g. maximum accelerations and displacements respectively in Figures 2.3a and b). In Figure 2.3c the periods associated with the displacements shown in Figure 2.3b are shown. It can be seen that in some regions, like for instance Central Italy around latitude 42°, long periods in the range between 20s and 30s are dominating. They are related with signals generated by strong earthquakes occuring at large distance from the site (about 90km), while the magnitude of the closer events, which are responsible for the higher frequencies (between 2s and 5s in our computations), is not big enough to let high frequencies dominate the scenario.

The results of the deterministic procedure are particularly suitable for civil engineers as seismic input for the design of special buildings. In fact, the relevance of the displacements at periods of the order of 10s or so is a particularly relevant issue for seismic isolation and in general for lifelines with large linear dimensions, like bridges and pipelines, where differential motion plays a relevant role on their stability.

2.1.2. Validation of the synthetic models against independent observations

A quantitative validation is made using the observed accelerograms recorded during the Irpinia earthquake on 23 November 1980 and the Friuli earthquake on 6 May 1976. The source rupturing process of the Irpinia event is very complex (e.g., Bernard and Zollo, 1989) and the dimension of the source has been estimated to be of the order of several tens of km. Nevertheless, it seems that the signal recorded at the station of Sturno is mostly due to a single sub-event that occurred rather close to the station itself, while the energy contributions coming from other parts of the source seem unimportant (Vaccari et al., 1990). With the cut-off frequency at 1 Hz, the horizontal components accelerograms recorded at Sturno have been low-pass filtered to be compared with the computed signals for the Irpinia region. The example shown in Figure 2.4a refers to the NS component but the same considerations can be applied to the EW component of motion. The early phases and the AMAX of the recorded signal (upper trace) and the synthetic one computed in the point-source approximation (middle trace), are in good agreement. The later part of the observed recording is more complicated and this is mostly related to the complexity of the

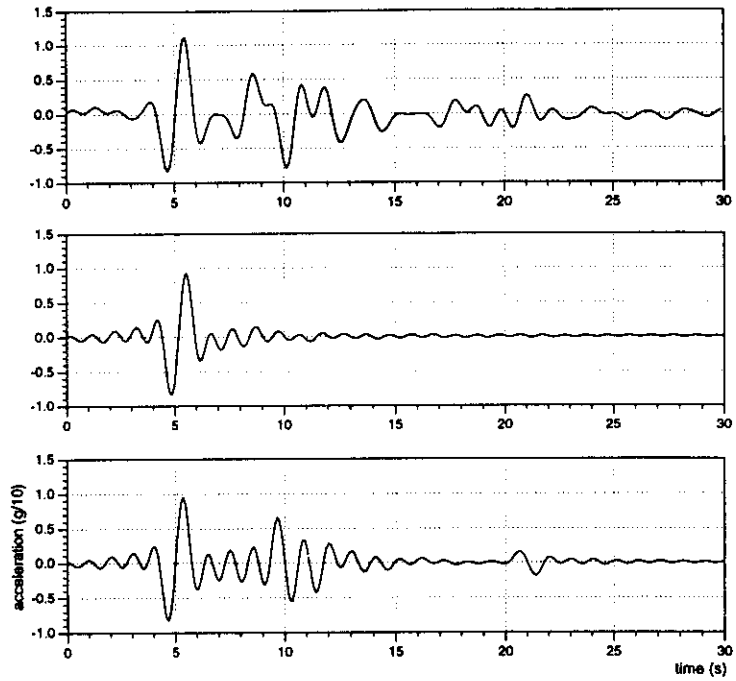

Figure 2.4a Irpinia (Southern Italy). Comparison between NS acceleration recorded at the Sturno station during the Irpinia earthquake of 23 November, 1980 (upper trace), one synthetic signal computed for that area (middle trace) in section 2.1.2 and the sum of four synthetic sub-events built using the middle trace (with proper weights and time shifts). Accelerations are low-pass filtered with a cut-off frequency of 1Hz.

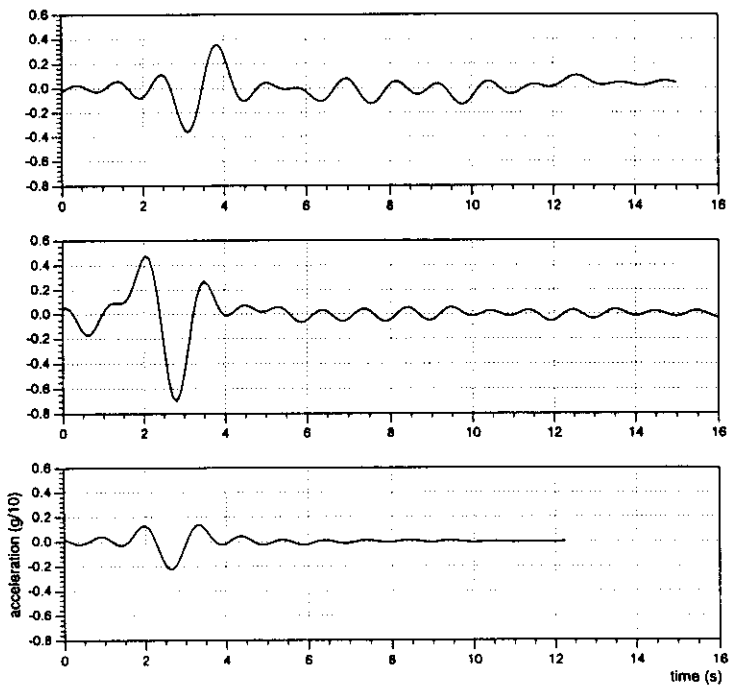

Figure 2.4b Friuli (Northern Italy). Comparison between NS acceleration recorded at the Tolmezzo station (upper trace) and two synthetic signals computed for that area (middle and lower traces).

source, which is deliberately neglected in the computation of the synthetic signal, to be used in the first-order zoning. The lower trace is shown as an example of modelling of the source complexity. It is the result of a superposition of four sub-events, each one modelled with the middle trace properly weighted and shifted in time accordingly with the model by Vaccari et al. (1990).

The same approach has been used in the comparison between the NS component recorded at Tolmezzo during the Friuli (1976) earthquake (Figure 2.4b, upper trace) and two synthetic signals obtained for that area (middle and lower traces). In the case of the Friuli event, the point-source approximation seems to be a sufficient approximation even for an event with M_S=6.1.

2.2. FIRST ORDER ZONING OF ETHIOPIA

Gouin (1976) produced the first seismic hazard map of Ethiopia using a probabilistic approach. Since the production of that map, quite a large number of destructive earthquakes have occurred in the country causing damages both to property and human life. Furthermore, destructive earthquakes that occurred in the neighbouring countries are not included in the production of the first map. Following the procedure described in section 2.1, Kebede and Vaccari (1996), produced a new seismic hazard map of Ethiopia and northern neighbouring countries.

The smoothed magnitude distribution for the seismogenic zones is given in Figure 2.5. The

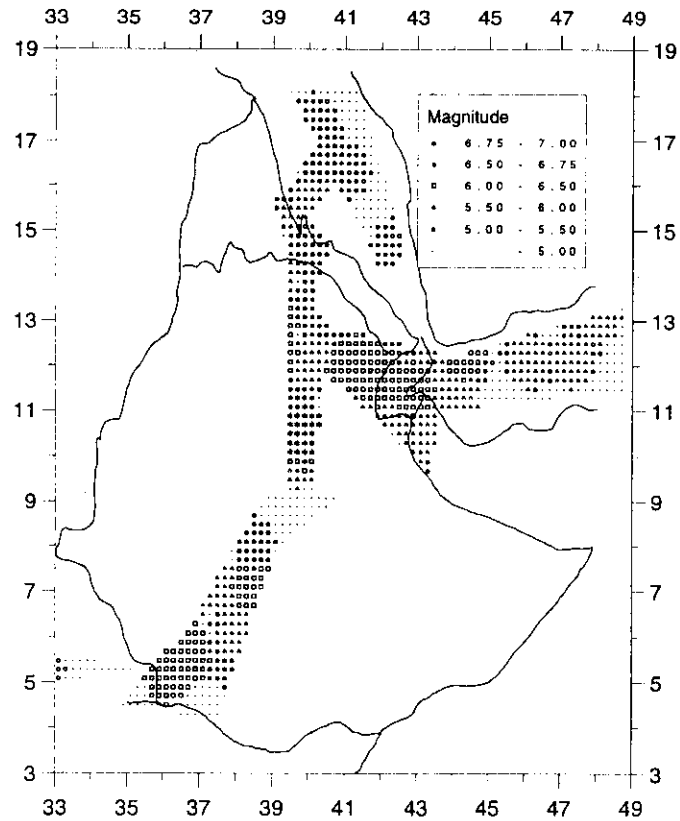

Figure 2.5 Smoothed magnitude (M_L) distribution for the cells belonging to the seven seismogenic zones, defined for Ethiopia after Kebede and Vaccari (1996).

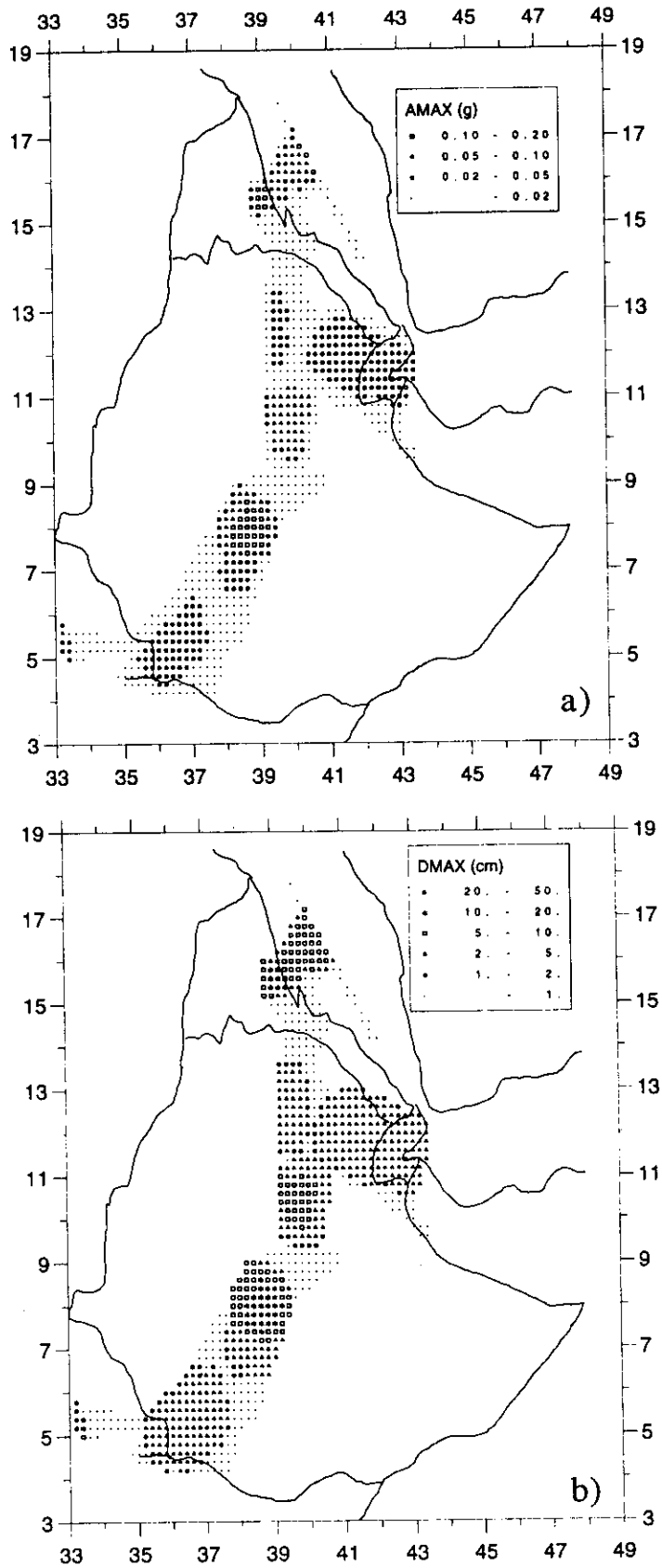

Figure 2.6 Horizontal AMAX (a) and DMAX (b) distribution for Ethiopia after Kebede and Vaccari (1996). Maximum frequency 1 Hz.

focal mechanisms and other related source parameters for the representative earthquakes that occurred in the seven seismogenic zones and the three main lithospheric structures (one for the rift and two for the eastern and western plateaux) used in this study, are based on the existing literature. The different magnitudes present in the earthquake catalogue have been converted to M_L, therefore, the magnitude-moment relation proposed by Boore (1987) has been used instead of the relation by Kanamori (1977).

Figure 2.6a shows the zoning map obtained for the region under study from the calculated AMAX, as a fraction of g (acceleration due to gravity). A glance at the figure shows that the higher values of AMAX (0.1 - 0.2g) are obtained for the main Ethiopian rift around latitude 8°N and in Eritrea around latitude 15°N, and are compatible with the values estimated by Gouin (1976) using a probabilistic approach. The corresponding displacements DMAX can be found in Figure 2.6b.

Given that the main Ethiopian rift is a region where various economic development activities are currently undertaken, and knowing that in this region the seismic hazard is high, necessary precautions should be taken both in the development of the new built environment and in the reinforcement of the existing one.

The seismic region of central and eastern Afar belongs to a different scenario. This area is characterised by the occurrence of intermediate-size earthquakes with M_L never exceeding 6.2. Even though the seismic activity rate is high (about 4 earthquakes per year with $m_b \geq 4.6$), a relatively low (as compared to that of the main Ethiopian rift) AMAX value is obtained for the region. The probabilistic approach used by Gouin (1976) leads to more conservative results than the deterministic one.

2.3. FIRST ORDER ZONING OF THE BULGARIAN TERRITORY

The same methodology (Section 2.1) has been applied to the Bulgarian territory by Orozova-Stanishkova et al. (1996), who discuss extensively the necessay input data. The map showing the smoothed distribution of seismicity within the seismogenic zones is given in Figure2.7.

As shown in Figure 2.8a, the highest values of AMAX are obtained in southwestern Bulgaria (0.3-0.4g), Struma zone, where the strongest earthquake in Bulgaria (M_S=7.8) occurred. Values between 0.2g and 0.3g have been estimated also in Southern Bulgaria and in the north-eastern part of the country. Near Trun, Sofia, and the western and central part of Maritza zone, as well as in Gorna Oryakhovitza zone AMAX varies in the range 0.1-0.2g. The northwestern and southeastern parts of Bulgaria are the less dangerous zones: AMAX is below 0.05g.

The largest Bulgarian cities, with relevant economical and cultural importance, such as Sofia, Plovdiv and Varna are situated in the zones with high seismic hazard. The values of AMAX calculated there are about 0.1-0.3 g. The corresponding displacements are shown in Figure 2.8b.

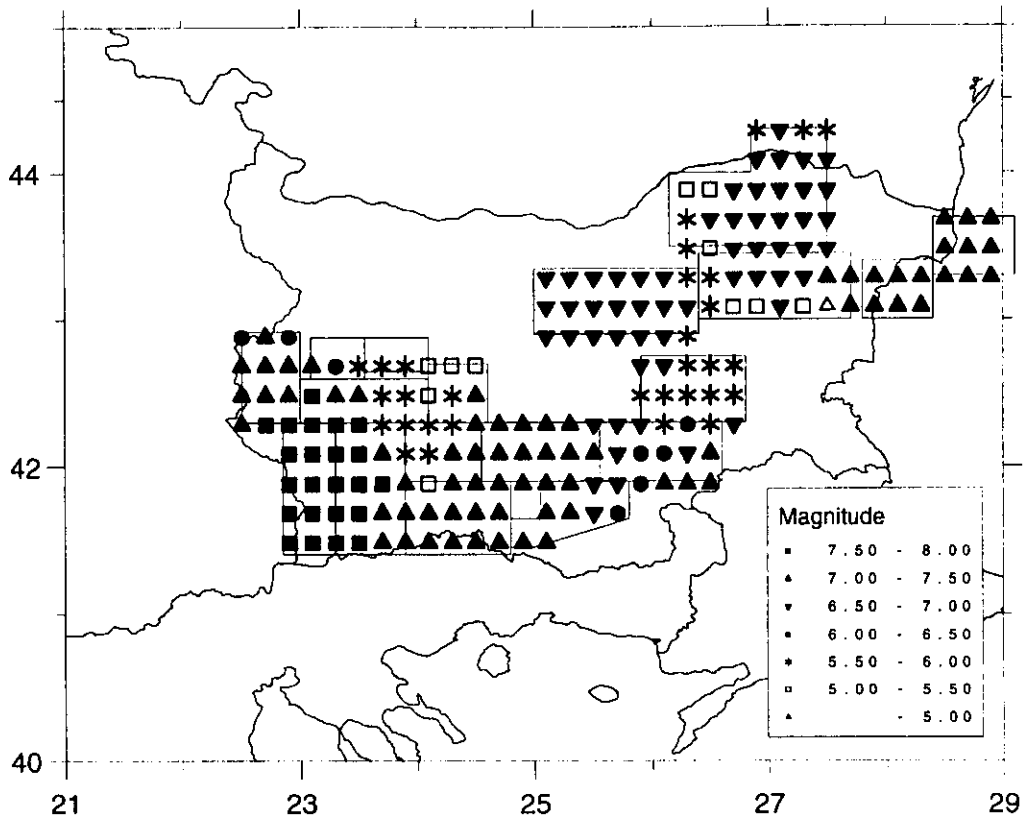

Figure 2.7 Smoothed M_S magnitude distribution for the cells belonging to the seismogenic zones, defined for Bulgaria after Orozova-Stanishkova et al. (1996).

2.4. DETAILED ZONING COMBINING OBSERVATION AND MODELLING OF GROUND MOTION

It is not possible to refine the results obtained with a first-order zoning by simply assuming a higher cut-off frequency (> 1 Hz) in the computation of the synthetic seismograms. A more detailed zoning requires a better knowledge of the seismogenic process in the region. Furthermore, to model wave propagation in greater detail the structural model used in the computation of synthetic seismograms must take into account lateral heterogeneities.

Detailed numerical simulations play an important role in the estimation of ground motion in regions of complex geology. They can provide synthetic signals for areas where recordings are absent. Numerical simulations are, therefore, useful for the design of earthquake-resistant structures, in particular when seismic isolation techniques are applied. In fact the number of available strong motion recordings containing reliable information at periods of a few seconds is very small, and will not increase very rapidly, since strong earthquakes in densely instrumented areas are rare events.

The computations that are at the base of the maps shown in Figures 2.3, 2.6 and 2.8 allow us to determine immediately the ground acceleration response spectra for periods, T, larger than 1 s, that are of special interest for seismically isolated buildings. For practical purposes, these

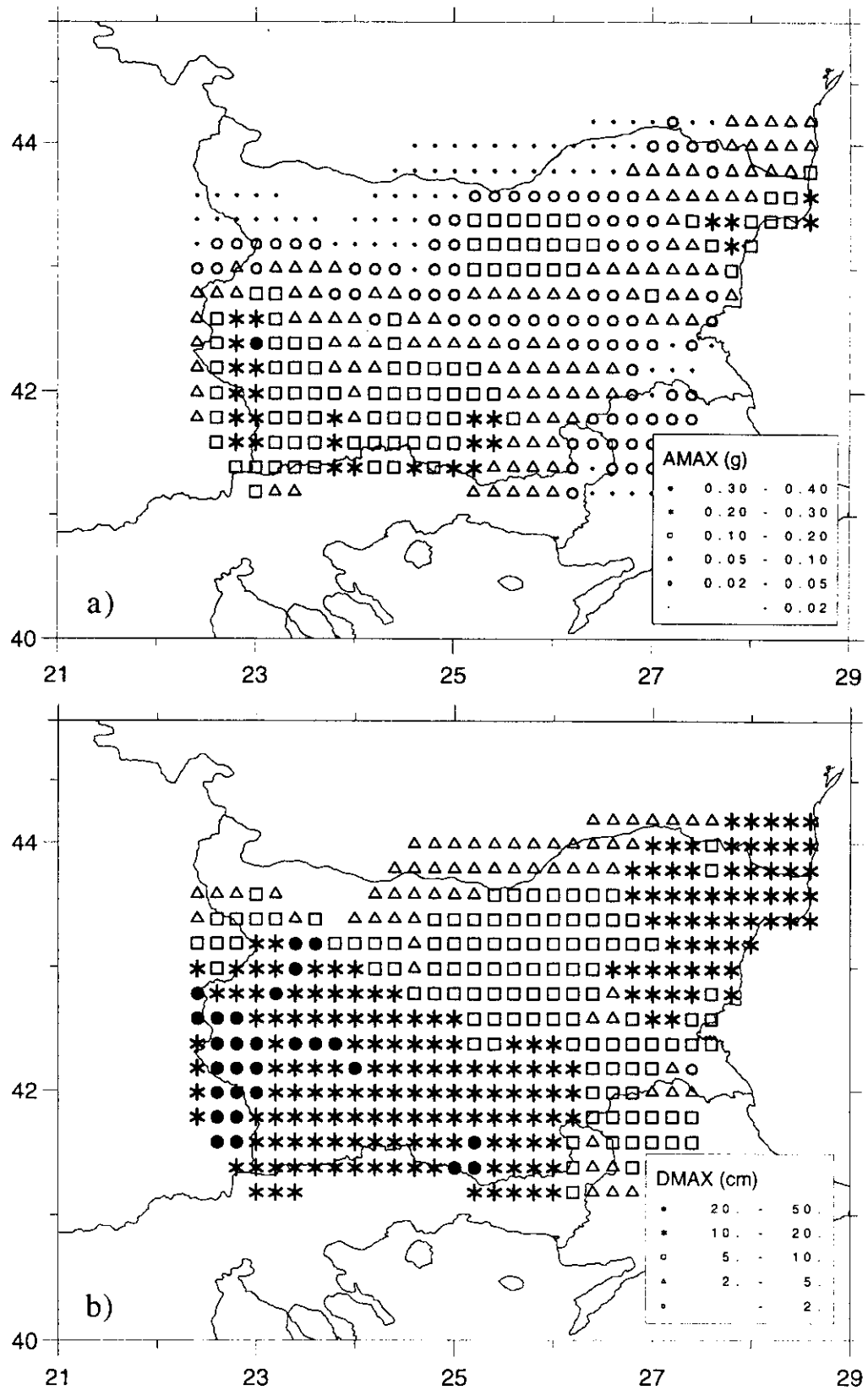

Figure 2.8 Horizontal AMAX (a) and DMAX (b) distribution for Bulgaria after Orozova-Stanishkova et al. (1996). Maximum frequency 1 Hz.

results can be generalized to higher frequencies by the use of the existing standard codes. For instance, Eurocode 8 (1993) defines the normalized elastic acceleration response spectrum, $\beta(T)$, of the ground motion, for 5% critical damping. Therefore, the matching of the long-period portion of the normalized spectra with the ones computed from synthetic accelerograms, allows us to obtain, for any portion of the considered territory, an absolute spectrum, provided a satisfactory classification of soils is available. An example is given in Figure 2.9. The preliminary soil classification of Eurocode 8 (1993) considers three classes, A, B, and C, ranging from hard rock to loose uncemented sands. Accordingly with Eurocode 8 (1993) for sites with soil conditions not matching the three classes A, B and C, special studies for the definition of the ground acceleration response spectrum are necessary (examples of such special studies are given in section 2.4.1).

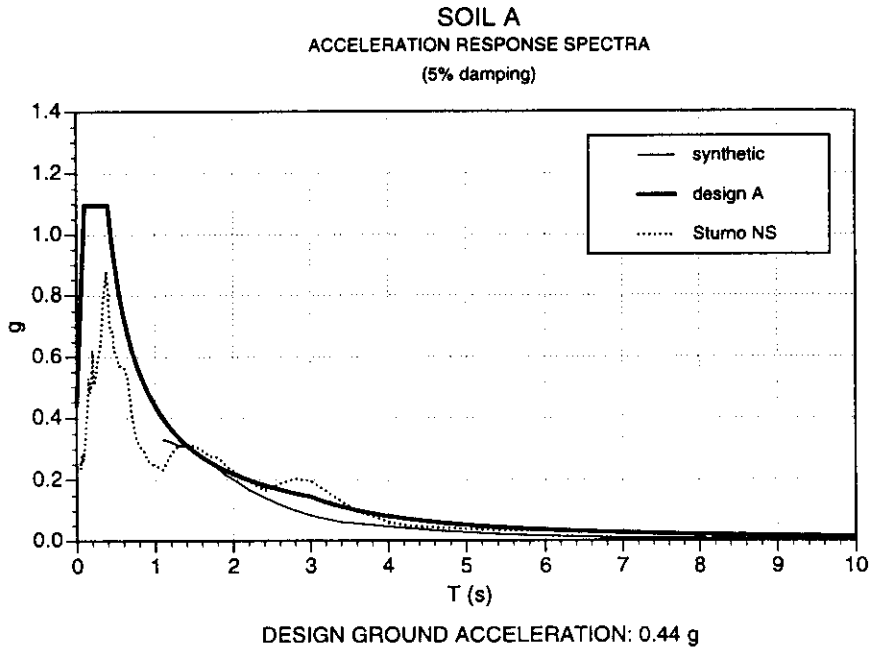

Figure 2.9 Elastic acceleration response spectra. Absolute values (thick line) have been obtained scaling the normalized Eurocode8 response spectrum for subsoil A with the long period response spectrum (thin line), determined from the synthetic signal obtained in section 2.1 for the Irpinia (Southern Italy) area. The spectrum of the NS component observed at Sturno during the 1980 Irpinia earthquake is shown by the dotted line.

When detailed special studies are required by Eurocode 8 or by the presence, in the built environment, of special objects, the standard seismic prospecting techniques, used for the detailed definition of the elastic properties of sub-surface geology, do not give satisfactory results since they treat wave propagation in laterally heterogeneous structures with asymptotic forms for high frequencies. These methods, called "ray methods", can only be applied to smoothly varying media, where the characteristic dimensions of the inhomogeneities are considerably larger than the prevailing wavelength. They fail to predict ground motion at sites close to lateral heterogeneities such as edges of sedimentary basins and at sites above irregular bedrock-sediment interfaces, where excitation of local surface waves and resonance effects can become important.

Far away from lateral heterogeneities, a local structure can sometimes be approximated by a horizontally-layered structural model, and the mode summation method is the most powerful tool for computing broadband synthetic seismograms. This method is still suitable when lateral variations can be schematized with vertical discontinuities (Vaccari et al., 1989), but it is presently not applicable to local irregular structures, which cannot be reduced to plane-layered models. When dealing with special detailed investigations the influence of these local and irregular heterogeneities must be included in the numerical modelling. This can be done combining the modal summation and the finite difference techniques (Fäh et al., 1990; Fäh, 1992).

2.4.1. Modelling strong ground motion observed in Mexico City

Mexico City has experienced extensive damage in the recent past from strong earthquakes with hypocentres in the Mexican subduction zone. The Michoacan earthquake of September 19,

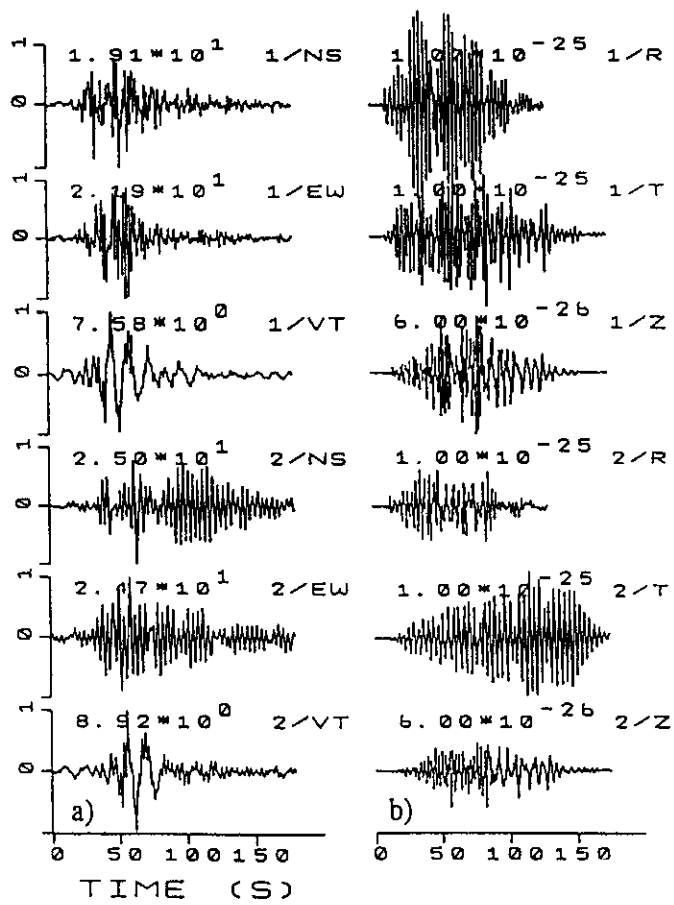

Figure 2.10 a) Observed horizontal and vertical components of displacements recorded at two stations (1 and 2) in the valley of Mexico City. N denotes the North-South, E the East-West and Z the vertical component. b) Synthetic displacements computed with the hybrid technique (Fäh et al., 1990; Fäh, 1992). R is the radial, T is the transverse and Z is the vertical component. The signals are normalised to a seismic moment of 10^{-7} Nm, and the peak displacement is indicated in units of cm (modified from Fäh et al., 1994a).

1985 (M_S=8.1), together with its aftershocks, produced the worst earthquake damage in the history of Mexico. More than 10,000 people died in Mexico City, 300,000 people were rendered homeless, and about 1,000 buildings were destroyed (Beck and Hall, 1986). Although the epicentre of the earthquake is close to the Pacific coastline, damage at coastal sites was relatively small. The reason for this is that most of the populated areas near the coast are sited on hard bedrock. In contrast, Mexico City, which is about 400 km from the epicentre, suffered extensive damage. This can be attributed to the geotechnical characteristics of the sediments in the valley of Mexico City. As the Michoacan earthquake was one of the most precisely-monitored events affecting a large metropolitan area, it is of particular interest to compare observed (Figure 2.10a) and computed (Figure 2.10b) strong ground motion, containing reliable information also at long periods.

The area of severe damage in Mexico City is characterized by the increasing thicknesses of the deep sediments and of the clay layer. The large impedance contrast between these two units causes strong resonance effects in the clay layer, as it is shown by the computed seismograms (Figure 2.10b) which are characterized by almost monochromatic wavetrains of long duration and large amplitude in the horizontal components, but absent in the vertical. The small influence of sedimentary basins on the vertical component of motion is frequently observed, and the computations (Fäh et al., 1994a) give a solid theoretical explanation of this fact.

The model used by Fäh et al. (1994a), directly obtained from the exisiting litterature, explains the observed difference in amplitudes for receivers located inside and outside the lake-bed zone in Mexico City, the ratio being in the range from 5 to 7 between the computed and the

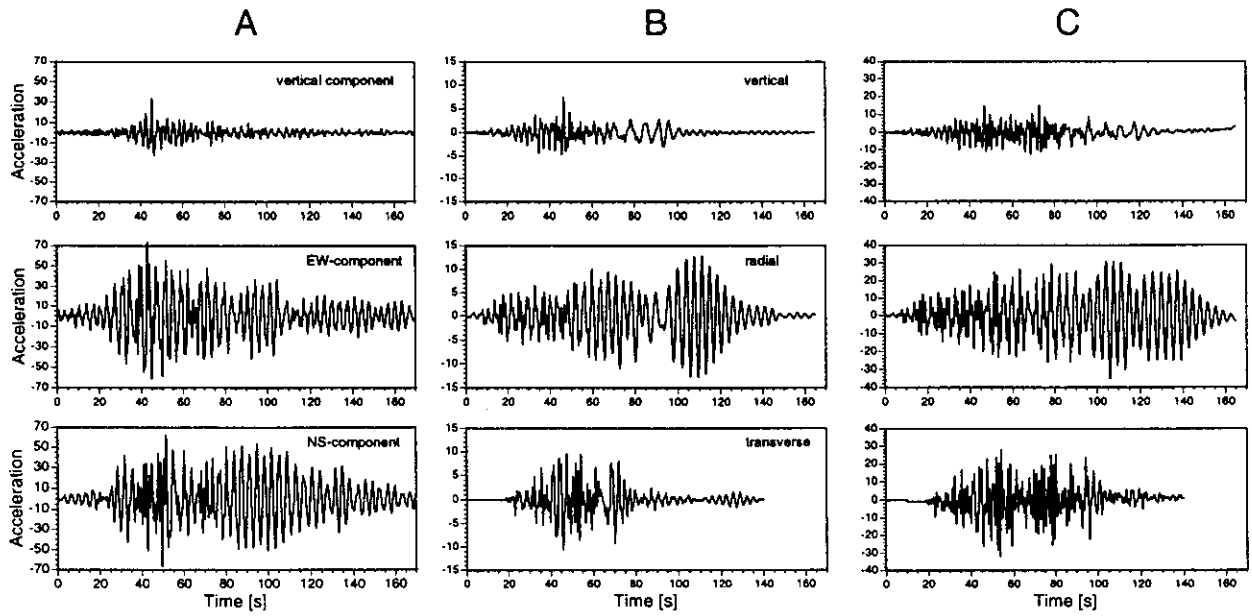

Figure 2.11 Michoacan earthquake (1985). Comparison between (A) the record at station CD and synthetic signals, computed at the eastern edge of the basin, 409.5 km from the source, corresponding to (B) one point source, (C), three point sources, with different strength and shifted in time (after Fäh and Panza, 1994).

observed time series. The use of an instantaneous source time-function gives rise to synthetic signals that contain too much energy at high frequency (above 0.6 Hz). This drawback can be removed by applying the ω^2 scaling law for the seismic moment rate spectrum, proposed by Kanamori et al. (1993) for the events occurring in the Mexican subduction zone:

$$\hat{\dot{M}} = M_0 \omega_c^2 (\omega^2 + \omega_c^2)^{-1}$$

M_0 is the seismic moment and ω_c is the corner angular frequency. Following Kanamori et al. (1993), ω_c=0.196 s^{-1} and M_0=0.5·10^{21} Nm. These values permit to obtain a good reproduction of the shape of the observed signals over the entire frequency spectrum, but the absolute observed accelerations are underestimated by a factor ranging from 6 to 3. This last discrepancy can be reconciled considering the errors affecting the estimates of ω_c and M_0, and taking into account the subsequent rupture episodes of the Michoacan earthquake, mainly the one occurring about 26 s after the origin time, as shown in Figure 2.11 (Fäh and Panza, 1994). This data fitting is, however, unrelevant for the computation of spectral amplifications and for the more general purpose of defining the seismic input for engineering purposes.

At the site of interest, spectral amplification, computed with respect to a reference site, gives a good representation for micro-zoning purposes, especially from the engineering point of view. Fäh and Panza (1994) computed the spectral amplification, i.e. the relative spectral accelerations and velocities for one hundred frequencies of the oscillator in the frequency range 0.1-1.0 Hz. From these values the maximum spectral amplification (MSA) for the entire basin has been computed and is shown in Figure 2.12. The results for the relative spectral accelerations and velocities are similar, due to the approximate relation existing between them: $Sa(\omega) \approx \omega\, Sv(\omega)$, where ω is the angular frequency of the oscillator. In the following we will therefore limit ourselves to the relative spectral velocities, which we will call spectral amplification.

In two-dimensional modelling, the SH-waves (transverse component of motion) and the P-SV-waves (radial component of motion) are two independent wave fields. The direction of propagation of the local surface waves in the sedimentary basin is therefore well correlated with the source-receiver direction. In Mexico City, the local surface-waves are excited at different locations of the interface between the bedrock and the sediments, and the direction of propagation of the local surface-waves in the lake-bed zone may not correspond anymore to the source-receiver direction. Therefore, to justify the comparison between the observed ground motion and the synthetic signals, the spectral amplification for the complete horizontal ground motion must be computed. This has been done by Fäh and Panza (1994), who applied the horizontal ground motion to an oscillator with two degrees of freedom. The results for the synthetic signals are shown in Figure 2.12. Due to the large amplitudes of SH-waves, the MSA obtained for the horizontal ground motion are similar to the result obtained for the transverse component. The maximum peaks in the MSA in Figure 2.12 can be attributed to sites where a strong interaction between the deep sediments and the surficial clay layer occurs. At such sites, the resonance frequencies of the two layers are almost the same. The MSA obtained from the numerical simulation is rather independent from the shape of the seismic moment rate spectrum, as can be seen in Figure 2.13, where the results obtained with the seismic moment rate spectrum proposed by Kanamori et al. (1993) are compared with the results obtained for a frequency-independent spectrum.

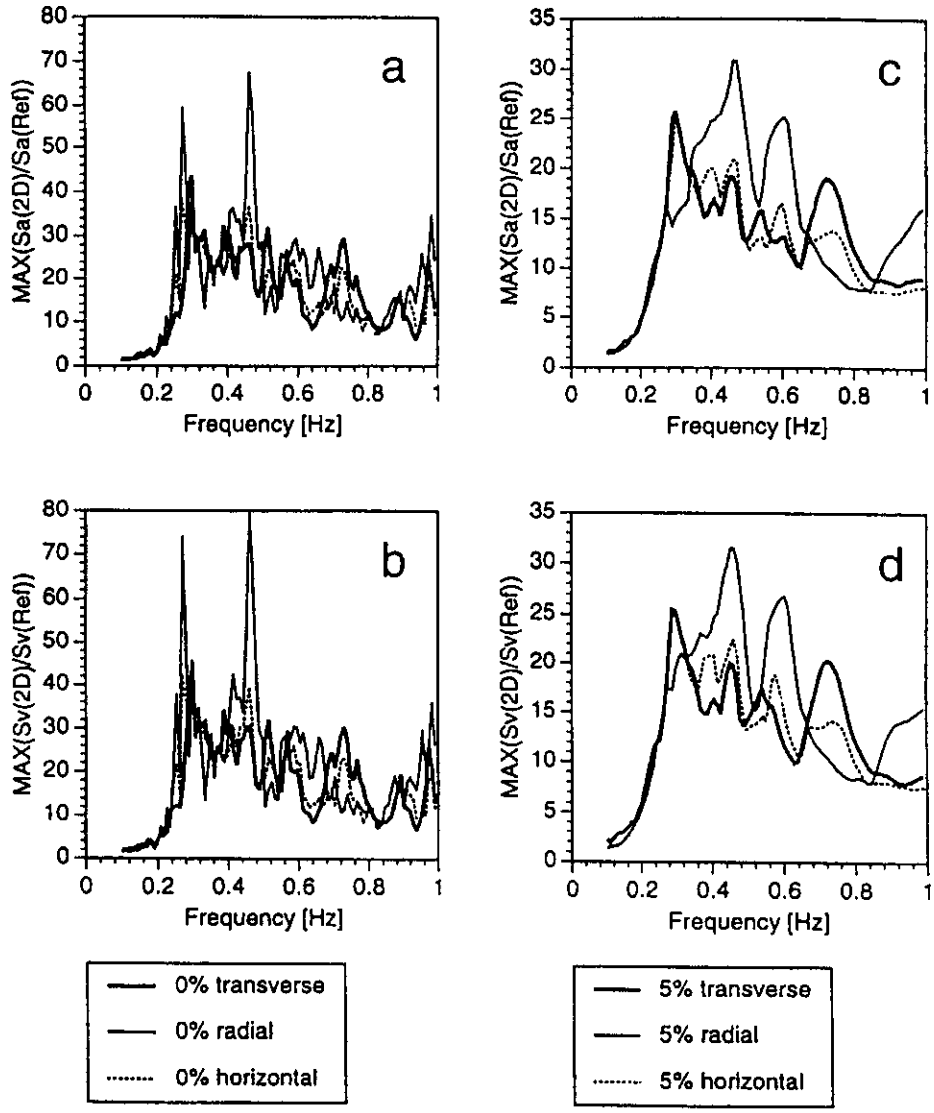

Figure 2.12 Maximum relative spectral accelerations Sa(2D)/Sa(Ref) and velocities Sv(2D)/Sv(Ref) for zero damping (a,b) and 5% damping (c,d) obtained with synthetic signals. The results are shown for a single-degree of freedom oscillator for the transverse and the radial component of motion, and for an oscillator with two degrees of freedom for the horizontal ground motion. The synthetic signals are scaled assuming the seismic moment rate spectrum proposed by Kanamori et al. (1993) (after Fäh and Panza, 1994).

The relation existing between the properties of strong motion records, the geological setting and the distribution of damage in Mexico City widens the spectrum of the possible applications of synthetic seismograms for seismic zoning purposes, allowing us the use of earthquakes for which instrumental data are not available (historical events). An example of such possibilities is given in Section 2.4.2.

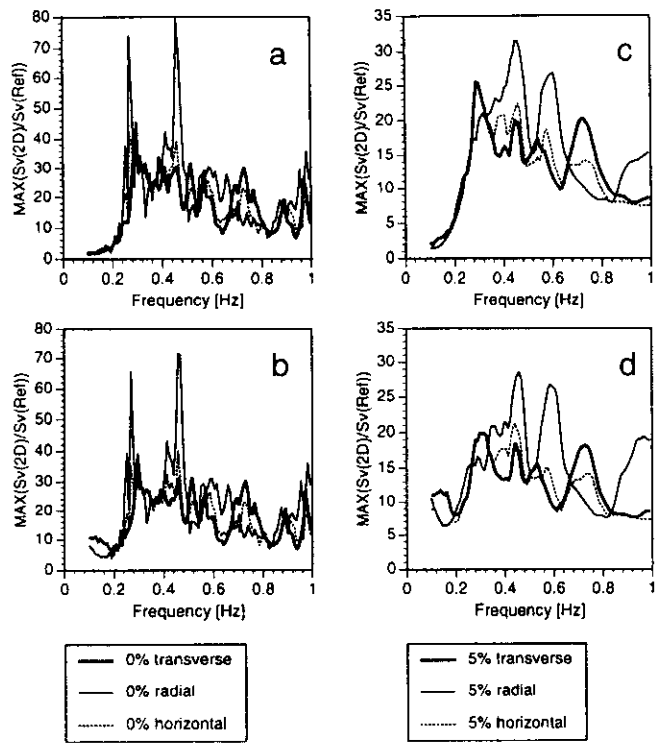

Figure 2.13 Maximum relative spectral velocities Sv(2D)/Sv(Ref) for zero damping (a,b) and 5% damping (c,d) obtained with the synthetic signals, which are scaled by assuming the seismic moment rate spectrum proposed by Kanamori et al. (1993) (a,c) and by assuming a constant, frequency independent, spectrum (b,d) (after Fäh and Panza, 1994).

2.4.2. Microzoning of Rome

A large quantity of descriptions of earthquakes that have been felt in Rome is available (Ambrosini et al., 1986; Molin et al., 1986; Basili et al., 1987). The use of the hybrid method (Fäh et al., 1993) allows us to give a simple and natural explanation of the damage disribution observed as a consequence of the the January 13, 1915 Fucino earthquake - one of the strongest events that have occurred in Italy during this century (Intensity XI on the Mercalli-Cancani-Sieberg, MCS, scale). The well-documented distribution of damage in Rome, caused by the Fucino earthquake, is successfully compared by Fäh et al. (1993) with the results of a series of different numerical simulations, using AMAX and the so called total energy of acceleration, W (Jennings, 1983), which is proportional to the Arias Intensity.

High relative AMAXs are obtained where the impedance of the surficial sediments is small, whereas relative AMAXs are low where the volcanic rocks are thick, and this is in good agreement with the observed damage distribution. An even better correlation with the observed damage is obtained considering the relative W. There are four peaks: at the edges of the Tiber basin, within the alluvial valley of the Aniene, and a broad peak at the end of the Siciliano low-velocity zone. An additional important result of Fäh et al. (1993) is the demonstration that sharp variations in the

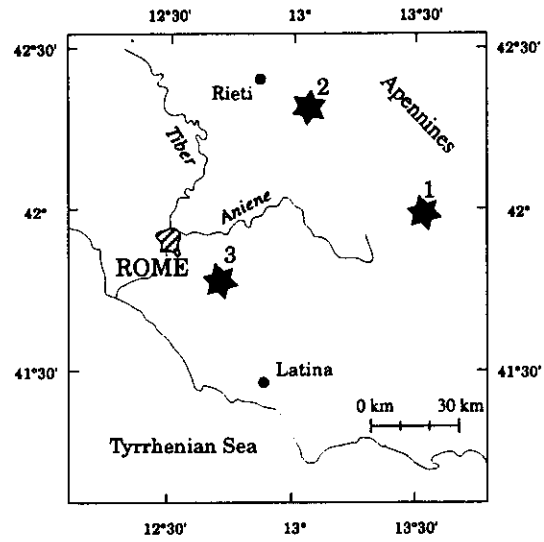

Figure 2.14 Epicenter locations of the events considered in the numerical simulations used for the microzoning. The source positions are (1) the epicenter of the January 13, 1915 Fucino earthquake, (2) the Carseolani Mountains, and (3) the Alban Hills.

spatial distribution of the spectral ratios can be due to the polarization of P-SV waves in the sediments, even when the geometry of the different sedimentary layers is relatively regular. This is a quite logical explanation of the often observed concentration of damage in very small, scattered zones, and is easier to accept than the often invoked presence of unlikely abrupt variations in the geotechnical properties of the subsoil.

Since the correlation is good between AMAX, W and the damage statistics, it is possible to extend the zoning to the entire city of Rome, thus providing a basis for the prediction of the expected damage from future strong events.

In addition to the Central Apennines, whose earthquakes caused in the town maximum intensity VII-VIII (MCS) and may generate significant perturbations at long period, the most important seismogenetic zone (Figure 2.14) which can cause structural damage in Rome are the Alban Hills (observed maximum MCS in Rome VI-VII) (Molin et al., 1986). Therefore, Fäh et al. (1993) used the sources shown in Figure 2.14: (1) the epicenter of the January 13, 1915 Fucino earthquake, (2) the Carseolani Mountains where, from the study of pattern recognition (Caputo et al., 1980), a strong earthquake is expected to occur, and (3) the Alban Hills. The source mechanisms assigned to these earthquakes are the mechanism of the Fucino earthquake (Gasparini et al., 1985) for event 1 and 2, and the mechanism of a recent earthquake in the Alban Hills (Amato et al., 1984) for event 3.

For a first order microzoning, in order to minimize the effects of the radiation pattern and of the regional propagation, Fäh et al. (1994b) consider the relative spectral accelerations or spectral amplification Sa(2D)/Sa(bedrock), computed along the profiles of Figure 2.15. Sa(2D) indicates Sa computed for the two-dimensional models of Figure 2.16, while Sa(bedrock) is the Sa obtained for the one-dimensional reference bedrock models given by Fäh et al. (1993).

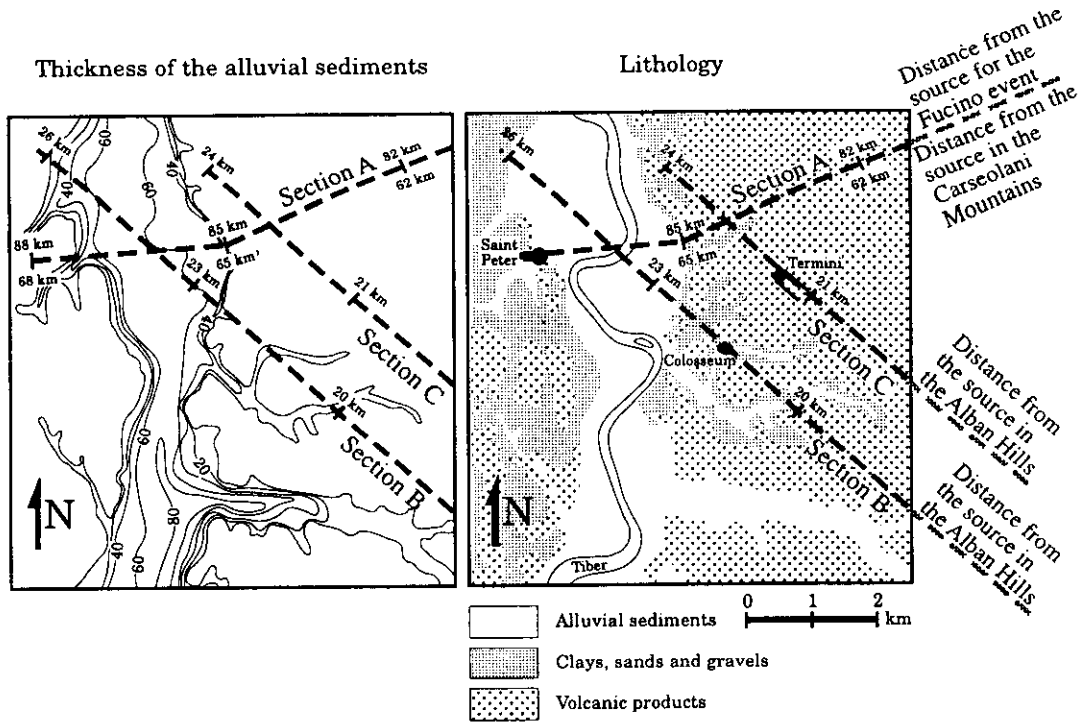

Figure 2.15 Lithology and thickness of alluvial sediments in Rome (Ventriglia, 1971; Funiciello et al., 1987; Feroci et al., 1990). The dashed lines indicate the positions of the cross sections, for which numerical modelling is performed.

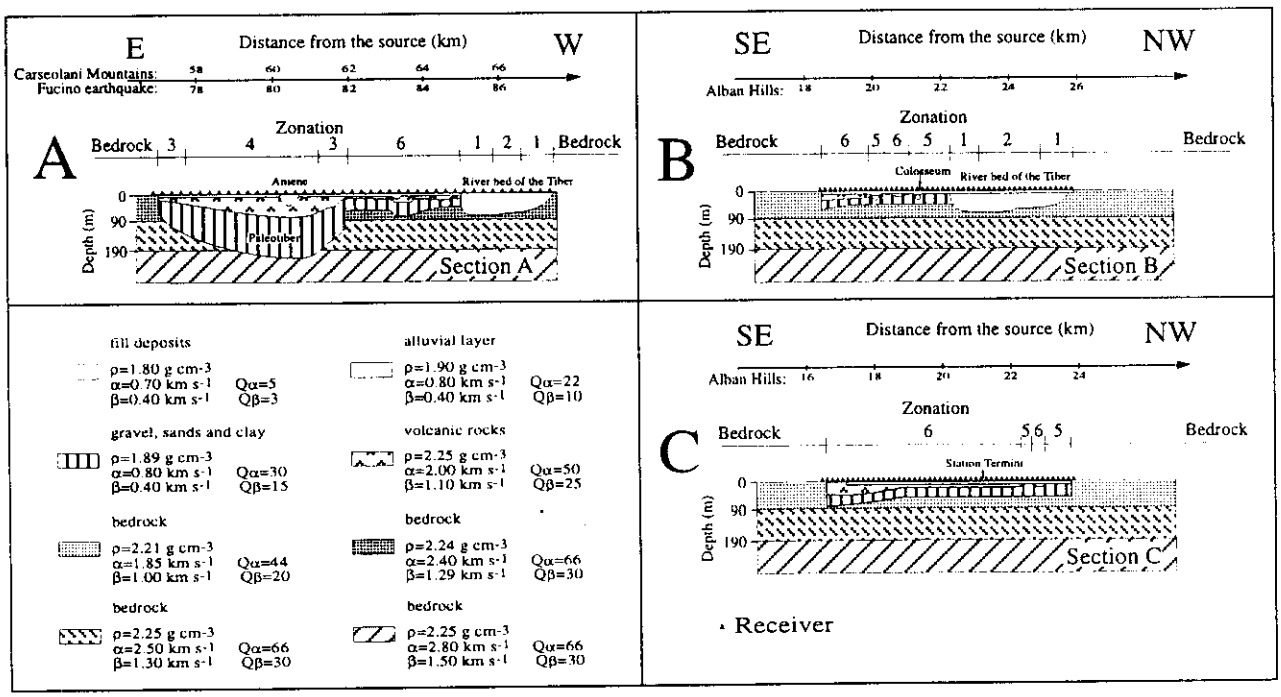

Figure 2.16 Two-dimensional models corresponding to the dashed lines shown in Figure 2.15. Only the part near to the surface is shown, where the 2D model deviates from the horizontally-layered reference models. The general microzonation is explained in the text (after Fäh et al., 1994b).

For general microzonation purposes, using the results obtained from the modelling of the Fucino event, it is possible to define the six zones shown in Figure 2.16: (1) *zone 1* includes the edges of the Tiber river, (2) *zone 2* extends over the central part of the alluvial basin of the Tiber, (3) *zone 3* includes the edges of the Paleotiber basin, and (4) *zone 4* extends over the central part of the Paleotiber basin. The *zones 5* and *6* include areas which are located outside the large basins of the Tiber and Paleotiber where we distinguish between areas (5) without and (6) with a layer of volcanic rocks close to the surface. These zones can be recognized also in the sections considered in relation with the events located in the Carseolani Mountains and the Alban Hills (Figure 2.16).

For all the sites located in each of the six zones, and for all the two-dimensional models, shown in Figure 2.16, and the studied events, located in Figure 2.14, the spectral amplifications Sa(2D)/Sa(bedrock) have been computed. From these values the average and the maximum spectral amplification, which are shown in Figure 2.17, for zero and 5% damping of the oscillator, are determined for each given zone.

The zoning performed along the three sections can be extrapolated, with cautions, to a larger area using the information available on geological and geotechnical conditions. The result of such tentative extrapolation is shown in Figure 2.18.

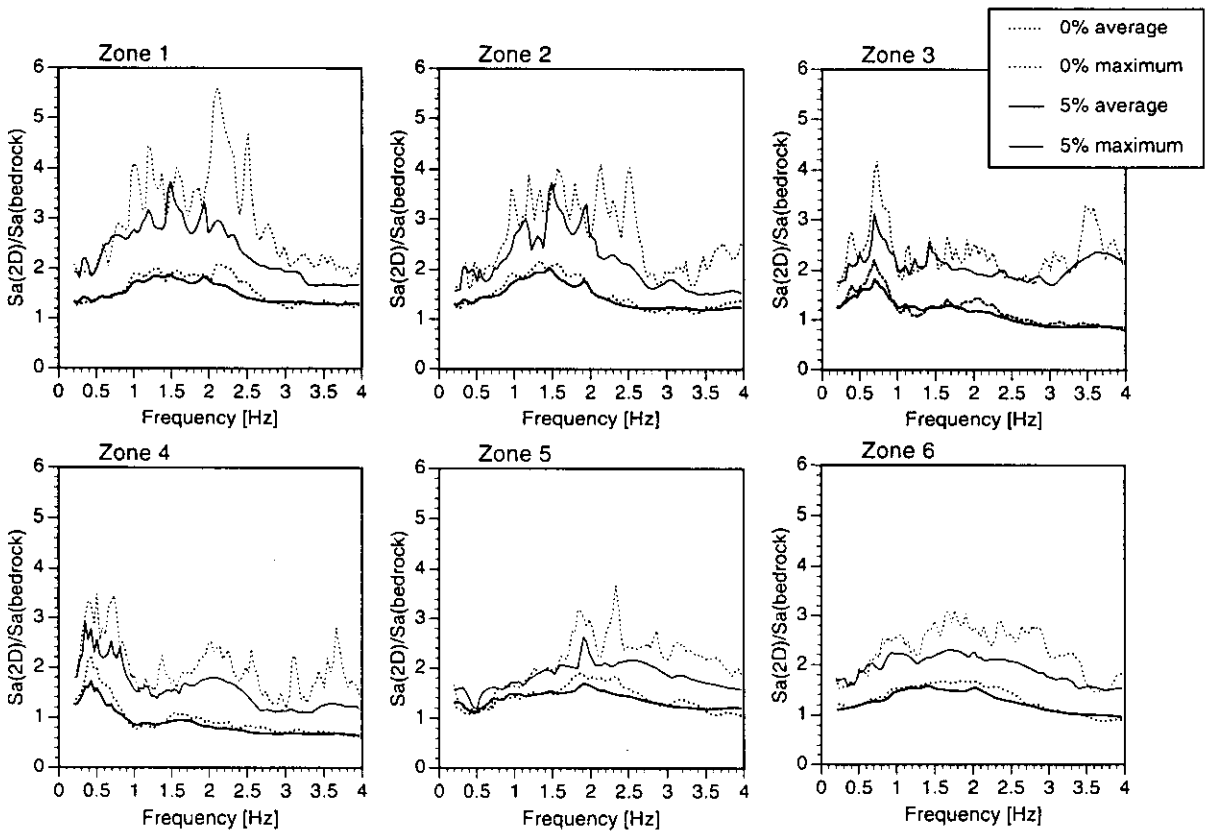

Figure 2.17 Maximum and average relative spectral accelerations for the zones defined in Figure 2.16, for zero damping and 5% damping (after Fäh et al., 1994b).

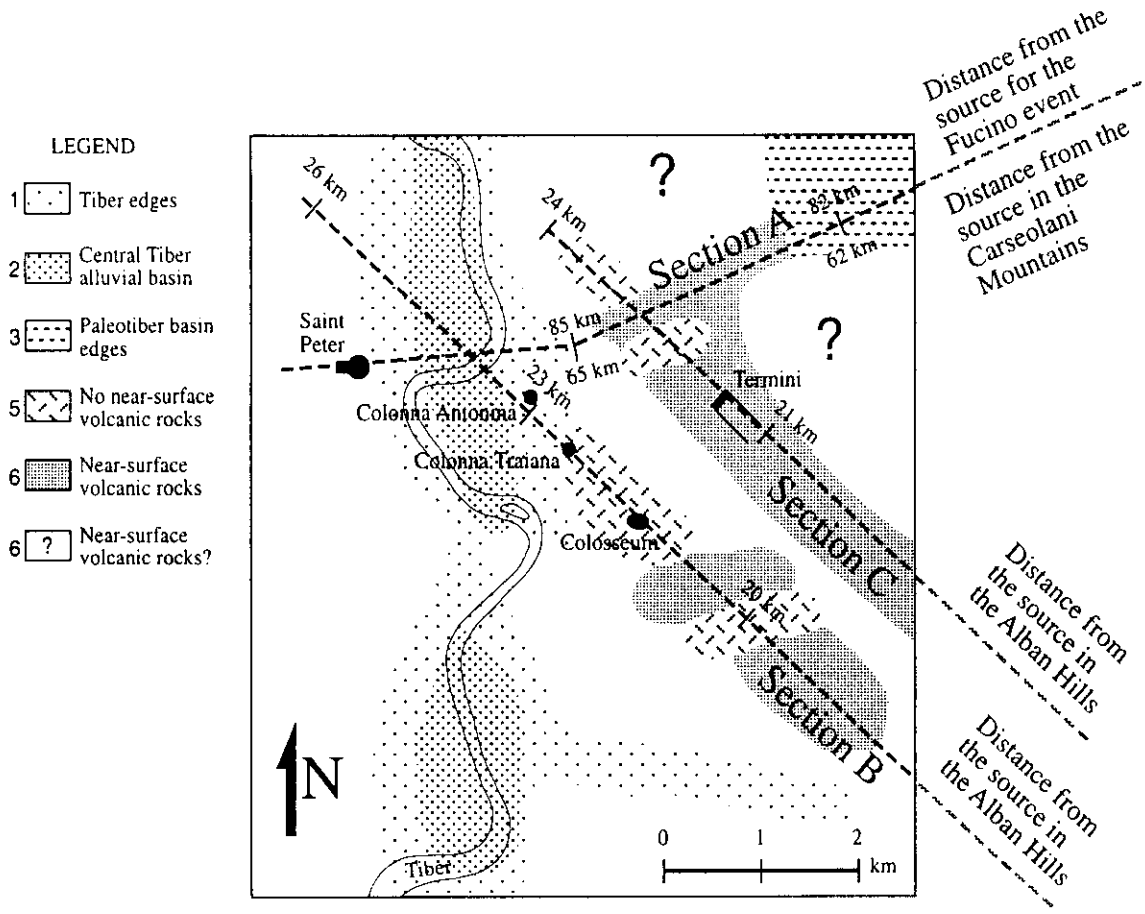

Figure 2.18 Microzoning for the city of Rome.

Thus, in absence of instrumental data, and without having to await for a strong earthquake to occur, a realistic numerical simulation of the ground motion, has been used for the first order microzonation of the city of Rome. The highest values of the spectral amplification are observed at the edges of the sedimentary basin of the Tiber, strong amplification are observed in the Tiber's river bed. This is caused by the large amplitudes and long duration of the ground motion due to (1) low impedance of the alluvial sediments, (2) resonance effects, and (3) excitation of local surface waves. The presence near to the surface of rigid volcanic rocks is not sufficient to classify a location as a "hard-rock site", since the existence of an underlying sedimentary complex can cause amplifications due to resonance effects. A correct zonation requires the knowledge of both the thickness of the surficial layer and of the deeper parts of the structure, down to the real bedrock. This is especially important in volcanic areas, where volcanic flows often cover alluvial basins.

Up to now we have seen examples of the possibility to reproduce most of the features of experimental records and to explain the damage distribution using as input data the information that can be retrieved in the literature. The agreement between observations and models is not obtained by an inversion procedure, that has not prognostic capabilities, but is the result of a direct computation. The ground motion is theoretically predicted on the base of the available knowledge about the seismic source and the medium through which waves propagate. In the following two

sections we present examples of such predictions for areas where experimental data are not available or extremely scarce.

2.5. DETAILED ZONING FROM THE MODELLING OF GROUND MOTION, AND COMPARISON OF 1-D VERSUS 2-D METHODS.

The standard one-dimensional method, developed by Thomson (1950) and Haskell (1953), and by Schnabel et al. (1972) (computer program Shake), that uses incident SH-waves in a structure composed of plane parallel layers, when applied to laterally heterogeneous structures, is often not sufficient to account for effects such as the excitation of local surface waves, resonances, and different incidence angles relative to the geometry of the heterogeneities. This limitation produces significant discrepancies between the ground response predicted by one-dimensional modelling, and the response computed for realistic two-dimensional structural models and incident wavefields. Therefore, for the computation of the local seismic response, here we use (1) the standard one-dimensional method (Schnabel et al., 1972), from now on method 1, and (2) the hybrid method (Fäh et al., 1990; Fäh, 1992), from now on method 2. The results obtained with the two methods are compared in order to define the limits and possibilities of the generally used standard one-dimensional method for reliable microzoning actions.

2.5.1. Modelling of ground motion in Naples

Naples is not within a seismogenetic area, but it has often been severely damaged by earthquakes which occurred in the Southern Apennines. The last strong event, November 23, 1980 (M_S=6.9), produced serious damage in Naples, and mostly in the historical centre and in the eastern area (Rippa and Vinale, 1983), where a ten-storied building was completely destroyed causing tens of human deaths. For the historical buildings, the damage distribution is easily explained by their degraded conditions, but for the most damaged buildings of the eastern district, which are tall and made in reinforced concrete, it is necessary to consider the combined effects of the incident wavefield, the local soil conditions and the properties of the buildings. The nearest available accelerogram was recorded at a seismic station installed on a lava deposit at Torre del Greco, on the flanks of Vesuvius, about 20 km closer to the epicentral zone than Naples. Thus, at present, the only possibility for a detailed zoning for the town, that accordingly with historical records may experience a shaking of intensity VIII on the MCS scale, is given by the use of realistic synthetic seismograms.

Nunziata et al. (1995) performed the numerical modelling of the propagation of the wavefield, generated by the main rupture event of the 1980 earthquake, up to a profile trending N86°W, and located in a test area in the eastern district of Naples, and made an accurate and realistic evaluation of the seismic ground motion.

The causative fault of the 1980 earthquake is located about 90 km from the cross-section, representative of the eastern part of Naples, shown in Figure 2.19. The choice of the mechanism of the seismic source is made accordingly with the mechanism of the main event: a normal fault

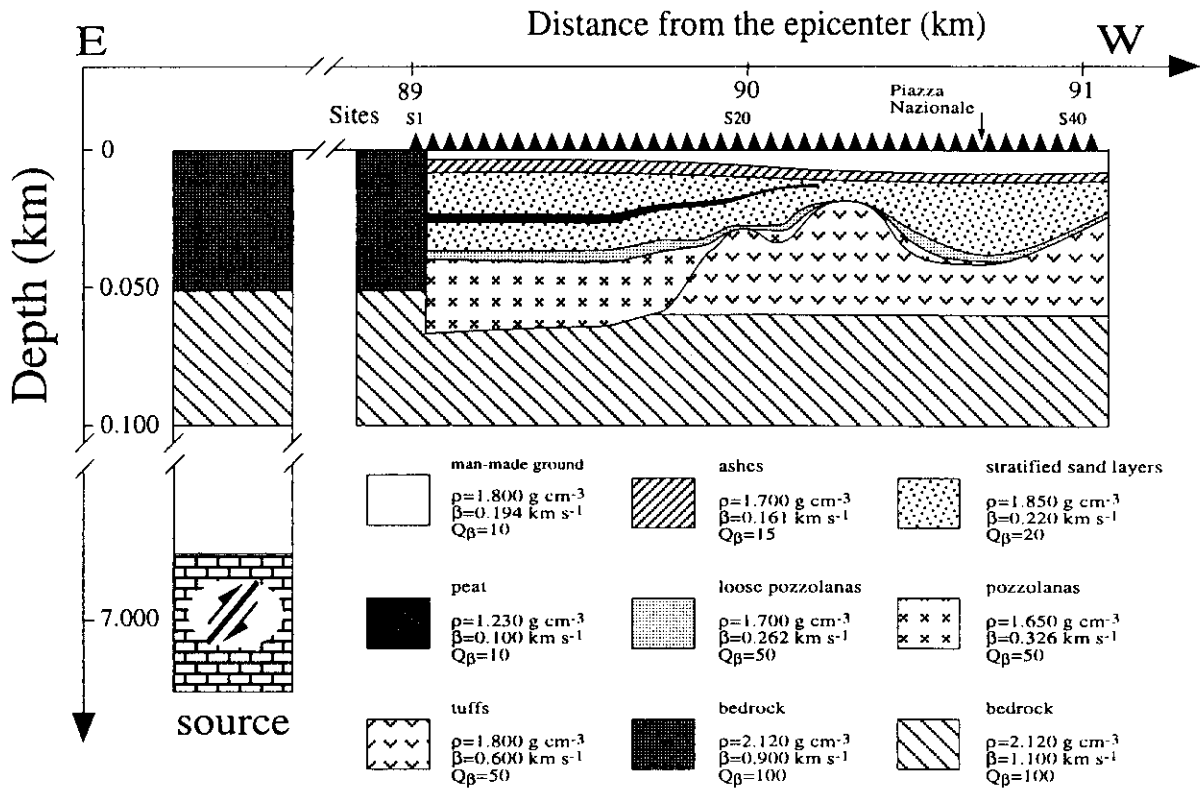

Figure 2.19 Geological cross-section in the eastern district of Naples, used in the computations (after Nunziata et al., 1995).

with little transcurrent component. Since there is no agreement between authors about the amount of the strike-slip component (e.g. Bernard and Zollo, 1989; Vaccari et al., 1990), Nunziata et al. (1995) adopt a pure normal fault with dip 65°, rake 270°, strike 315° and depth 7.0 km. The angle between the strike of the fault and the epicenter-cross section line is 36°.

The propagation of the waves from the source up to the two-dimensional structural model has been computed with method 2. The source is located in the laterally homogeneous part, and the propagation of the waves from the source up to the 2-D structure (Figure 2.19) is computed with the modal summation technique for the layered one-dimensional model representative of the path to Naples (Vaccari et al., 1990). Acceleration time series for SH-waves (Figure 2.20) are computed in several sites of different cross-sections: (1) a one-dimensional reference model for the bedrock, which corresponds to the structural model for the region between the source position and Naples, (2) a two-dimensional model with a peat layer, and (3) a two-dimensional model without the peat layer. All scaling values are related to a source seismic moment $M_0 = 10^{-7}$ Nm, and in each column, the signals are normalized to the same value. The time scale is shifted by 22 s with respect to the origin time, and the distance between two sites is 100 m. If we scale the signals of Figure 2.20 following Gusev (1983) relation using $M_0 = 2\ 10^{19}$ Nm, that is for $M_S = 6.9$ (Kanamori, 1977), we obtain acceleration values, associated with SH waves, in the range 45cm/s^2-60 cm/s^2, in good agreement with the regressions of Sabetta and Pugliese (1987).

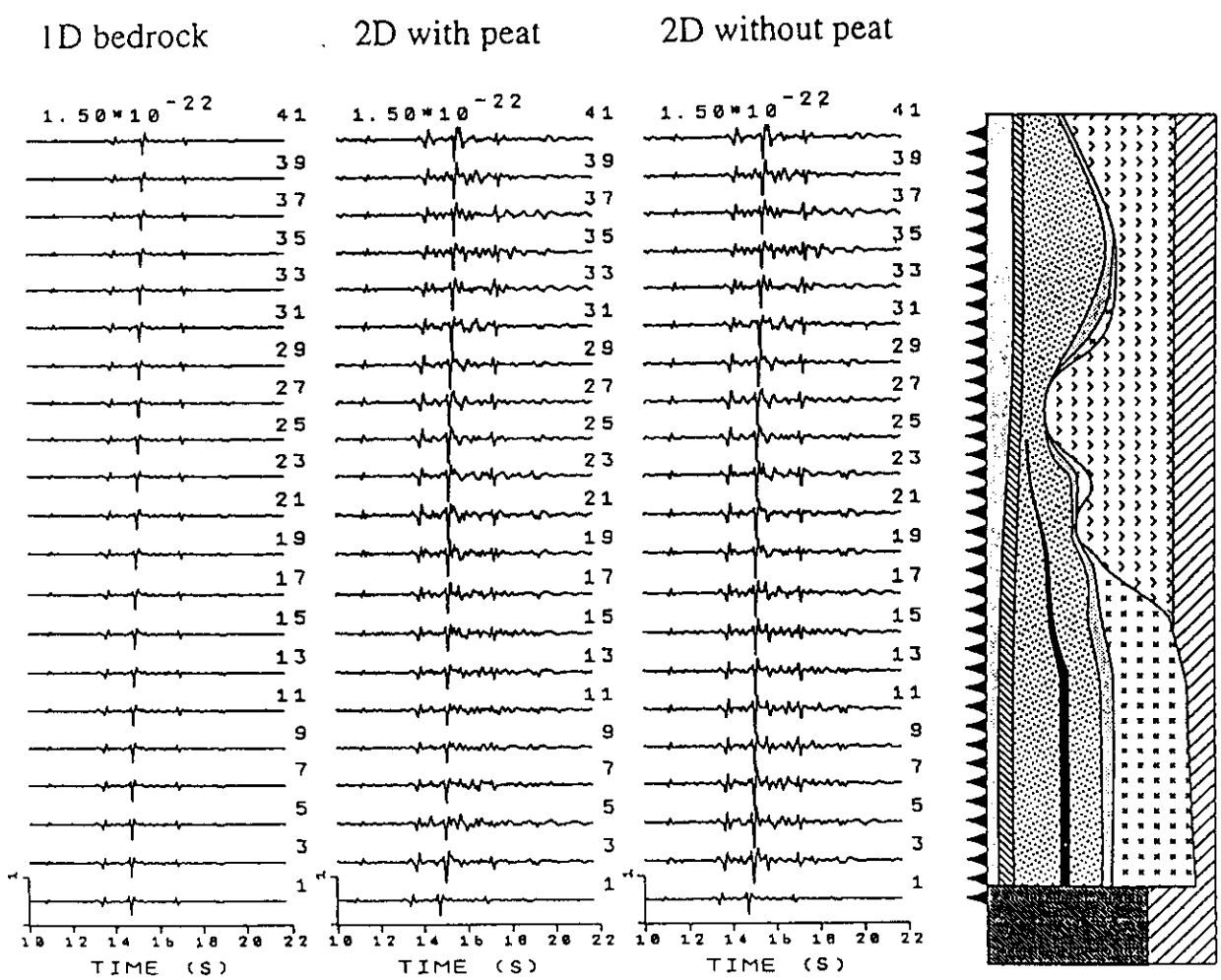

Figure 2.20 Acceleration time series for SH-waves computed for the reference model (1D bedrock), the 2-D structural model with the peat layer, and the 2-D structural model without the peat layer (after Nunziata et al., 1995).

The presence of unconsolidated sediments causes an increase of the signal's amplitudes and duration, more pronounced for the model without the peat layer. For the model with the peat layer, between sites 1 and 15, the maximum amplitudes are similar to the maximum amplitudes observed for the one-dimensional bedrock model.

Looking at the spectral ratios at the sites S7, S17, S23, S26, S33 it is quite evident the large variability of ground motion within a few hundred meters (Figure 2.21). The main peak moves from frequencies less than 1 Hz, site S7, where the peat layer reaches the maximum thickness, to frequencies slightly higher than 1 Hz, sites S17 and S33, and to frequencies around 2 Hz, sites S23 and S26. The amplification factor of the ground motion is in general around five, and this value is exceeded only at site S17. A secondary significant peak is present at higher frequencies, between 2Hz and 3Hz at site S7, between 3Hz and 4Hz at sites S26 and S33, and around 5Hz for site S17.

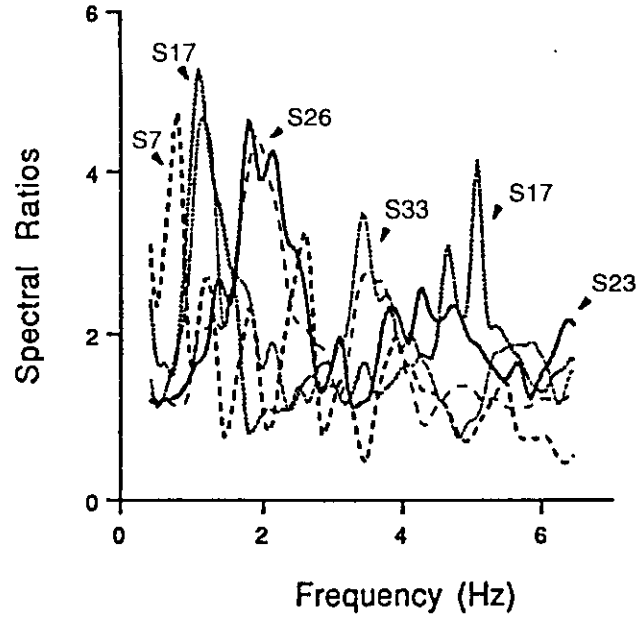

Figure 2.21 Smoothed spectral ratios computed with the hybrid method at the sites S7, S17, S23, S26, S33 - see Figure 2.19 for their location (after Nunziata et al., 1995).

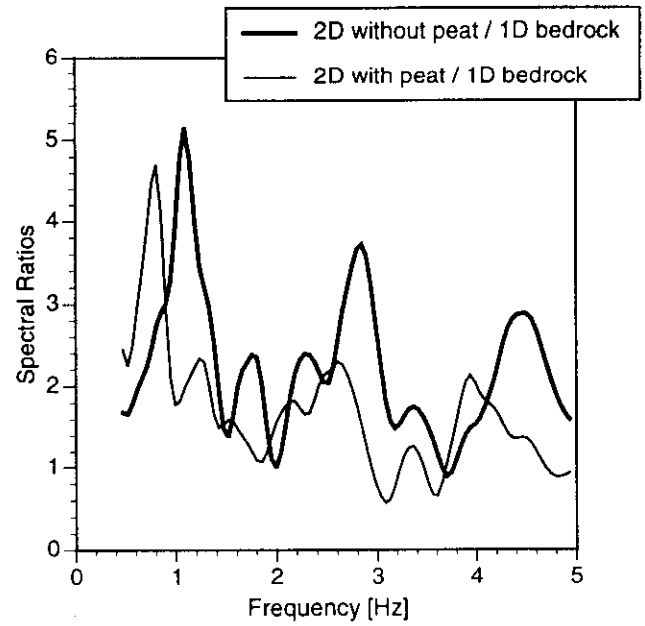

Figure 2.22 Example of the effect of the peat at site S9 (see Figure 2.19 for its location), with respect to its removal. Smoothing applied (after Nunziata et al., 1995).

The damping effect of the peat layer is clearly shown by the comparison of the spectral ratios computed at the same site (S9) when the peat layer is removed (Figure 2.22). The maximum peak increases in amplitude and is shifted towards higher frequencies, when the peat layer is removed.

The peat layer, even though with a thickness of only 3 m, reduces significantly the amplification effects induced by the unconsolidated sediments.

The discrepancies between the amplifications computed with method 1 and method 2 are clearly illustrated in Figures 2.23, 2.24 and 2.25 for sites S7, S23 and S26. At site S7, the main peak is reached at the same frequency with both modellings, but the amplitude obtained with method 1 is 30% smaller than that obtained with method 2. Moreover, other peaks, at frequencies which are important for engineering purposes, and characterizing the results obtained with the finite differences method, are absent in the results obtained with method 1. At site S23 a frequency shift of the main peak is observed in addition to a disagreement for the other peaks. The picture changes for site S26, as the spectral amplifications, computed with method 1, overestimate those obtained with method 2, even if they have a similar shape.

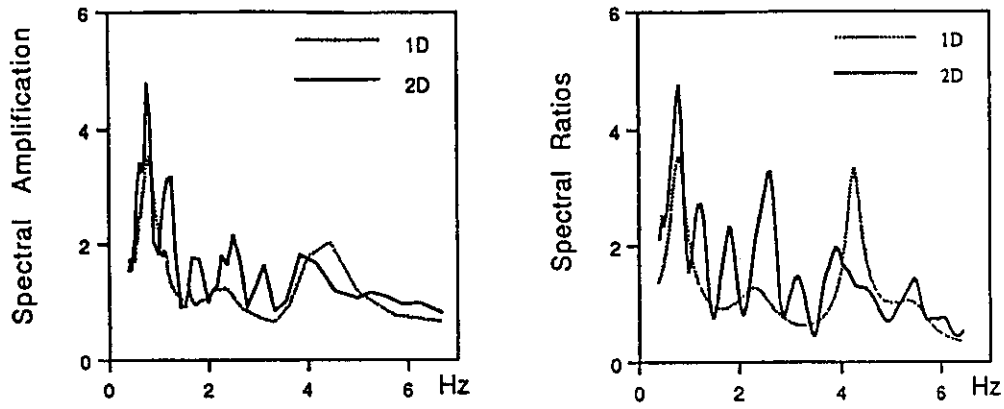

Figure 2.23 Spectral ratios (smoothed) and spectral amplification (not smoothed) for zero damping computed with 1-D and 2-D methods at site S7 - see Figure 2.19 for its location (after Nunziata et al., 1995).

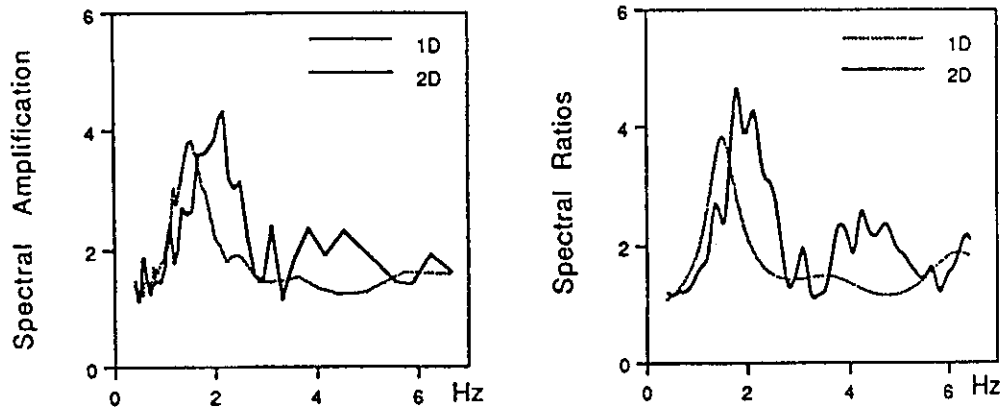

Figure 2.24 Spectral ratios (smoothed) and spectral amplification (not smoothed) for zero damping computed with 1-D and 2-D methods at site S23 - see Figure 2.19 for its location (after Nunziata et al., 1995).

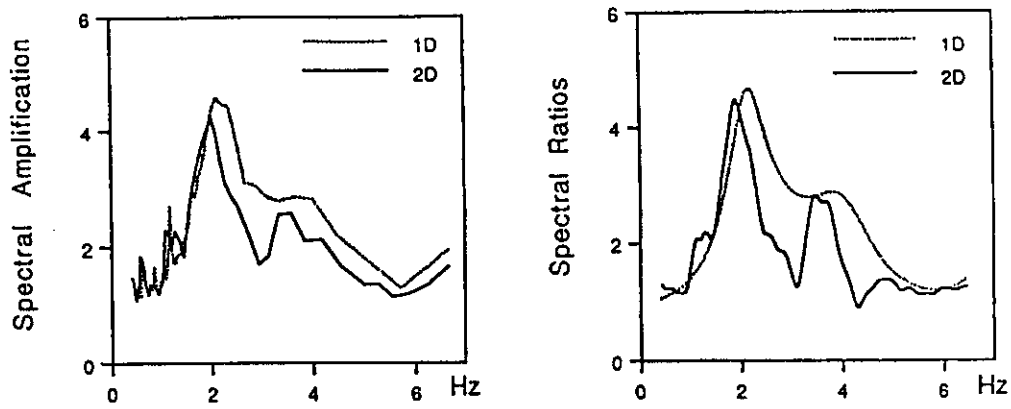

Figure 2.25 Spectral ratios (smoothed) and spectral amplification (not smoothed) for zero damping computed with 1-D and 2-D methods at site S26 - see Figure 2.19 for its location (after Nunziata et al., 1995)

Therefore, the seismic vulnerability of a megacity like Naples, with a large cultural heritage and a very high number of people to safeguard, can be drastically reduced, without having to await for another strong earthquake to occur.

2.6. THE SEISMIC MICROZONATION OF BENEVENTO: AN EXAMPLE OF PARAMETRIC STUDY

The average structural model for the region between the source position and the town of Benevento, used as the reference structure for the bedrock, is given by Vaccari et al. (1990). Following Fäh and Suhadolc (1994), the ground motion computed with the hybrid method for the different sites in the two-dimensional models is always discussed with respect to the results obtained for the same seismic source and this one-dimensional structure.

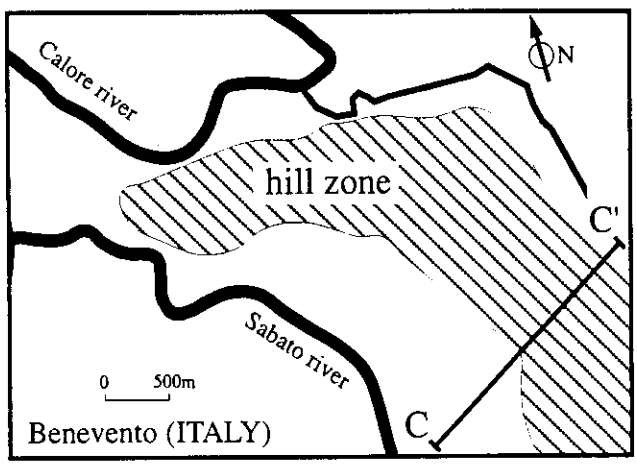

Figure 2.26 Area of the city of Benevento with the location of the profile C-C' used for the numerical modelling (after Fäh and Suhadolc, 1994).

At the western border of the Benevento hill, a Pliocenic clay formation abruptly disappears, probably due to the presence of a fault. To study the influence of this abrupt transition, different geometries of the expected fault are considered, and since material properties of the different soils are not well known, a parametric study for the shear-wave velocities is performed (Fäh and Suhadolc, 1994).

The locations of the different layers and the values of the seismic velocities, shown in Figure 2.26, are based on the information given in Marcellini et al. (1991). The resulting cross-section and the examined different geometries of the transition between pliocenic clay and cemented conglomerate are shown in Figure 2.27. More details about the material properties which characterize the different layers and the type of extended seismic source considered are given by Fäh and Suhadolc (1994).

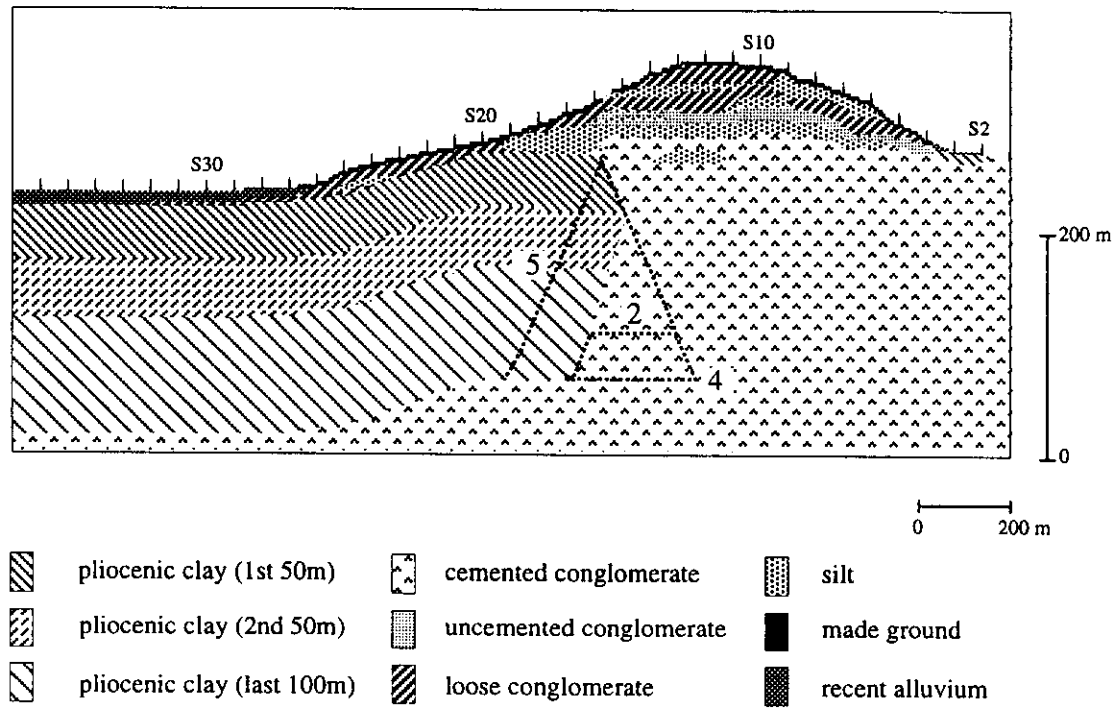

Figure 2.27 Two-dimensional model (1) of the studied Profile. Only the part of the structure near to the surface is shown, where the 2D model deviates from the 1D layered reference model. The assumed geometries of the transition between pliocenic clay and cemented conglomerate are indicated by numbers from 2 to 5, labeling the different thick dashed lines. The site positions are shown by small triangles - Site S1 at the right edge of the figure (after Fäh and Suhadolc, 1994).

The results of the study of the spatial variation of the site response, as determined by W, are shown in Figure 2.28a. The differences between the results obtained for the four geometries are smaller than the variations along the four single cross-sections. The biggest differences between

the four geometries are observed, as expected, just above the transition between pliocenic clay and cemented conglomerate. The peaks of relative W values, observed at distances between 13.7 and 13.9 km from the source, become slightly smaller for the two cases considered in Geometry 4 and Geometry 5. The result obtained for different shear-wave velocities are given in Figure 2.28b.

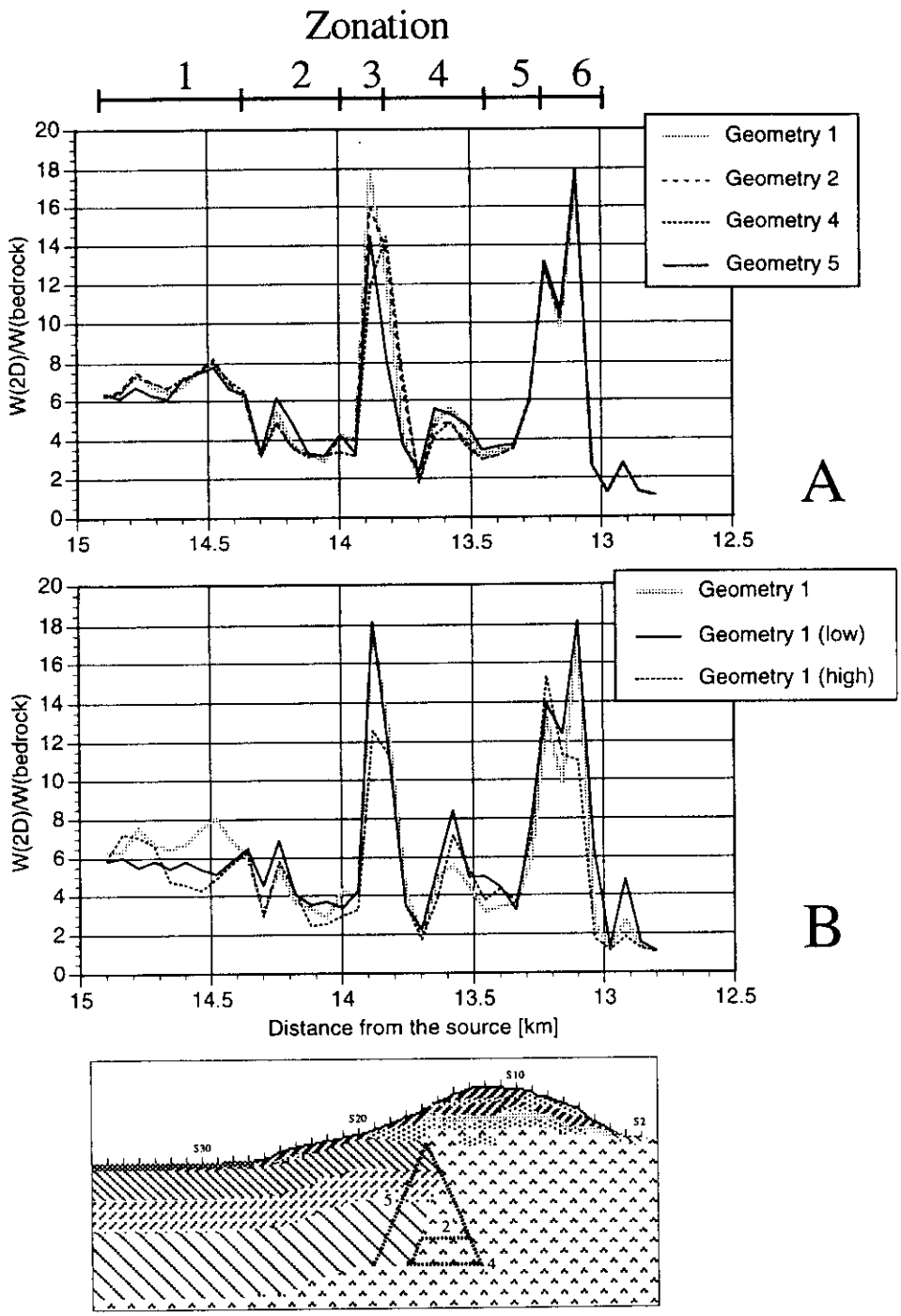

Figure 2.28 Relative energy of acceleration W: a) for different geometries, and b) by assuming low shear-wave velocities (low b), or high shear-wave velocities (high b) in the uppermost layer. The general zonation is explained in the text (after Fäh and Suhadolc, 1994).

The stability of the results obtained for the different models allows us to identify six zones, each characterized by a typical strong ground motion response, indicated in Figure 2.28. *Zone 1* extends over the lower valley of the Sabato river, where pliocenic clay is overlaid by a surficial layer of recent alluvium, including in some parts a thin buried layer of loose conglomerates. *Zone 2* represents the transition zone from the lower valley of the Sabato river to the hill zone of Benevento, where we have assumed a surface layer composed of loose conglomerate of variable thickness. Also present is a buried "silt lens". The hill zone of Benevento is divided into: *Zone 3* that includes the transition between pliocenic clay and cemented conglomerate, with a thick silt deposit, "made ground" within the surface layer, and in some parts a thin layer of loose conglomerate; *Zone 4* that extends over the areas of the hill where a thick layer of loose conglomerate is located close to the free surface; and *Zone 5* that spreads over the eastern part of the hill, where a silt layer is buried below the surface layer of "made ground". *Zone 6* is characterized by areas with only a thin sedimentary cover, located above the cemented conglomerate (bedrock).

In each of the six zones, for all sites and for all two-dimensional models, Fäh and Suhadolc (1994) have computed the relative spectral amplifications, Sa(2D)/Sa(bedrock), and the average and maximum spectral amplifications, that are shown, both for zero damping and 5% damping in Figure 2.29.

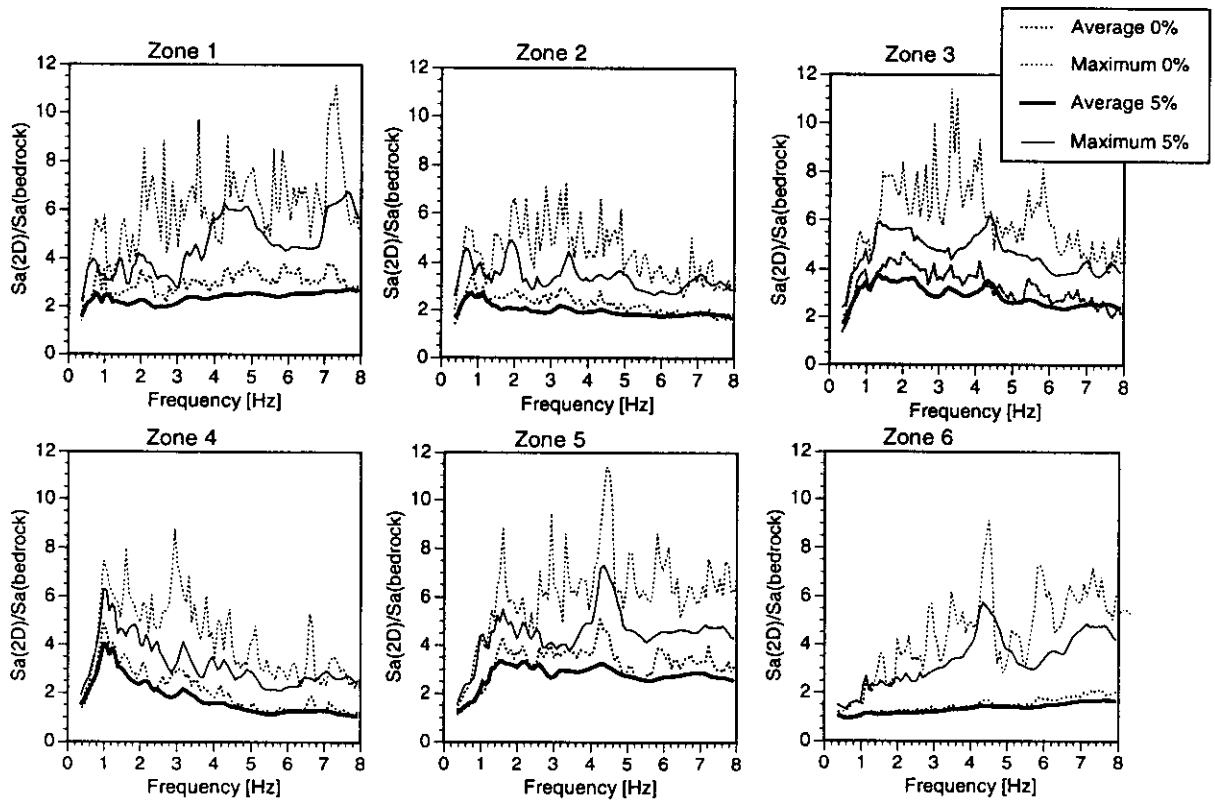

Figure 2.29 Maximum and average relative spectral amplifications, for the zones defined in Figure 2.28, for zero damping and 5% damping. The results include all computations made for the different two-dimensional structural models (after Fäh and Suhadolc, 1994).

3. CONCLUSIONS

Traditional deterministic methods for seismic zoning can only lead to a kind of "post-event" zoning whose validity cannot be easily extrapolated in time and to different regions and which, therefore, must be considered obsolete.

On the contrary the computation of realistic synthetic seismograms, using methods that make it possible to take source and propagation effects into account, utilizing the huge amount of geological, geophysical and geotechnical data, already available, goes well beyond the conventional deterministic approach and gives a powerful and economically valid scientific tool for seismic zonation and microzonation.

Because of its flexibility, the method is suitable for inclusion in new integrated procedures, a kind of compromise between probabilistic and deterministic approaches, that can be developed in order to minimize the drawbacks of each of the two procedures.

The ability to estimate accurately seismic hazard at very low probability of exceedance may be important in protecting, against rare earthquakes, the existence of special objects in the built environment. The deterministic approach, based upon the assumption that several earthquakes can occur within a predefined seismic zone, represents a conservative definition of seismic hazard for pre-event localized planning for disaster mitigation, over a quite broad-band of periods.

The results of tests made against instrumentally recorded accelerograms show that, even an approximate knowledge of the geometry and of the mechanical properties of the uppermost layers and the use of commonly available data on the seismic source geometry, is sufficient to make a realistic prediction of the ground motion.

Severe discrepancies are found between the amplifications computed with the 1-D standard method (method 1) and the 2-D hybrid method (method 2), and they cannot be ignored when formulating building codes and retrofitting the built environment. For example, in the area of Naples, in presence of a peat layer, the amplifications computed with method 1 are smaller then the "true" ones computed with method 2, and this is a clear evidence of the danger intrinsic in the application of method 1 for risk assessment. If the peat layer is absent, a similarity in shape exists between the amplifications computed with the two methods, but the amplification determined with method 1 overestimates the results obtained with method 2, with consequent implication of not necessary larger costs for the reduction of vulnerability.

Similar conclusion can be drawn from the computations made in Benevento. For an extended seismic source which is not located beneath the site of interest, in a laterally homogeneous structure, vertical incidence of waves (method 1) significantly overestimates the local hazard, with respect to the results obtained with the more realistic method 2. This is due to the different incidence angles related to different phase velocities of a realistic wavefield. The hybrid approach (method 2) allows us the simulation of the complete wavefield in given frequency and phase-velocity bands, and, in these bands, it accounts automatically for all surface waves and body waves, characterized by any incidence angle consistent with the bands considered. For a laterally

heterogeneous area, one-dimensional modelling fails to correctly estimate the seismic hazard, whereas for a seismic source which is not located beneath the site of interest, two-dimensional modelling with vertical incidence of plane polarized body-waves does not allow us to correctly estimate the frequency bands at which amplifications occur.

These considerations point to the problem of the definition of the seismic source in time-domain computations, and to the differences that can be obtained when using an empirical definition of the incident wavefield or a numerical simulation of the seismic source. Numerical simulations of the seismic source are a more adequate technique than making estimates based on recorded accelerograms (empirical Green functions), since such records are always influenced by the local soil condition of the recording site. On the other hand, numerical simulations require the knowledge or the estimate of many parameters for the definition of the source-site path and of the source rupture process, which are often, but not always at hand. With method 2, it is possible to obtain, at low cost and exploiting large quantities of already available data - like geotechnical parameters, surface geology data, seismological and geophysical data - the definition of realistic seismic input for the existing or planned built environment, including special objects. The hybrid method is, at present, the only quantitative procedure that permits, for realistic seismic sources, to compute reliable complete seismograms that take into account the propagation effects, including detailed local conditions and the anelastic behaviour of soils.

The definition of realistic seismic input can be obtained from the computation of a wide set of time histories and spectral information, corresponding to possible seismotectonic scenarios for different source and structural models. Such a data set can be fruitfully used by civil engineers in the design of new seismo-resistant constructions and in the reinforcement of the existing built environment, and therefore supply a particularly powerful tool for the prevention aspects of Civil Defence.

The procedure is scientifically and economically valid for the immediate (no need to wait for a strong earthquake to occur), first order, seismic microzonation of any urban area, where the geotechnical data are available. The possibility to model broad-band seismic input is a useful tool for the engineering design and for the retrofitting of special objects, with relatively long free periods, that is acquiring a continuously increasing importance, due to the widespread existence, in the built environment, of special objects.

4. ACKNOWLEDGMENTS

We thank Dr. F. Kebede, Dr. C. Nunziata and Dr. I. Orozova-Stanishkova for their consent to use some results about the city of Naples (CN), the zoning of Bulgaria (IO-S) and Ethiopia (FK).

Most of the computations were performed on the IBM3090E computer at the ENEA INFO BOL Computer Center, to whom we would like to express our deep gratitude.

We acknowledge support by European Union contracts EPOC-CT91-0042, EV5V-CT94-0491 and EV5V-CT94-0513, Italian MURST 40% and 60% funds (1992-1994), and CNR grants

91.02550.PF54, 91.02539.PF54, 91.02692.CT15, 92.02867.CT54, 92.02876.CT54, 92.02422.CT15, 93.04179.CT15 and 94.00193.CT05, and Swiss National Science Foundation Grant Nr. 8220-037189. This research has been carried out in the framework of the ILP Task Group II.4 contribution to the IDNDR project "Physical Instability of Megacities".

5. REFERENCES

Amato A., De Simoni B. and Gasparini C. 1984. Considerazioni sulla sismicità dei Colli Albani. Atti del 3° Convegno del Gruppo Nazionale di Geofisica della Terra Solida, CNR, Roma, 2:965-976.

Ambrosini S., Castenetto S., Cevolani F., Di Loreto E., Funiciello R., Liperi L. and Molin D. 1986. Risposta sismica dell'area urbana di Roma in occasione del terremoto del Fucino del 13 gennaio 1915. Risultati preliminari. *Mem. Soc. Geol. It.*, 35:445-452.

Arias, A. 1970. A measure of earthquake intensity. In: Seismic design for nuclear power plants (Ed. R. Hansen), Cambridge, Massachussets.

Basili A., Favali P., Scalera G. and Smriglio G. 1987. Valutazione della pericolosità sismica in Italia centrale con particolare riguardo alla città di Roma. Atti del 6° Convegno del Gruppo Nazionale di Geofisica della Terra Solida, CNR, Roma, 379-393.

Beck J. L. and Hall J. F. 1986. Factors contributing to the catastrophe in Mexico City during the earthquake of September 19, 1985. *Geophys. Res. Lett.* 13:593-596.

Bernard P. and Zollo A. 1989. The Irpinia (Italy) 1980 earthquake: detailed analysis of a complex normal faulting. *J. Geophys. Res.*, 94:1631-1647.

Boore D.M. 1987. The prediction of strong ground motion. In: M.Ö. Erdik and M.N. Toksöz (Eds), Strong ground motion seismology. Reidel Publishing Company, Dordrecht, 109-141.

Costa, G., Panza, G.F., Suhadolc, P. and Vaccari, F. 1992. Zoning of the italian region with synthetic seismograms computed with known structural and source information. Proc. 10th WCEE, July 1992, Madrid, Balkema, 435-438.

Costa G., Panza G.F., Suhadolc P. and Vaccari F. 1993. Zoning of the Italian territory in terms of expected peak ground acceleration derived from complete synthetic seismograms. In: R. Cassinis, K. Helbig and G.F. Panza (Eds), Geophysical Exploration in Areas of Complex Geology, II. *J. Appl. Geophys.*, 30:149-160.

Eurocode 8 1993. Eurocode 8 structures in seismic regions - design - part 1 general and building, Doc TC250/SC8/N57A.

Fäh D. 1992. A hybrid technique for the estimation of strong ground motion in sedimentary basins.

Ph.D. thesis Nr. 9767, Swiss Federal Institute of Technology, Zürich.

Fäh D. and Panza G.F. 1994. Realistic modelling of observed seismic motion in complex sedimentary basins. *Ann. Geofis.* 37:1771-1797.

Fäh D. and Suhadolc P. 1994. Application of numerical wave-propagation techniques to study local soil effects: the case of Benevento (Italy). *Pure and Applied Geophys.* 143:513-536.

Fäh D., Suhadolc P. and Panza G.F. 1990. Estimation of strong ground motion in laterally heterogenenous media: modal summation - finite differences. Proc. 9-th European Conference of Earthquake Engineering, Sept. 11-16, 1990, Moscow, 4A, 100-109.

Fäh D., C. Iodice, P. Suhadolc and G.F. Panza 1993. A new method for the realistic estimation of seismic ground motion in megacities: the case of Rome. *Earthquake Spectra* 9: 643-668.

Fäh D., Suhadolc P., Mueller St. and Panza G.F. 1994a. A hybrid method for the estimation of ground motion in sedimentary basins: quantitative modeling for Mexico City. *Bull. Seism. Soc. Am.* 84: 383-399.

Fäh D., Iodice C., Suhadolc P. and Panza G.F. 1994b. Estimation of strong ground motion and micro-zonation for the city of Rome. Pre-print, IC/94/48, ICTP, Trieste, Italy.

Feroci M., Funiciello R., Marra F. and Salvi S. 1990. Evoluzione tettonica e paleogeografica plio-pleistocenica dell'area di Roma. *Il Quaternario* 3:141-158.

Florsch N., Fäh D., Suhadolc P. and Panza G.F. 1991. Complete synthetic seismograms for high-frequency multimode SH-waves. *Pure and Applied Geophys.* 136:529-560.

Funiciello R., Lori G. and Salvi S. 1987. Ricostruzione delle superfici strutturali del sottosuolo della città di Roma. Atti del 6° Convegno del Gruppo Nazionale Geofisica della Terra Solida, CNR, Roma, 395-415.

Gasparini C., Iannaccone G. and Scarpa R. 1985. Fault-plane solutions and seismicity of the Italian peninsula. *Tectonophysics* 117:59-78.

GNDT 1992. Convegno Nazionale sul Modello Sismotettonico d'Italia. Milano, 25-26 May 1992

Gouin P. 1976. Seismic zoning in Ethiopia, *Bull. Geophys. Obs.* (Ethiopia) 17:1-46.

Gusev, A.A. 1983. Descriptive statistical model of earthquake source radiation and its application to an estimation of short period strong motion. *Geophys. J.R. Astron. Soc.* 74:787-800.

Haskell N. A. 1953: The dispersion of surface waves in multilayered media. *Bull. Seism. Soc. Am.* 43:17-34.

ING 1980-1991. Istituto Nazionale di Geofisica, Seismological reports. ING, Roma.

Jennings P.C. 1983. Engineering seismology. Terremoti: osservazione, teoria ed interpretazione. Rendiconti della Scuola Internazionale di Fisica 'Enrico Fermi', LXXXV Corso. Società Italiana di Fisica (ed.), 138-173.

Kanamori H. 1977. The energy release in great earthquakes. *J. Geophys. Res.* 82:2981-2987.

Kanamori H., Jennings P.C., Singh S.K. and Astiz L. 1993. Estimation of strong ground motions in Mexico City expected for large earthquakes in the Guerrero seismic gap. *Bull. Seism. Soc. Am.* 83:811-829.

Kebede F. and Vaccari F. 1996. Deterministic estimates of ground motion for Ethiopia, Djibouti and Eritrea. In preparation.

Manos G.C. and Demosthenous M. 1992. Design of R.C. structures according to the Greek Seismic Code Provisions. *Bull. of IISEE* 26:559-578.

Marcellini A., Bard P.-Y., Vinale F., Bousquet J.C., Chetrit D., Deschamps A., Franceschina L., Grellet B., Iannaccone G., Lentini E., Lopez Arroyo A., Meneroud J.P., Mouroux J.P., Pescatore T., Rippa F., Romeo R., Romito M., Sauret B., Scarpa R., Simonelli A., Tento A. and Vidal, S. 1991. Benevento Seismic Risk Project. Progress report (Report for the Commission of the European Communities, 1991).

Molin D., Ambrosini S., Castenetto S., Di Loreto E., Liperi L. and Paciello A. 1986. Aspetti della sismicità storica di Roma. *Mem. Soc. Geol. It.* 35:439-444.

Nunziata C., Fäh D. and Panza G.F. 1995. Mitigation of seismic hazard of a megacity: the case of Naples. *Annali di Geofisica* 38:649-661.

Orozova-Stanishkova I., Costa G., Vaccari F. and Suhadolc P. 1996. Estimates of 1Hz maximum acceleration in Bulgaria for seismic risk reduction purposes. *Tectonophysics* 258:263-274.

Panza G.F. 1985. Synthetic seismograms: The Rayleigh waves modal summation. *J. Geophysics* 58:125-145.

Panza, G. F., Prozorov, A. and Suhadolc, P. 1990. Is there a correlation between lithosphere structure and statistical properties of seismicity?, in: The structure of the Alpine - Mediterranean area: contribution of geophysical methods (Eds. R. Cassinis and G. F. Panza), *Terra nova* 2:585-595.

Panza, G. F. and Vaccari, F. 1994. Avanced criteria of seismic zoning and synthetic seismograms, Proc. Europrotech, Ed. G. Verri, CISM, Udine, 63-92.

Reiter L. 1990. Earthquake hazard analysis: issues and insights. Columbia University Press, New

York.

Rippa F. and Vinale F. 1983. Effetti del terremoto del 23 Novembre 1980 sul patrimonio edilizio di Napoli. Ass. Geotecnica Italiana, Atti XV Convegno Nazionale di Geotecnica, 193-206.

Sabetta F. and Pugliese A. 1987. Attenuation of peak horizontal acceleration and velocity from Italian strong-motion records. *Bull. Seism. Soc. Am.* 77:1491-1513.

Schnabel B., Lysmer J. and Seed H. 1972. Shake: a computer program for earthquake response analysis of horizontally layered sites. Rep. E.E.R.C. 70-10, Earthq. Eng. Research Center, Univ. California, Berkeley.

Stucchi M. et al., 1993. NT: il catalogo di lavoro del GNDT. GNDT internal report. Reserved.

Thomson W. T. 1950. Transmission of elastic waves through a stratified solid medium. *J. Appl. Phys.* 21:89-93.

Vaccari F., Gregersen S., Furlan M. and Panza G. F. 1989. Synthetic seismograms in laterally heterogeneous anelastic media by modal summation of P-SV-waves. *Geophys. J. Int.* 99:285-295.

Vaccari, F, Suhadolc, P. and Panza, G. F. 1990. Irpinia, Italy, 1980 earthquake: waveform modelling of strong motion data. *Geophys. J. Int.* 101:631-647.

Ventriglia U. 1971. La geologia della città di Roma. Amm. Prov. di Roma, Roma.